IMMUNOLOGICAL INVESTIGATIONS TO RE-ENGINEER A PLASMODIUM FALCIPARUM BLOOD-STAGE HUMAN MALARIA VACCINE

A DISSERTATION SUBMITTED TO THE GRADUATE DIVISION OF THE UNIVERSITY OF HAWAI'I AT MĀNOA IN PARTIAL FULFILLMENT OF THE REQUIREMENTS FOR THE DEGREE OF

DOCTOR OF PHILOSOPHY
IN
BIOMEDICAL SCIENCES
(TROPICAL MEDICINE)

MAY 2012

By
Kae M. Pusic

Dissertation Committee:

George Hui, Chairperson
Sandra Chang
Kenton Kramer
David Clements
Paul Nachtigall

Keywords: malaria, vaccine, adjuvant

ACKNOWLEDGMENTS

I would like to first give my utmost thanks to my Committee Chairperson Dr. George Hui for all his support, mentoring, and guidance through out this whole process. I would also like to thank my Committee members Dr. Sandra Chang, Dr. David Clements, Dr. Kenton Kramer, and Dr. Paul Nachtigall for their support.

For their technical support in the laboratory I would like to thank: Mazie Tsang, Natasha Cortez, Alyssa Fujimoto, Danielle Clements, Jackie McLaughlin, Acasia Hokama, Aliea Apana, Sophie Kobuch, and Andrew Stridiron.

For their help in animal immunizations I would like to thank: Dr. Sandra Chang, Dr. William Gosnell, Dr. Kenton Kramer, Ann Hashimoto, and Steve Case.

From Hawaii Biotech Inc. I would like to thank David Clements, James Senda, and Bo Liu for assistance in transformation and culture of *Drosophila* S2 cells expressing the truncated MSP1-42 proteins.

From Oceannanotech LLC I would like to thank Dr. Andrew Wang, Dr. Zoraida Aguilar, and Dr. Hong Xu for their collaboration and providing the nanoparticles and performing the conjugation of the malaria antigen to the nanoparticle.

I would lastly like to thank the RMATRIX and the NIH/NCRR COBRE for their technical support and help with the statistical analysis of the data.

ABSTRACT

Despite decades of intensive research, malaria remains one of the most prevalent and devastating infectious diseases in the developing world. There is dire need for an effective malaria vaccine. The Merozoite Surface Protein of *P. falciparum*, MSP1-42, is one of the leading candidates for a blood-stage malaria vaccine. However, clinical trials of MSP1-42 show no efficacy. Here, we provide *in vivo* evidence that T cell epitope regions at the N-termjnus of MSP1-42 (MSP1-33) provide functional help in inducing antibodies to the C-terminal protective fragment (MSP1-19). We further demonstrated that these T cell epitopes positively or negatively influenced antibody responses directed towards MSP1-19. Differential recognition of these regions by humans may play a critical role in natural immunity to MSP1-4;, and may also be a critical determinant of vaccine efficacy . This study provides the rational basis to re-engineer more efficacious MSP1-42 vaccines by selective inclusion and exclusion of MSP1-33 specific T cell epitopes.

Another major obstacle in the development of a subunit recombinant MSP1-42 malaria vaccine is the availability of safe and effective adjuvants that can potentiate a robust protective immune response. Currently, the adjuvant formulations suitable for clinical testing are very limited. Alternate strategies to enhance vaccine immunogenicity need to be explored and developed. One such strategy is the use of particle-mediated delivery systems such as nanoparticles. Here, we demonstrated the use of inorganic nanoparticles (<15nm) as a potent vaccine delivery platform to enhance the immunogenicity of the recombinant malaria vaccine antigen without additional adjuvants. Results showed that the inorganic nanoparticle delivery platform was as effective in enhancing immunogenicity as the malaria antigen administered with a clinically acceptable adjuvant. Moreover, the malaria vaccine/nanoparticle formulation induced parasite inhibitory antibodies in more than one animal species. Preliminary toxicity studies showed no significant

deviations from normal clinical values. We also investigated the effects of nanoparticle uptake by dendritic cell and macrophages and showed that targeting to these antigen presenting cells may be one of the principle modes of action in enhancing vaccine induced immune responses. Our results indicate that the inorganic nanoparticles is a viable vaccine delivery platform for further clinical development.

TABLE OF CONTENTS

INDEX OF TABLES

INDEX OF FIGURES

INTRODUCTION

Despite decades of intensive research, malaria remains one of the most prevalent and devastating infectious diseases in the developing world. Each year 350 to 500 million new cases of malaria are detected worldwide [1], with over one million deaths. Current methods to prevent and treat malaria, including drugs, insecticides and bed nets, have met with limited success [1]. Consequently, there is dire need for an effective malaria vaccine to aid in combating this debilitating and deadly parasitic disease. To date, malaria vaccine development efforts have focused on targeting a number of antigens from different developmental stages of the parasite's life cycle [2,3,4,5]. Vaccines are now being developed to target the sporozoite stage/the liver stage, the erythrocyctic stage, and gamete/gametocyte stages [2,3,4,5,6]. The sporozoite stage requires a vaccine which can induce sterile immunity, however, a successful vaccine can halt the infection and prevent the appearance of clinical symptoms and gametocytes. A vaccine targeting the gamete/gametocyte stage can reduce the number of mosquitos which harbor the parasite, nevertheless the vaccine must be able to eliminate all of the gametocytes present in the blood in order to reduce the chance of up take by feeding mosquitos. Morbidity, mortality, and all the clinical symptoms are associated with the erythrocytic stages of malaria [1], individuals living in endemic regions acquire clinical immunity to malaria after repeated exposures to the parasite [7,8,9]. This suggests that a vaccine targeting the blood stage has the potential to confer protection without having to induce sterile immunity. Blood stage vaccines also have a number of advantages; blocking parasites coming from the liver, reducing clinical symptoms associated with malaria, priming the immune response for shared antigens with the liver stage, and reducing the number of gametocytes present in the blood for up take by feeding mosquitos.

The majority of erythrocytic stage vaccine candidates target the free merozoites or antigens expressed on the surface of infected erythrocytes

[10,11,12,13,14,15,16,17,18,19,20]. These antigens are readily accessible as targets of both humoral and cellular immune effectors. Some of the erythrocytic vaccine candidates under evaluation include but are not limited to: Merozoite Surface Proteins (MSPs), Apical Membrane Antigen (AMA-1), the *P. falciparum* Erythocyte Membrane Protein 1 (PfEMP1), and Erythrocyte Binding Antigen (EBA-175) [5,6]. Of the eleven identified MSPs, the Merozoite Surface Protein 1 (MSP1) is one of the most studied and promising antigens for development as a malaria blood stage vaccine.

The MSP1 is a 195kDa protein that is proteolytically processed during schizogony into four smaller fragments: 83kDa, 30kDa, 38kDa, and 42kDa [20,21]. The C-terminal 42kDa fragment is then further cleaved during merozoite invasion into 33kDa and 19kDa fragments [21]. The 19kDa fragment (MSP1-19) is carried into the infected erythrocyte by the invading merozoite, while the 33kDa fragment (MSP1-33) is released into blood plasma [22]. MSP1 has been shown to form non-covalent complexes with other MSPs, namely MSP6 and MSP7 [23,24]. Their role in the merozoite invasion processes is an area that is actively investigated. Many vaccine studies have focused on the MSP1 C-terminal fragments, MSP1-42 and MSP1-19.

Epidemiological studies provide strong evidence that protective immunity against blood stage parasite infections is antibody mediated [7,8,9,25,26], with the majority having specificity for either MSP1-42 or MSP1-19 [25,26,27]. Research to date indicates that MSP1-42 or MSP1-19 antibodies may act by inhibiting and/or blocking merozoite invasion [8,25,28]. Vaccination studies based on MSP1-42 or MSP1-19 have demonstrated protection against blood infections *in vivo* rodent and monkey models [29,30,31,32,33]. Passive transfer of monoclonal or polyclonal antibodies specific for MSP1-19 protect against malaria [27]. Parasite growth inhibitory antibodies have been induced by vaccination with MSP1-19 and MSP1-42

[29,30,31,32] suggesting that vaccine-induced protective antibodies also inhibit parasite growth [29,31,32]. Besides the ability of anti-MSP1 antibodies to directly inhibit parasite growth or block invasion, studies have demonstrated a role of accessory cells (ie. monocytes) in antibody mediated effector mechanisms for MSP1 [34].

Statement of Problem and Hypothesis

Although there are promising data supporting the protective potential of these two MSP1 antigens, the immunological responses against MSP1-42/MSP1-19 are still unclear. There are a several distinctions between MSP1-42 and MSP1-19, the most significant being a difference in the specificity of antibodies they are capable of inducing [35]. Rodent and rabbit studies have shown that MSP1-42 elicits a broader and more consistent immune response, whereas MSP1-19 is capable of inducing stronger protection and/or parasite inhibiting antibodies, but only in a subset of the immunized animals [35,36,37]. This may be due to the cross-reactivity of antibody responses produced by MSP1-42 with other allelic forms of MSP1, and suggests that MSP1-42 may contain additional epitopes that are able to stimulate and/or help with specific parasite inhibiting antibody production [35].

As mentioned above, a number of animal studies with MSP1-42 based vaccines have demonstrated protection against malaria blood infections [29,30,31,32,33]. Unfortunately, clinical studies utilizing MSP1-42 vaccines have not been successful in inducing protection [38,39]. A number of factors may cause this discrepancy. First, unlike immunization in animal models, human antibodies induced by MSP1-42 vaccines do not possess specificity toward parasite inhibitory epitopes, as indicated by the lack of inhibitory response in the vaccinated individuals [38]. Second, the magnitude of antibody responses (titers) induced by the MSP1-42 vaccines in humans were lower in comparison to animals immunized with the same vaccine [38,39,40,41,42] and these antibody responses may also have been too

short lived to induce protection and/or memory responses [38,41,43]. A better understanding of MSP1-42 vaccine-induced immunity will aid in the design of more effective MSP1 C-terminal based vaccines to overcome the obstacles encountered to date.

To address this unmet need, studies designed to investigate the immunity induced by MSP1-42 are proposed. Specifically, the influence of T cell epitopes found on Merozoite Surface Protein 1-33 (MSP1-33) on MSP1-42 vaccine efficacy. Few studies have examined the role of MSP1-33 in protective responses elicited by MSP1-42. The majority of these studies merely focused on mining for T cell epitopes on MSP1-33 [44,45,46]. This is significant, since MSP1-19 does not possess adequate T cell help to stimulate antibody response in a genetically diverse population [36,45]. Therefore, we hypothesize that T cell epitopes on MSP1-33 can provide cognate helper function which is specific for anti-MSP1-19 antibody response and may also increase vaccine responsiveness in a population of diverse MHC make up [36,37,45,46,47,48]. It is further hypothesize that these MSP1-33 T cell epitopes will influence the quality of antibody response as demonstrated in other antigen models [49,50,51,52]. Thus, the goal of the proposed research is to identify the T epitope regions on MSP1-33 that provide help and contribute to induction of antibodies with specificity to inhibitory epitopes. Subsequently, selective inclusion of T cell epitopes that are identified as beneficial have the potential to be utilized in the design of a more effective MSP1-42 vaccine. Following the same rational, T cell epitopes that are identified as non-beneficial and not inducing specific MSP1-19 antibodies to inhibitory epitopes can be eliminated from vaccine design.

Another major obstacle in the development of a subunit recombinant MSP1-42 malaria vaccine is the availability of safe and effective adjuvants that can potentiate a robust protective immune response. Currently, the adjuvant formulations deemed suitable for clinical testing are very limited, with some that

have produced unacceptable adverse effects, and/or unable to induce sufficient levels of biologically active antibodies [39,41]. Alternate strategies to enhance vaccine immunogenicity need to be explored and developed. One such strategy that is being explored for other vaccine systems is the use of particle-mediated delivery systems such as micro or nanoparticles [53,54,55,56,57]. The particles currently being evaluated are composed of organic materials such as the lipid polymer particles (eg. PLGA, PGA, PLA) [58,59,60,61]; Virus-Like Particles (VLPs) [62,63]; Immune Stimulating Complexes (ISCOMS) [64,65]; and chitosans [66,67,68]. More recently, Self-Assembling, Polypeptide-based Nanoparticles (SAPN) have also been tested as a delivery platform for a peptide sporozoite malaria vaccine [69]. These SAPNs have proven to be highly effective for small peptide antigens, but do not have the capability to incorporate large polypeptide antigens, such as the MSP1-42 [69].

While the previous studies have demonstrated the effectiveness of organic nanoparticles as vaccine delivery vehicles with low toxicity, there have been very few studies investigating the use of inorganic nanoparticles for the delivery of recombinant and peptide based vaccines. Inorganic nanoparticles are being used and/or being developed for many clinical applications [70]. Currently, iron oxide based nanoparticles are utilized in the clinic as MRI agents [71]. Other potential clinical applications include drug delivery, cancer imaging, and stem cell tracking [70]. The safety profiles of some of the inorganic nanoparticles have been demonstrated to be highly acceptable, thus opening up opportunities to exploit their use for vaccine delivery. Furthermore, studies on nanoparticle based delivery, organic or inorganic, have concentrated on examining particles sizes above 50 nm in diameter, as smaller sized particles have short half-lives [72,73]. Towards the goal of developing a more effective malaria MSP-1 C-terminal vaccine, it is hypothesized that smaller sized nanoparticles, eg. <20 nm, may be advantageous for vaccine delivery purposes. At sizes <10 nm, particles behave as true solutions and thus can

be readily dispersed and penetrate tissues and organs. Therefore, the use of such nanoparticles will be effective for vaccine delivery since their small sizes will have the potential to reach to key immunological tissues/organs such as lymph nodes and spleen. Furthermore, the potential of these nanoparticles to be taken up by antigen presenting cells (APC) may improve vaccine effectiveness by leading to activation of innate immune responses and subsequent enhancement of adaptive responses to potentiate vaccine immunogenicity.

Based on this hypothesis of the role of small inorganic nanoparticles in improving vaccine immunogenicity, a portion of the current research is designed to evaluate the ability of solid inorganic nanoparticles (<15 nm) to act as delivery platforms for our recombinant MSP1-42 antigens. Furthermore, the mode of action of these nanoparticles will be investigated based on the hypothesis that they may be taken up by professional APCs and modulate innate responses. Successful use of these nanoparticles will provide for the first time a proof of concept that inorganic nanoparticles may be used as a delivery platform for recombinant vaccine antigens without additional adjuvants. This would have the potential to accelerate the development of not only the MSP1 vaccines but also vaccines for other infectious diseases in need of an alternate delivery systems.

In summary, we plan to identify and investigate T helper epitope regions of MSP1-33 in order to understand their influence on MSP1-42 vaccine immunogenicity and specificity of MSP1-19. We hypothesize that T helper epitope regions will have the ability to provide help and contribute to the induction of MSP1-19 antibodies, however they will vary in their ability to broaden vaccine response and focus antibody response to inhibitory epitopes. We hope that this will lead to the selective inclusion of only the beneficial T cell epitopes. Additionally, we plan to investigate the use of solid, inorganic nanoparticles as an effective strategy for the delivery of MSP1-42 based vaccines without the use of adjuvants. Here we hypothesize that

nanoparticle immunizations will be able to enhance the immunogenicity of the MSP1-42 vaccine and will have efficacy equal to or surpassing conventional adjuvants. We believe that one of the modes of action of the immunoenhancement will be at the level of APCs; affecting antigen uptake, APC activation, and presentation.

Specific Aims

Aim 1. To identify and investigate T helper epitope regions on MSP1-33 and their influence on vaccine immunogenicity and specificity of MSP1-19.

Hypothesis. (i). T helper epitope regions on MSP1-33 have varying capabilities to a) broaden vaccine response to MSP1-19, and b) focus antibody response to inhibitory epitopes on MSP1-19/MSP1-42. (ii). T cells induced with truncated T helper epitope regions of MSP1-33 can be re-called during exposure to full length MSP1-33 and/or MSP1-42.

Aim 2. To identify and characterize putative T cell epitopes of the down selected truncated MSP1-42 constructs.

Hypothesis. Putative T cell epitopes that are confirmed by in vitro antigen re-stimulation will differ in their ability to mount an immune response and/or to be recalled by the full length MSP1-42.

Aim 3. To investigate the use of solid, inorganic nanoparticles (<15 nm) as an effective strategy for the delivery of MSP1-42 based vaccines without the use of additional adjuvants.

Hypothesis. (i). Nanoparticle immunizations will enhance the immunogenicity of truncated MSP1-42 constructs, and will have efficacy equal to or surpassing conventional adjuvants. (ii). The route of nanoparticle delivery affects immunogenicity. (iii). One of the modes of action of nanoparticle immunizations will be at the level of antigen presenting cells (dendritic cells), affecting antigen uptake; presentation; and DC activation. (iv). Modifications of nanoparticle surface will affect immunogenicity and (v). The in vivo efficacy of the nanoparticle platform is independent of animal species.

References

1. World Malaria Report 2009.

2. Chauhan VS, Bhardwaj D (2003) Current status of malaria vaccine development. Adv Biochem Eng Biotechnol 84: 143-182.

3. Moorthy VS, Good MF, Hill AV (2004) Malaria vaccine developments. Lancet 363: 150-156.

4. Haque A, Good MF (2009) Malaria vaccine research: lessons from 2008/9. Future Microbiol 4: 649-654.

5. Vekemans J, Ballou WR (2008) Plasmodium falciparum malaria vaccines in development. Expert Rev Vaccines 7: 223-240.

6. Richards JS, Beeson JG (2009) The future for blood-stage vaccines against malaria. Immunol Cell Biol 87: 377-390.

7. al-Yaman F, Genton B, Kramer KJ, Chang SP, Hui GS, et al. (1996) Assessment of the role of naturally acquired antibody levels to Plasmodium falciparum merozoite surface protein-1 in protecting Papua New Guinean children from malaria morbidity. Am J Trop Med Hyg 54: 443-448.

8. John CC, O'Donnell RA, Sumba PO, Moormann AM, Koning-Ward TF, et al. (2004) Evidence that invasion-inhibitory antibodies specific for the 19-kDa fragment of merozoite surface protein-1 (MSP-1 19) can play a protective role against blood-stage Plasmodium falciparum infection in individuals in a malaria endemic area of Africa. The Journal of Immunology 173: 666-672.

9. Perraut R, Marrama L, Diouf B, Sokhna C, Tall A, et al. (2005) Antibodies to the conserved C-terminal domain of the Plasmodium falciparum merozoite

surface protein 1 and to the merozoite extract and their relationship with in vitro inhibitory antibodies and protection against clinical malaria in a Senegalese village. Journal of Infectious Diseases 191: 264-271.

10. Marshall VM, Silva A, Foley M, Cranmer S, Wang L, et al. (1997) A second merozoite surface protein (MSP-4) of Plasmodium falciparum that contains an epidermal growth factor-like domain. Infect Immun 65: 4460-4467.
11. Ramasamy R, Ramasamy M, Yasawardena S (2001) Antibodies and Plasmodium falciparum merozoites. Trends Parasitol 17: 194-197.
12. Black CG, Wu T, Wang L, Hibbs AR, Coppel RL (2001) Merozoite surface protein 8 of Plasmodium falciparum contains two epidermal growth factor-like domains. Mol Biochem Parasitol 114: 217-226.
13. Black CG, Wang L, Wu T, Coppel RL (2003) Apical location of a novel EGF-like domain-containing protein of Plasmodium falciparum. Mol Biochem Parasitol 127: 59-68.
14. Sharma P, Kumar A, Singh B, Bharadwaj A, Sailaja VN, et al. (1998) Characterization of protective epitopes in a highly conserved Plasmodium falciparum antigenic protein containing repeats of acidic and basic residues. Infect Immun 66: 2895-2904.
15. Wu T, Black CG, Wang L, Hibbs AR, Coppel RL (1999) Lack of sequence diversity in the gene encoding merozoite surface protein 5 of Plasmodium falciparum. Mol Biochem Parasitol 103: 243-250.
16. Oeuvray C, Bouharoun-Tayoun H, Gras-Masse H, Bottius E, Kaidoh T, et al. (1994) Merozoite surface protein-3: a malaria protein inducing antibodies

that promote Plasmodium falciparum killing by cooperation with blood monocytes. Blood 84: 1594-1602.

17. Smythe JA, Peterson MG, Coppel RL, Saul AJ, Kemp DJ, et al. (1990) Structural diversity in the 45-kilodalton merozoite surface antigen of Plasmodium falciparum. Mol Biochem Parasitol 39: 227-234.

18. Pachebat JA, Ling IT, Grainger M, Trucco C, Howell S, et al. (2001) The 22 kDa component of the protein complex on the surface of Plasmodium falciparum merozoites is derived from a larger precursor, merozoite surface protein 7. Mol Biochem Parasitol 117: 83-89.

19. Trucco C, Fernandez-Reyes D, Howell S, Stafford WH, Scott-Finnigan TJ, et al. (2001) The merozoite surface protein 6 gene codes for a 36 kDa protein associated with the Plasmodium falciparum merozoite surface protein-1 complex. Mol Biochem Parasitol 112: 91-101.

20. Holder AA, Freeman RR (1984) The three major antigens on the surface of Plasmodium falciparum merozoites are derived from a single high molecular weight precursor. J Exp Med 160: 624-629.

21. Holder AA, Lockyer MJ, Odink KG, Sandhu JS, Riveros-Moreno V, et al. (1985) Primary structure of the precursor to the three major surface antigens of Plasmodium falciparum merozoites. Nature 317: 270-273.

22. Blackman MJ, Ling IT, Nicholls SC, Holder AA (1991) Proteolytic processing of the Plasmodium falciparum merozoite surface protein-1 produces a membrane-bound fragment containing two epidermal growth factor-like domains. Mol Biochem Parasitol 49: 29-33.

23. Kadekoppala M, Holder AA (2010) Merozoite surface proteins of the malaria parasite: the MSP1 complex and the MSP7 family. Int J Parasitol 40: 1155-1161.

24. Pearce JA, Triglia T, Hodder AN, Jackson DC, Cowman AF, et al. (2004) Plasmodium falciparum merozoite surface protein 6 is a dimorphic antigen. Infect Immun 72: 2321-2328.

25. Egan AF, Burghaus P, Druilhe P, Holder AA, Riley EM (1999) Human antibodies to the 19kDa C-terminal fragment of Plasmodium falciparum merozoite surface protein 1 inhibit parasite growth in vitro. Parasite Immunology 21: 133-139.

26. O'Donnell RA, Koning-Ward TF, Burt RA, Bockarie M, Reeder JC, et al. (2001) Antibodies against merozoite surface protein (MSP)-1(19) are a major component of the invasion-inhibitory response in individuals immune to malaria. Journal of Experimental Medicine 193: 1403-1412.

27. Chappel JA, Holder AA (1993) Monoclonal antibodies that inhibit Plasmodium falciparum invasion in vitro recognise the first growth factor-like domain of merozoite surface protein-1. Mol Biochem Parasitol 60: 303-311.

28. Guevara Patino JA, Holder AA, McBride JS, Blackman MJ (1997) Antibodies that inhibit malaria merozoite surface protein-1 processing and erythrocyte invasion are blocked by naturally acquired human antibodies. J Exp Med 186: 1689-1699.

29. Singh S, Miura K, Zhou H, Muratova O, Keegan B, et al. (2006) Immunity to recombinant plasmodium falciparum merozoite surface protein 1 (MSP1):

protection in Aotus nancymai monkeys strongly correlates with anti-MSP1 antibody titer and in vitro parasite-inhibitory activity. Infect Immun 74: 4573-4580.

30. Kumar S, Collins W, Egan A, Yadava A, Garraud O, et al. (2000) Immunogenicity and efficacy in aotus monkeys of four recombinant Plasmodium falciparum vaccines in multiple adjuvant formulations based on the 19-kilodalton C terminus of merozoite surface protein 1. Infect Immun 68: 2215-2223.
31. Chang SP, Case SE, Gosnell WL, Hashimoto A, Kramer KJ, et al. (1996) A recombinant baculovirus 42-kilodalton C-terminal fragment of Plasmodium falciparum merozoite surface protein 1 protects Aotus monkeys against malaria. Infect Immun 64: 253-261.
32. Stowers AW, Cioce V, Shimp RL, Lawson M, Hui G, et al. (2001) Efficacy of two alternate vaccines based on Plasmodium falciparum merozoite surface protein 1 in an Aotus challenge trial. Infect Immun 69: 1536-1546.
33. Hirunpetcharat C, Tian JH, Kaslow DC, van Rooijen N, Kumar S, et al. (1997) Complete protective immunity induced in mice by immunization with the 19-kilodalton carboxyl-terminal fragment of the merozoite surface protein-1 (MSP1[19]) of Plasmodium yoelii expressed in Saccharomyces cerevisiae: correlation of protection with antigen-specific antibody titer, but not with effector CD4+ T cells. J Immunol 159: 3400-3411.
34. McIntosh RS, Shi J, Jennings RM, Chappel JC, de Koning-Ward TF, et al. (2007) The importance of human FcgammaRI in mediating protection to malaria. PLoS Pathog 3: e72.

35. Hui G, Hashimoto C (2007) Plasmodium falciparum anti-MSP1-19 antibodies induced by MSP1-42 and MSP1-19 based vaccines differed in specificity and parasite growth inhibition in terms of recognition of conserved versus variant epitopes. Vaccine 25: 948-956.

36. Tian JH, Miller LH, Kaslow DC, Ahlers J, Good MF, et al. (1996) Genetic regulation of protective immune response in congenic strains of mice vaccinated with a subunit malaria vaccine. J Immunol 157: 1176-1183.

37. Stanisic DI, Martin LB, Good MF (2003) The role of the 19-kDa region of merozoite surface protein 1 and whole-parasite-specific maternal antibodies in directing neonatal pups' responses to rodent malaria infection. J Immunol 171: 5461-5469.

38. Ogutu BR, Apollo OJ, McKinney D, Okoth W, Siangla J, et al. (2009) Blood stage malaria vaccine eliciting high antigen-specific antibody concentrations confers no protection to young children in Western Kenya. PLoS One 4: e4708.

39. Malkin E, Long CA, Stowers AW, Zou L, Singh S, et al. (2007) Phase 1 study of two merozoite surface protein 1 (MSP1(42)) vaccines for Plasmodium falciparum malaria. PLoS Clin Trials 2: e12.

40. Angov E, Bergman-Leitner ES, Duncan EH, Brent-Kirk A, McCasland M, et al. (2007) Measurement of antibody fine specificities induced by malaria vaccine FMP1/ASO2A from a pediatric phase 2B trial in western Kenya. . American Journal of Tropical Medicine and Hygiene 77 Abstract 12.

41. Ellis RD, Martin LB, Shaffer D, Long CA, Miura K, et al. (2010) Phase 1 trial of the Plasmodium falciparum blood stage vaccine MSP1(42)-C1/Alhydrogel with and without CPG 7909 in malaria naive adults. PLoS One 5: e8787.

42. Stoute JA, Gombe J, Withers MR, Siangla J, McKinney D, et al. (2007) Phase 1 randomized double-blind safety and immunogenicity trial of Plasmodium falciparum malaria merozoite surface protein FMP1 vaccine, adjuvanted with AS02A, in adults in western Kenya. Vaccine 25: 176-184.

43. Lee EA, Flanagan KL, Minigo G, Reece WH, Bailey R, et al. (2006) Dimorphic Plasmodium falciparum merozoite surface protein-1 epitopes turn off memory T cells and interfere with T cell priming. Eur J Immunol 36: 1168-1178.

44. Lee EA, Flanagan KL, Odhiambo K, Reece WH, Potter C, et al. (2001) Identification of frequently recognized dimorphic T-cell epitopes in plasmodium falciparum merozoite surface protein-1 in West and East Africans: lack of correlation of immune recognition and allelic prevalence. Am J Trop Med Hyg 64: 194-203.

45. Udhayakumar V, Anyona D, Kariuki S, Shi YP, Bloland PB, et al. (1995) Identification of T and B cell epitopes recognized by humans in the C-terminal 42-kDa domain of the Plasmodium falciparum merozoite surface protein (MSP)-1. J Immunol 154: 6022-6030.

46. Malhotra I, Wamachi AN, Mungai PL, Mzungu E, Koech D, et al. (2008) Fine specificity of neonatal lymphocytes to an abundant malaria blood-stage

antigen: epitope mapping of Plasmodium falciparum MSP1(33). J Immunol 180: 3383-3390.

47. Hui GS, Gosnell WL, Case SE, Hashiro C, Nikaido C, et al. (1994) Immunogenicity of the C-terminal 19-kDa fragment of the Plasmodium falciparum merozoite surface protein 1 (MSP1), YMSP1(19) expressed in S. cerevisiae. J Immunol 153: 2544-2553.

48. Tian JH, Good MF, Hirunpetcharat C, Kumar S, Ling IT, et al. (1998) Definition of T cell epitopes within the 19 kDa carboxylterminal fragment of Plasmodium yoelii merozoite surface protein 1 (MSP1(19)) and their role in immunity to malaria. Parasite Immunol 20: 263-278.

49. Datta SK (1998) Production of pathogenic antibodies: cognate interactions between autoimmune T and B cells. Lupus 7: 591-596.

50. Milich DR, McLachlan A, Moriarty A, Thornton GB (1987) A single 10-residue pre-S(1) peptide can prime T cell help for antibody production to multiple epitopes within the pre-S(1), pre-S(2), and S regions of HBsAg. J Immunol 138: 4457-4465.

51. Milich DR (1988) T- and B-cell recognition of hepatitis B viral antigens. Immunol Today 9: 380-386.

52. Lanzavecchia A (1985) Antigen-specific interaction between T and B cells. Nature 314: 537-539.

53. Bramwell VW, Perrie Y (2005) Particulate delivery systems for vaccines. Crit RevTherDrug Carrier Syst 22: 151-214.

54. O'Hagan DT, Singh M (2003) Microparticles as vaccine adjuvants and delivery systems. Expert Rev Vaccines 2: 269-283.

55. O'Hagan DT, Singh M, Ulmer JB (2006) Microparticle-based technologies for vaccines. Methods 40: 10-19.

56. Peek LJ, Middaugh CR, Berkland C (2008) Nanotechnology in vaccine delivery. AdvDrug DelivRev 60: 915-928.

57. Singh M, Chakrapani A, O'Hagan D (2007) Nanoparticles and microparticles as vaccine-delivery systems. ExpertRevVaccines 6: 797-808.

58. Akagi T, Wang X, Uto T, Baba M, Akashi M (2007) Protein direct delivery to dendritic cells using nanoparticles based on amphiphilic poly(amino acid) derivatives. Biomaterials 28: 3427-3436.

59. Shive MS, Anderson JM (1997) Biodegradation and biocompatibility of PLA and PLGA microspheres. AdvDrug DelivRev 28: 5-24.

60. Mundargi RC, Babu VR, Rangaswamy V, Patel P, Aminabhavi TM (2008) Nano/micro technologies for delivering macromolecular therapeutics using poly(D,L-lactide-co-glycolide) and its derivatives. JControl Release 125: 193-209.

61. Lu JM, Wang X, Marin-Muller C, Wang H, Lin PH, et al. (2009) Current advances in research and clinical applications of PLGA-based nanotechnology. ExpertRevMolDiagn 9: 325-341.

62. Chackerian B (2007) Virus-like particles: flexible platforms for vaccine development. ExpertRevVaccines 6: 381-390.

63. Ludwig C, Wagner R (2007) Virus-like particles-universal molecular toolboxes. CurrOpinBiotechnol 18: 537-545.

64. Skene CD, Sutton P (2006) Saponin-adjuvanted particulate vaccines for clinical use. Methods 40: 53-59.

65. Sun HX, Xie Y, Ye YP (2009) ISCOMs and ISCOMATRIX. Vaccine 27: 4388-4401.

66. Masotti A, Ortaggi G (2009) Chitosan micro- and nanospheres: fabrication and applications for drug and DNA delivery. MiniRevMedChem 9: 463-469.

67. Illum L, Jabbal-Gill I, Hinchcliffe M, Fisher AN, Davis SS (2001) Chitosan as a novel nasal delivery system for vaccines. AdvDrug DelivRev 51: 81-96.

68. van dLI, Verhoef JC, Borchard G, Junginger HE (2001) Chitosan for mucosal vaccination. AdvDrug DelivRev 52: 139-144.

69. Kaba SA, Brando C, Guo Q, Mittelholzer C, Raman S, et al. (2009) A nonadjuvanted polypeptide nanoparticle vaccine confers long-lasting protection against rodent malaria. Journal of Immunology 183: 7268-7277.

70. Figuerola A, Di Corato R, Manna L, Pellegrino T From iron oxide nanoparticles towards advanced iron-based inorganic materials designed for biomedical applications. Pharmacol Res 62: 126-143.

71. Raynal I, Prigent P, Peyramaure S, Najid A, Rebuzzi C, et al. (2004) Macrophage endocytosis of superparamagnetic iron oxide nanoparticles: mechanisms and comparison of ferumoxides and ferumoxtran-10. Invest Radiol 39: 56-63.

72. Peer D, Karp JM, Hong S, Farokhzad OC, Margalit R, et al. (2007) Nanocarriers as an emerging platform for cancer therapy. NatNanotechnol 2: 751-760.

73. Ferrari M (2005) Cancer nanotechnology: opportunities and challenges.

NatRevCancer 5: 161-171.

Chapter 1

Title: T Cell Epitope Regions of the *P. falciparum* MSP1-33 Critically Influence Immune Responses and *in vitro* Efficacy of MSP1-42 Vaccines

Kae M. Pusic[1], Caryn N. Hashimoto[1], Axel Lehrer[2,3], Charmaine Aniya[3,4], David E. Clements[3], George S. Hui[1]

[1]*University of Hawaii, Honolulu, John A. Burns School of Medicine, Department of Tropical Medicine, Medical Microbiology, and Pharmacology, HI, USA;* [2]*Current affiliation: PantheraBioPharma. Aiea, HI, USA;* [3]*Hawaii Biotech Inc. Aiea, HI, USA;* [4] *Current affiliation: City and County of Honolulu, Police Department, Scientific Investigation Section, Drug Analysis Unit, HI, USA.*

Pusic KM, Hashimoto CN, Lehrer A, Aniya C, Clements DE, Hui GS: ***T cell epitope regions of the P. falciparum MSP1-33 critically influence immune responses and in vitro efficacy of MSP1-42 vaccines****. PLoS One 2011,* ***6****(9):e24782.*

Abstract

The C-terminal 42 kDa fragment of the *P. falciparum* Merozoite Surface Protein 1, MSP1-42, is a leading malaria vaccine candidate. MSP1-33, the N-terminal processed fragment of MSP1-42, is rich in T cell epitopes and it is hypothesized that they enhance antibody responses toward MSP1-19. Here, we provide *in vivo* evidence that T cell epitope regions of MSP1-33 provide functional help in inducing anti-MSP1-19 antibodies. Eleven truncated MSP1-33 segments were expressed in tandem with MSP1-19 and immunogenicity was evaluated in Swiss Webster mice and New Zealand White rabbits. Analyses of the anti-MSP1-19 antibody responses revealed striking differences in helper function of these segments despite that they all possess T cell epitopes. Only a few fragments were able to induce a responses in 100% of the outbred mice immunized. These responses were comparable to or surpassed the responses observed with the full length MSP1-42. In rabbits, only a subset of truncated antigens induced potent parasite growth inhibitory antibodies. Notably, two constructs elicited a more robust response than MSP1-42, one of which is composed of only conserved segments of sequence from the MSP1-33 region. Moreover, a T cell epitope region was identified that induces high titers of non-inhibitory antibodies that interfered with the inhibitory activities of anti-MSP1-42 antibodies. In mice, this region also induced a skewed TH2 cellular response. This is the first demonstration that T cell epitope regions of MSP1-33 positively or negatively influenced antibody responses directed towards MSP1-19. Differential recognition of these regions by humans may play a critical role in vaccine induced and/or natural immunity to MSP1-42. This study provides the rational basis to re-engineer more efficacious MSP1-42 vaccines by selective inclusion and exclusion of MSP1-33 specific T cell epitopes.

Introduction

The C-terminal fragment of the Merozoite Surface Protein 1 (MSP1) of *P. falciparum*, MSP1-42, is one of the leading candidates for a blood-stage malaria vaccine [1]. MSP1 is a 195kDa protein that is proteolytically processed during schizogony into four smaller fragments: 83kDa, 30kDa, 38kDa, and 42kDa [2,3]. The C-terminal 42kDa protein is then further processed during merozoite invasion into a 33kDa and a 19kDa fragment [3]. The 19kDa fragment (MSP1-19) is carried into the infected erythrocyte by the merozoites, while the 33kDa fragment (MSP1-33) is released into the blood plasma [4]. Protective immunity induced by MSP1-42/MSP1-19 has been shown to be antibody mediated [5,6,7,8,9]. It has been demonstrated that passive transfer of anti-MSP1-42 or MSP1-19 monoclonal and polyclonal antibodies can provide protection against malaria [10,11,12,13,14,15]; MSP1-42 or MSP1-19 specific antibodies may act by inhibiting merozoite invasion [9]. On the other hand, blocking antibodies specific for MSP1-42/MSP1-19 have also been detected, and these antibodies interfere with the activities of parasite inhibitory anti-MSP1-19 antibodies [16]. Vaccination studies with MSP1-42 or MSP1-19 have demonstrated strong or complete protection against blood infections in rodent and monkey models [17,18,19,20,21]. Monkeys protected by MSP1-42 vaccinations produce parasite inhibitory antibodies [17,19,20], thus suggesting that vaccine-induced immunity is also antibody mediated.

Although the above studies have convincingly demonstrated the vaccine potential of MSP1-42/MSP1-19, a Phase II clinical trial using MSP1-42 resulted in no *in vivo* protection [22]. The inability of the MSP1-42 vaccine formulation to induce protection in this clinical trial could be attributed to very low levels (titers) of parasite inhibitory antibodies [22,23]. Two Phase I trials of MSP1-42 using Alum and Alum+CPG adjuvants also resulted in low levels of inhibitory antibodies [24,25]. The failure to elicit protective immunity and/or high levels of parasite inhibitory

antibodies in these clinical trials may be attributed to a number of factors: a) serum samples from vaccinated individuals have no parasite inhibitory activity suggesting that the MSP1-42 vaccine induced antibodies of the wrong specificity [22,24]: b) the magnitude of antibody titers induced by the MSP1-42 vaccines were not high enough to have biological activity [23,24,26]: c) antibodies were relatively short-lived to confer protection [22,25]: and d) inadequate induction of memory responses [27]. A better understanding of the vaccine-induced immune response to MSP1-42 may help to overcome these shortcomings and may help to design a more efficacious MSP1-42 vaccine.

Unlike MSP1-42/MSP1-19, there have been few studies on MSP1-33. Studies on MSP1-33 primarily focus on mining T cell epitopes [28,29,30] since it has been shown that MSP1-19 does not possess adequate T helper epitopes to stimulate robust antibody responses in a diverse genetic population [29,31]. Thus, it has been suggested that T cell epitopes on MSP1-33 may provide cognate helper function specific for anti-MSP1-19 antibody response [29,30,31,32,33,34]. It is assumed that MSP1-33 specific T cell epitopes will all contribute positively to the induction of biologically active anti-MSP1-19 antibodies. However, it has been well established in other model systems that T cell epitopes can influence the development antibody response to B cell epitopes [35,36,37,38]. Indeed, previous studies have observed differences in antibody specificity induced by MSP1-19 versus MSP1-42 (ie. MSP1-33 + MSP1-19) [39]. In a genetically diverse population, MSP1-42 is more effective in inducing parasite growth inhibitory antibody responses than MSP1-19 [39]. In addition, *in vivo* protection induced by MSP1-19 is also regulated by the host's immune response, (IR) genes [31,33]. Moreover, MSP1-42 induces antibodies that are more broadly cross-reactive with other allelic forms of MSP1-19 than the MSP1-19 fragment [39], suggesting that MSP1-42 may elicit antibodies to additional epitopes with in MSP1-19 [39]. It is possible that MSP1-33, which harbors abundant

T cell epitopes, may influence antibody responses directed towards MSP1-19 when MSP1-42 is used as an immunogen. To address this hypothesis, we investigated the ability of T cell epitopes of MSP1-33 to provide help, and whether they can critically influence anti-MSP1-19 antibody specificity. Outbred Swiss Webster mice were used to examine the efficacy of eleven recombinant MSP1 C-terminal subunit proteins consisting of truncated segments of MSP1-33 linked to MSP1-19. Additionally, the recombinant subunit proteins, formulated with ISA51, were evaluated in New Zealand White (NZW) rabbits for the induction of parasite growth inhibitory antibodies. The results presented demonstrate that T cell epitopes of MSP1-33 have a profound influence on the ability to influence anti-MSP1-19 antibody responses.

Material and Methods

Ethics Statement

All experiments involving animals (mice and rabbits) were approved by the University of Hawaii Institutional Animal Care and Use Committee (IACUC). Procedures were designed to minimize pain and distress. The use of animals for experimentation strictly adhered to the "Guide for the Care and Use of Laboratory Animals" published by the Institute for Laboratory Animal Research (ILAR). Immunized animals were monitored for unusual pain and distress and they would have been euthanized if such symptoms appeared. Euthanasia was performed according to the methods recommended by the American Veterinary Medical Association (AVMA). University of Hawaii's Animal Care Assurance number is A3423-01. For all animal studies, the IACUC approved specific protocol number is 08-389.

Mouse and Rabbit strains

Outbred Swiss Webster mice (female, 6-8 weeks old) were obtained from four different vendors, Taconic (Albany, NY), Simonsen (San Clara, CA), Harlan Spraque Dawley Inc. (Indianapolis, IA), and Charles River Laboratory (Wilmington, MA) to ensure genetic heterogeneity. New Zealand White (NZW) rabbits (female, 8-10 lbs) were obtained from Western Oregon Rabbit Company (Philomath, Oregon). The use of mice and rabbits were approved by the University of Hawaii's Institutional Animal Care and Use Committee.

MSP1-specific antibody assays

Mouse and rabbit sera were assayed for anti-MSP1 antibodies (MSP1-42 and MSP1-19) by direct binding ELISAs as previously described [40]. Recombinant MSP1-42 and MSP1-42 antigens used for coating ELISA plates were produced based on *P. falciparum* FUP strain and were obtained from previous studies. The MSP1-42 was

expressed in baculovirus [33],and, MSP1-19 was expressed in yeast [32]. Recombinant MSP1-33 was expressed in *E. coli* and was based on the 3D7 strain, which has identical MSP1-33 sequence as FUP [41]. Briefly, 96-well ELISA plates (Costar, Acton, MA) were coated with the appropriate test antigen at a concentration of 0.4µg/mL. Plates were then blocked with 1% Bovine Serum Albumin (BSA) in Borate Buffered Saline (BBS). Test sera were serially diluted in 1% BSA/0.5% yeast extract/BBS and then incubated for 60 minutes in the antigen-coated ELISA wells. Wells were washed seven times with High Salt Borate Buffered Saline (HSBBS) and incubated for 60 minutes with horseradish peroxidase conjugated anti-rabbit (H & L chain specific, Kirkgaard and Perry Laboratories, Gaithersburg, MD) at a dilution of 1:2000 or anti-mouse antibodies (H & L chain specific, Kirkgaard and Perry Laboratories, Gaithersburg, MD) at a dilution of 1:2000. Wells were subsequently washed as above and then developed using the peroxidase substrates, H_2O_2 and 2.2'-azinobis (3-ethylbenzthiazolinesulfonic acid)/ABTS (Kirkgaard and Perry Laboratories, Gaithersburg, MD). Optical densities (O.D.) were determined at 405nm and endpoint titers were calculated and graphed using Sigma Plot 10. End point titers were calculated using the serum dilutions that gave an O.D. of 0.2, which is greater than 4 fold of background O.D. obtained using normal mouse or rabbit serum.

Expression and purification of recombinant MSP1 C-terminal subunit proteins in Drosophila S2 cell

The recombinant MSP1 C-terminal subunit proteins were produced in the *Drosophila* S2 expression system. The expression system consists of the *Drosophila* S2 cells [42] and a series of broad host plasmid vectors that direct the expression of heterologous proteins [43]. The expression plasmid, pMttbns (derived from pMttPA) contains the following elements: *Drosophila melanogaster* metallothionein promoter,

the human tissue plasminogen activator secretion leader (tPAL) and the SV40 early polyadenylation signal. A 14 base pair BamHI fragment was excised from the pMttbns vector to yield pMttΔXho creating a unique XhoI. This expression vector results in the secretion of the target protein into the culture medium. The MSP-1 sequences were introduced into the pMttΔXho vector using the unique BglII and XhoI sites.

Eleven constructs, referred hereto as Constructs 33-A – 33-K, were designed to express regions of MSP1-33 fused to MSP1-19 (Figure 1.1). These constructs were selected based on T-cell epitope predictions via the computer algorithm, Propred [44] or data empirically generated by antigen driven human PBMC proliferation assays [28,29,30]. Table 1.1 lists the amino acid sequence of the identified and predicted T cell epitopes used in the design of the Constructs 33-A – 33-K. For the construction of Constructs 33-A – 33-K expression plasmids, two strategies were used either separately or in combination. The first strategy utilized PCR amplified DNA sequences encoding T cell epitope regions from the MSP1-33 fragment that was derived from the FUP strain genomic DNA (Table 1.2). The second strategy utilized oligonucleotides encoding for T cell epitope containing fragment(s) (Table 1.2). All PCR and oligonucleotide generated MSP1 C-terminal subunit gene fragments were designed to include restriction endonuclease sites that were used for cloning into the vectors or linking of MSP1 sequences (fragments).

S2 cells were cultured in Excel 420 serum free medium (SAFC, St. Louis, MO). The cells were co-transformed with the pMttΔXho-MSP1 expression plasmids and the pCoHygro selection plasmid, which encodes hygromycin resistance, utilizing the calcium phosphate co-precipitation method (Invitrogen Kit, Carlsbad, CA) according to the manufacturer's recommendations. Cells were co-transformed with 20 μg total DNA at a 20:1 ratio of expression plasmid to selection plasmid. Transformants were selected with hygromycin B (Roche Molecular Biochemicals, Indianapolis, IN) at a

concentration of 300 µg/mL. For expression studies, cells were induced with 200 µM $CuSO_4$. The recombinant proteins were purified from the culture supernatant by immunoaffinity chromatography utilizing the mAb 5.2 [45], and analyzed by SDS-PAGE.

Immunization with recombinant MSP1 C-terminal subunit proteins

Swiss Webster mice were divided into eleven different vaccination groups (12 mice per group). Each mouse group was immunized with a different MSP1 C-terminal construct and two control groups were immunized with either MSP1-19 or MSP1-42. All mice were immunized three times at 21 days intervals, via the IP route. The first immunization consisted of a sub-optimal dose of 2 µg antigen, followed by two booster injections with an optimal dose of 5 µg [46]. The immunogens were emulsified in Complete Freund's Adjuvant (CFA) for the primary injections and in Incomplete Freund's Adjuvant (IFA) for booster injections. Sera were obtained through tail bleeds, 14 days after each immunization.

New Zealand White rabbits were divided into 10 different immunization groups (3 rabbits per group). NZW rabbits were immunized with nine of the S2 cell expressed recombinant MSP1 C-terminal subunit proteins formulated in Montanide ISA51 adjuvant. Each dose of vaccine contained 50 µg of antigen in 250 µl PBS, which was then emulsified with an equal volume of ISA51 as per the manufacturer's recommendations. The emulsion was injected via the IM route into the left and right thighs. A total of four immunizations were given at 4 weeks intervals and sera was collected 21 days after the last immunization. Sera were analyzed by ELISA and parasite growth inhibition assays. As control, rabbits were similarly immunized with S2 cell expressed full length MSP1-42.

ELISPOT Assay

ELISPOTS were performed using splenocytes from immunized mice according to methods previously described [47]. Ninety-six well PVDF plates (Millipore Inc., Bedford, MA) were coated with 10 ug/mL of anti-IFN-γ mAb (R4-642) and 5 ug/mL of anti-IL-4 mAb (11B11) (BD Biosciences, San Diego, CA) and incubated overnight at room temperature. Plates were then washed five times with sterile phosphate buffered saline (PBS) and blocked for 60 minutes at 37ºC with DMEM/10% fetal bovine serum. Mice from each vaccination group were sacrificed by cervical dislocation, the spleen removed, and placed in DMEM. The spleen was crushed and individual suspensions of splenocytes were prepared by passing through a cell strainer and washing four times in DMEM. Splenocytes were plated at $0.5x10^6$ cells/well, $0.25\ x10^6$ cells/well, and $0.125\ x10^6$ cells/well, and the corresponding recombinant immunogen was added at a final concentration of 20 ug/mL as the stimulating antigen. Positive control wells were incubated with 5 ng/mL of phorbol myristate acetate (PMA) and 1 ng/mL ionomycin. Plates were incubated again at 37ºC for 48 hours and then processed by washing four times with PBS and five times with PBS with 0.05% Tween-20. Biotinylated monoclonal antibodies against IFN-γ at 2 µg/mL (XMG1.2), and monoclonal antibodies against IL-4 at 1 µg/mL (BVD6-24G2) (BD, Biosciences, San Diego, CA) were added to appropriate wells and incubated for three hours at 37ºC. Plates were again washed as mentioned above and incubated with peroxidase conjugated streptavidin (Kirkgaard and Perry Laboratories, Gaithersburg, MD) for 60 minutes at a concentration of 1:800. After seven washings, plates were developed with a solution consisting of 3,3'-Diaminobenzidine tetrahydrochloride (DAB) (Sigma-Aldrich St. Louis, MO, 1mg/ml) and 30% H_2O_2 (Sigma-Aldrich St. Louis, MO). Cytokine producing cells were counted microscopically and data presented as spot-forming-units (SFU) per million of plated splenocytes.

In vitro parasite growth inhibition assays

The ability of sera from rabbits immunized with nine of the MSP1 C-terminal subunit proteins to inhibit parasite growth was determined using an *in vitro* parasite growth inhibition assay [20,32,48,49]. The assay was performed using sorbitol synchronized parasite cultures (3D7 strain) as previously described [32]. Synchronized parasite cultures at a starting parasitemia of 0.2% and 0.8% hematocrit were incubated in 30% heat inactivated immune sera. Cultures were then incubated for 72 hours with periodic mixing. Parasitemia was then determined microscopically by Giemsa staining. The degree of parasite growth inhibition was determined by comparing the parasitemias of cultures incubated with pre-immune sera as previously described [32,48,49].

In vitro assay for blocking antibodies

To test for the presence of blocking antibodies that interfere with anti-MSP1 growth inhibitory antibodies, synchronized parasite cultures were incubated in a mixture of 20% heat inactivated anti-Construct 33-C sera and 15% anti-MSP1-42 inhibitory sera as previously described [50]. Normal rabbit sera were similarly mixed with the inhibitory anti-MSP1-42 sera as control. The inhibitory anti-MSP1-42 sera was obtained from a previous vaccination study [39]. In that study we produced highly inhibitory anti-MSP1-42 antibodies (>90% growth inhibition) by hyper-immunization of rabbits with full length MSP1-42 emulsified in CFA [39]. These sera were used because of their very high levels of parasite growth inhibition making their inhibitory activities less prone to dilution effects when mixing with other sources of rabbit sera.

Data handling and Statistics

Sigma Plot 10® and GraphPadPrism 4® were used to calculate end point titers. One-way Analysis of Variance (ANOVA) and Student t-test were used to determine

significant differences in antibody titers amongst the different test groups. Cytokine responses (ELISPOT) in mice and parasite growth inhibition of sera from rabbits immunized with the different MSP1 C-terminal subunit proteins were analyzed by Logistic Regression for Repeated Measures and Fisher Exact Test: respectively (IBM SPSS Statistics). A $p<0.05$ was considered statistically significant.

Results

Expression of recombinant MSP1 C-terminal subunit proteins

Induced culture supernatants from *Drosophila* S2 cells transformed with Constructs 33-A – 33-K were clarified and the recombinant proteins were purified by immuno-affinity chromatography. The purified proteins were analyzed by SDS-PAGE. A representative reducing gel of the purified proteins is shown in Figure 1.2. A protein doublet was observed after purification of Construct 33-A (~19 kDa) and 33-B (~21 kDa) (Figure 1.2, Lanes 1 and 2), which may result from different degrees of glycosylation in the insect cells. A single protein band was observed after purification of Construct 33-C – 33-K, with molecular sizes of ~14, 29, 32, 39, 21, 19, 17, 21, and 19 kDa; respectively (Figure 1.2, Lanes 3-11). All truncated MSP1 C-terminal recombinant subunit proteins maintained native-like conformation based on binding with conformationally sensitive monoclonal antibodies. As examples, Construct 33-A, 33-B, and 33-C were reactive to MSP1-19 specific monoclonal antibody, mAb 5.2 [51], mAb 12.8, and mAb 2.2 [52] on immunoblots when prepared under non-reducing conditions. These same antibodies did not bind to the recombinant subunit proteins when prepared under reducing conditions as shown in Figure 1.3. By ELISA the conformationally dependent mAb 5.2 reacted equally well with all eleven constructs as with MSP1-42 (data not shown). This suggests that all constructs retained similar conformation as MSP1-42 with respect to the mAb 5.2 epitope.

Immunogenicity of the recombinant MSP1 C-terminal subunit proteins in mice

Secondary and tertiary sera from immunized Swiss Webster mice were tested for antibodies specific for MSP1-19 by ELISA. Responders were defined as having an ELISA O.D. of >0.2 at a 1/50 serum dilution. This value is greater than four-fold the O.D. values observed for pre-immune mouse sera. As shown in Figure 1.4A, the

percent responsiveness of the immunogens varied from a low of 30% to a high of 100% after two immunizations. In comparison, MSP1-19 had the lowest response rate (18%) of all the constructs. Analysis of the tertiary sera, however, revealed that the additional immunization was able to increase the number of responders for the majority of the constructs with the exception of Construct 33-C, Construct 33-K, and MSP1-19 (Figure 1.4A, black bars). Constructs 33-D – 33-I induced response rates similar or comparable to the full length MSP1-42 (Figure 1.4A).

The immunogenicity of the recombinant MSP1 C-terminal subunit proteins was also evaluated in terms of MSP1-19 specific antibody titers. In each of the antigen groups there were high and low responders (Figure 1.4B). High responders were defined as having an ELISA O.D. of >0.6 at a 1/1250 serum dilution. There were significant differences in antibody titers across the immunized groups (One-way ANOVA [$F(10, 133) = 2.345$, $p = 0.014$]). Construct 33-D which represents the largest of the N-terminally truncated constructs induced significantly higher antibody titers than all other truncated constructs (Tukey post-hoc comparison, $p<0.05$).

Regions of MSP1-33 influenced cytokine responses

Splenocytes of immunized mice were stimulated *in vitro* with the immunogens and analyzed by IL-4/IFN-γ ELISPOTS (Figure 1.5A and B). For the purpose of analysis, constructs were separated into two groups, Construct 33-A – 33-D and Constructs 33-E – 33-K, basing on the fact that the Construct group 33-E – 33-K does not contain T cell epitopes within the 31 amino acid sequence immediately N-terminal of the MSP1-19. Accordingly, Construct group 33-E – 33-K induced significantly higher levels of IFNγ than Construct group 33-A – 33-D (Logistic Regression for Repeated Measures, $p<0.05$). No significant difference between the two groups was observed for the production of IL-4. Thus, Constructs containing T cell epitopes within the 31 amino acid sequence induced a skewed TH2 response (Figure 1.5A); whereas, those

without this sequence induced a more balanced TH1/TH2 response (Figure 1.5B). Constructs 33-J and 33-K were not further studied since mouse data indicated that they had a low percent responsiveness and were only weakly immunogenic.

Immunogenicity of the recombinant MSP1 C-terminal subunit proteins in rabbits

Rabbit sera from quaternary bleeds were tested by ELISA for MSP1-19 and MSP1-42 specific antibodies. All nine constructs were able to induce an antibody response (Table 1.3). When antibody endpoint titers were analyzed among the nine MSP1 C-terminal constructs, Construct 33-C induced the highest mean antibody titers (geometric mean) against both MSP1-19 and MSP1-42; whereas, Construct 33-F induced the lowest mean antibody titers. Construct 33-D and 33-I had significantly lower mean antibody titers than MSP1-42 ($p=0.02$ and $p=0.0003$; respectively). In addition, Construct 33-I had significantly lower titers than Construct 33-C ($p=0.02$).

In vitro parasite growth inhibitory activity of recombinant MSP1 C-terminal subunit protein antibodies

The ability of the rabbit sera generated by immunizations with the recombinant MSP1 C-terminal subunit proteins formulated with ISA51 to inhibit parasite growth was evaluated using an *in vitro* assay [20,32,48,49]. Inhibition greater than 50% is considered to be biologically significant [19,53,54]. As shown in Table 1.3, there were constructs which induced no significant inhibitory antibodies in the immunized rabbits (Construct 33-C and 33-G). For other constructs, one or two of the three immunized animals produced significant levels of inhibitory antibodies (Construct 33-A, 33-B, 33-D, 33-E, 33-F, and 33-H). The positive control, full length recombinant MSP1-42, resulted in two out of three animals having significant levels of inhibitory antibodies. Construct 33-D and 33-I were the only two immunogens able to induce significant levels of inhibitory antibody in all three immunized animals (Table 1.3).

The ability of Construct 33-D and 33-I to induce inhibitory antibodies greater than 50% in rabbits were found to be significant as compared to other construct groups (Fisher Exact Test, two sided p-value = 0.0051) (Table 1.3). It is also important to emphasize that Construct 33-C failed to induce significant inhibitory antibodies, despite producing the highest mean antibody titers. On the other hand, anti-Construct 33-I antibodies had the highest mean percent parasite inhibition (76%) despite having ELISA titers that were at least one log lower than those produced by Construct 33-C and the full length MSP1-42 (p=0.02). To a lesser extent, Construct 33-D also induced significant parasite inhibition despite the fact that antibody titers were significantly lower than MSP1-42 (p=0.02).

Anti-Construct 33-C antibodies interferes with inhibitory anti-MSP1-42 antibodies

Non-inhibitory anti-Construct 33-C antibodies were tested for interfering/blocking effects on inhibitory MSP1-42 sera. The highly inhibitory MSP1-42 sera were obtained from previous vaccination studies in which rabbits were hyper-immunized with full length MSP1-42 emulsified in CFA [39]. The data in Table 4 demonstrates that when anti-MSP1-42 sera with high levels of inhibitory activity, were mixed with anti-Construct 33-C sera from two different rabbits (anti-Construct 33-C sera #1 and anti-Construct 33-C sera #2) the levels of parasite growth inhibition were reduced. MSP1-42 inhibitory serum #1 alone had an 86% inhibition of parasite growth. The addition of anti-Construct 33-C serum #1 to MSP1-42 inhibitory serum #1 decreased the parasite growth inhibition from 86% to 59%. The addition of anti-Construct 33-C serum #2 reduced growth inhibition from 86% to 73%. Similarly for MSP1-42 inhibitory serum #2, which alone inhibited parasite growth at 93%, the level of p parasite inhibition was reduced from 93% to 73% when anti-Construct 33-C serum #1 was added; and from 93% to 89% when anti-Construct 33-C serum #2 was added. The data also shows that anti-Construct 33-C serum #1 had higher

blocking/interfering activity than anti-Construct 33-C serum #2. Mixing of normal rabbit serum with the MSP1-42 inhibitory sera had negligible effects on parasite inhibition.

Discussion

The development of recombinant MSP1-based malaria vaccines to date has primarily focused on MSP1-42 and its C-terminal sub-fragment, MSP1-19. The main purpose of this study was to examine immune responses to the N-terminal sub-fragment of MSP1-42, MSP1-33, in order to better understand its relevance and potential in enhancing the immunogenicity of MSP1-42 based vaccines.

Previous studies have shown that MSP1-19 has limited ability to induce an antibody response in a genetically diverse host population [31,33]. This is thought to be due to the scarcity of T helper epitopes on MSP1-19 [29,31]. Although inclusion of additional heterologous T cell epitopes may overcome this limitation [55], such vaccines lack the advantage of priming cognate T cell help that can be recalled during natural infections. A number of T cell epitopes have been identified in the MSP1-33 fragment [28,29,30,56], and many of these epitopes were included in the eleven recombinant subunit constructs described here. Previous studies of these T cell epitopes have only focused on T cell proliferation and/or cytokine production from PBMC's collected from malaria immune individuals [28,29,30]. Whether these epitopes can provide functional "help" to enhance anti-MSP1-19 antibody responses has not been investigated.

Our results demonstrate that all truncated MSP1-33 fragments, when fused to MSP1-19, were able to broaden the antibody responsiveness to MSP1-19 in outbred mice as compared to MSP1-19 alone. However, the degree in broadening responsiveness varied among the different MSP1-33 fragments when fused to MSP1-19. A number of constructs were able to induce a generalized response (80% -100% response rate), which was comparable/equal to MSP1-42 (Figure 1.4A). This suggests that some of the T cell epitope regions on MSP1-33 of *P. falciparum* can provide adequate levels of helper function for the induction of antibodies in a genetically diverse population. A previous study with *P. yoelii* shows that MSP1-33

can provide help in the induction of anti-MSP1-19 antibodies [57]. However, this study only focused on Balb/c restricted haplotype and did not address the ability to broaden the response in a population of diverse MHC makeup. Our data provides for the first time, experimental validation of the long-held assumption that MSP1-33 possesses T helper epitopes that can enhance antibody responses specific for MSP1-19 in a genetically diverse population.

Aside from providing T helper functions, our studies indicate that the T cell epitope regions of MSP1-33 critically affected the quality of the anti-MSP1-19 responses. This linkage of T cell help to B cell specificity has been previously observed in a number of studies [35, 36, 37, 38] and more recently it has been extended to large protein molecules [58]. One measurement of the specificity of the anti-MSP1 antibody responses is their ability to inhibit parasite growth in vitro. Accordingly, inclusion of certain T cell epitope regions may contribute positively or negatively towards the induction of inhibitory antibodies. As examples, Construct 33-D and 33-I consistently induced high levels of parasite inhibitory antibodies; whereas, Construct 33-C failed to induce appreciable amount of inhibitory antibodies despite producing high antibody titers. This suggests that the T cell epitope regions in Construct 33-C were unable to focus antibody responses to inhibitory epitopes. The inhibitory antibody responses observed are due to anti-MSP1-19 antibodies since negligible anti-MSP1-33 antibodies were induced (data not shown). Furthermore, the antibodies induced by Construct 33-C interfered with the parasite inhibitory activity of anti-MSP1-42 antibodies (Table 1.4). The MSP1-33 specific T cell epitope regions also influenced the relative balance of TH1 versus TH2 responses. Inclusion of the 31 amino acid sequence from Construct 33-C in other MSP1 C-terminal constructs had a tendency to bias responses towards the TH2 arm (Figure 1.5). Thus, based on our antibody and ELISPOT analyses the T cell epitope regions contained in Construct 33-C would not be beneficial because of their tendency to

potentiate undesirable antibody and T cell responses. The negative effects of these T cell epitopes may be modulated by virtue of their relative dominance when presented with other MSP1-33 specific T cell epitopes in outbred populations, and this could be the situation observed with other constructs in our study. Since it is difficult to predict and/or anticipate the relative dominance of T cell epitopes in a genetically diverse population, it may be prudent to preemptively eliminate the 33-C specific T cell epitopes from vaccine design in order to avoid production of undesirable antibodies and T cell responses. Accordingly, constructs such as 33-A, 33-B, and 33-D may possibly be made more effective as an immunogen by eliminating the T cell epitope regions found in Construct 33-C. Along the same line, since the T cell epitopes within Construct 33-C and Construct 33-I are recognized by humans from malaria endemic populations [28,29,30], selective exclusion and/or inclusion of these epitopes from a MSP1-42 based vaccine would ensure boosting of only the desirable preexisting anti-MSP1 responses, which in turn may enhance overall vaccine efficacy.

Epidemiological studies have provided evidence that protective immunity afforded by MSP1 is dependent on the production of inhibitory antibodies [5,59,60,61,62]. However, other studies have argued the lack of correlation between anti-MSP1 inhibitory antibodies alone with malaria immunity [28,63,64] and protective anti-MSP1-19 response may involve other immune effector mechanisms such as Antibody Dependent Cell Cytotoxicity (ADCC), which involves Fc-dependent killing of parasites through neutrophils and macrophages [65,66]. It is important to point out that although the present study demonstrated the influence of MSP1-33 specific T cell epitopes on the induction of parasite inhibitory antibodies, it is possible that these T cell epitopes may have a broader influence on the development of other protective anti-MSP1-42 immune effector responses.

Recently, a prime-boost immunization regimen utilizing simian adenoviral and poxviral vectors expressing four N-terminal conserved blocks of MSP1 fused with

both dimorphic forms of MSP1-42 was reported as a new candidate malaria vaccine [67]. These vaccines were found to induce high antibody titers against MSP1 and have high growth inhibitory activities [67]. The study did not examine the contribution of MSP1-42 specific T cell epitopes to the development of inhibitory antibodies. Further, since the N-terminal regions (Blocks 1, 3, 5, 12) are physically separated from MSP1-42 during merozoite development and invasion it may be difficult for these regions to provide cognate help in inducing or boosting antibody responses to MSP1-19. Previous studies have also utilized non-MSP1 derived T cell epitopes in conjunction with the MSP1-19 immunogen to overcome genetic restrictions of MSP1-19 induced protection [55]. The addition of these non-MSP1 T cell epitopes shows an impact on antibody subclass and protective efficacy [55]. However, these epitopes will not be able to boost anti-MSP1-19 antibodies during natural infections. The strategy of selective inclusion of MSP1-33 T cell epitopes has the potential advantage of boosting existing immunity to MSP1-42/MSP1-19 via cognate T cell help in malaria exposed populations.

The results presented here provide a fresh glimpse on the manner by which anti-MSP1-19 antibody response may be modulated during natural infections when a selected MSP1-42 specific T cell epitopes are presented. As example, dominant recognition of T cell epitopes within Construct 33-C in malaria-exposed individuals may skew responses toward the development of non-inhibitory and/or interfering types of antibodies. It is tempting to speculate that deployment of a full length MSP1-42 vaccine under this setting may not be able to potentiate the level(s) of protective immunity and specificity as has been observed with immunizations in naive animal models [17,18,19,20]. Moreover, our results may also help explain the lack of efficacy in a recent MSP1-42 clinical trial in malaria endemic areas.

An important outcome of this study is the identification of a more efficacious MSP1 vaccine than the current full length MSP1-42; namely, Construct 33-I.

Construct 33-I, along with Construct 33-D, were the only two immunogens able to induce significant parasite growth inhibitory antibodies (>50%) in all immunized rabbits; whereas all other vaccine groups including MSP1-42 failed to do so. Importantly for Construct 33-I, the levels of parasite inhibition were achieved at much lower antibody titers than what were induced by MSP1-42. The prevailing view of an efficacious MSP1-42 vaccine is the requirement of high antibody titers needed for in vivo protection or in vitro parasite inhibition. This would necessitate the use of powerful adjuvants to achieve the desired immunogenicity. Our data with Construct 33-I indicates that this MSP1 C-terminal subunit vaccine can induce potent anti-parasite antibodies at a much lower overall antibody response. This would eliminate the prerequisite for strong adjuvants for its deployment as a human malaria vaccine. An equally attractive attribute of Construct 33-I is the sequence compositions of T cell epitopes. First, the MSP1-33 specific T cell epitopes in this construct are based entirely of conserved sequences, thereby circumventing the potential complications of allelic variations. Second, computer algorithm analyses of the T cell epitope sequences revealed a promiscuous binding to all major HLA Class II molecules (Figure 1.6), suggesting a potential broad immune responsiveness that this vaccine can elicit in humans. The superior immunological characteristics that Construct 33-I has over MSP1-42 strongly justify further evaluations as a second generation MSP1-42 based human malaria vaccine. To further validate the vaccine candidacy of Construct 33-D and 33-I, it would be necessary to perform immunogenicity and efficacy studies in non-human primate models. Equally important is to evaluate whether the T cell epitope regions defined by Construct 33-D and 33-I are immunogenic in malaria exposed human populations; and whether human T cells specific for these epitopes will be able to provide necessary helper functions for the induction of protective antibodies.

Acknowledgements

We would like to thank James Senda and Bo Liu for their help in the transformation and culture of *Drosophila* S2 cells expressing the recombinant MSP1 C-terminal subunit proteins. Mazie Tsang and Natasha Cortez for their help in the isolation and purification of the recombinant MSP1 C-terminal subunit proteins. We would also like to thank Dr. Jim Davis of the RMATRIX for his help with the statistical analysis of the data.

References

1. Holder AA, Guevara Patino JA, Uthaipibull C, Syed SE, Ling IT, et al. (1999) Merozoite surface protein 1, immune evasion, and vaccines against asexual blood stage malaria. Parassitologia 41: 409-414.
2. Holder AA, Freeman RR (1984) The three major antigens on the surface of Plasmodium falciparum merozoites are derived from a single high molecular weight precursor. J Exp Med 160: 624-629.
3. Holder AA, Lockyer MJ, Odink KG, Sandhu JS, Riveros-Moreno V, et al. (1985) Primary structure of the precursor to the three major surface antigens of Plasmodium falciparum merozoites. Nature 317: 270-273.
4. Blackman MJ, Ling IT, Nicholls SC, Holder AA (1991) Proteolytic processing of the Plasmodium falciparum merozoite surface protein-1 produces a membrane-bound fragment containing two epidermal growth factor-like domains. Mol Biochem Parasitol 49: 29-33.
5. al-Yaman F, Genton B, Kramer KJ, Chang SP, Hui GS, et al. (1996) Assessment of the role of naturally acquired antibody levels to Plasmodium falciparum merozoite surface protein-1 in protecting Papua New Guinean children from malaria morbidity. Am J Trop Med Hyg 54: 443-448.
6. John CC, O'Donnell RA, Sumba PO, Moormann AM, de Koning-Ward TF, et al. (2004) Evidence that invasion-inhibitory antibodies specific for the 19-kDa fragment of merozoite surface protein-1 (MSP-1 19) can play a protective role against blood-stage Plasmodium falciparum infection in individuals in a malaria endemic area of Africa. J Immunol 173: 666-672.
7. Perraut R, Marrama L, Diouf B, Sokhna C, Tall A, et al. (2005) Antibodies to the conserved C-terminal domain of the Plasmodium falciparum merozoite surface protein 1 and to the merozoite extract and their relationship with in vitro

inhibitory antibodies and protection against clinical malaria in a Senegalese village. J Infect Dis 191: 264-271.

8. Egan AF, Blackman MJ, Kaslow DC (2000) Vaccine efficacy of recombinant Plasmodium falciparum merozoite surface protein 1 in malaria-naive, -exposed, and/or -rechallenged Aotus vociferans monkeys. Infect Immun 68: 1418-1427.
9. Egan AF, Burghaus P, Druilhe P, Holder AA, Riley EM (1999) Human antibodies to the 19kDa C-terminal fragment of Plasmodium falciparum merozoite surface protein 1 inhibit parasite growth in vitro. Parasite Immunol 21: 133-139.
10. Daly TM, Long CA (1995) Humoral response to a carboxyl-terminal region of the merozoite surface protein-1 plays a predominant role in controlling blood-stage infection in rodent malaria. J Immunol 155: 236-243.
11. Eslava I, Payares G, Pernia BM, Holder AA, Spencer LM (2010) Suppressive and additive effects in protection mediated by combinations of monoclonal antibodies specific for merozoite surface protein 1 of Plasmodium yoelii. Malar J 9: 46.
12. Spencer Valero LM, Ogun SA, Fleck SL, Ling IT, Scott-Finnigan TJ, et al. (1998) Passive immunization with antibodies against three distinct epitopes on Plasmodium yoelii merozoite surface protein 1 suppresses parasitemia. Infect Immun 66: 3925-3930.
13. McKean PG, O'Dea K, Brown KN (1993) Nucleotide sequence analysis and epitope mapping of the merozoite surface protein 1 from Plasmodium chabaudi chabaudi AS. Mol Biochem Parasitol 62: 199-209.
14. Burns JM, Jr., Parke LA, Daly TM, Cavacini LA, Weidanz WP, et al. (1989) A protective monoclonal antibody recognizes a variant-specific epitope in the precursor of the major merozoite surface antigen of the rodent malarial parasite Plasmodium yoelii. J Immunol 142: 2835-2840.

15. Burns JM, Jr., Daly TM, Vaidya AB, Long CA (1988) The 3' portion of the gene for a Plasmodium yoelii merozoite surface antigen encodes the epitope recognized by a protective monoclonal antibody. Proc Natl Acad Sci U S A 85: 602-606.

16. Guevara Patino JA, Holder AA, McBride JS, Blackman MJ (1997) Antibodies that inhibit malaria merozoite surface protein-1 processing and erythrocyte invasion are blocked by naturally acquired human antibodies. J Exp Med 186: 1689-1699.

17. Singh S, Miura K, Zhou H, Muratova O, Keegan B, et al. (2006) Immunity to recombinant plasmodium falciparum merozoite surface protein 1 (MSP1): protection in Aotus nancymai monkeys strongly correlates with anti-MSP1 antibody titer and in vitro parasite-inhibitory activity. Infect Immun 74: 4573-4580.

18. Kumar S, Collins W, Egan A, Yadava A, Garraud O, et al. (2000) Immunogenicity and efficacy in aotus monkeys of four recombinant Plasmodium falciparum vaccines in multiple adjuvant formulations based on the 19-kilodalton C terminus of merozoite surface protein 1. Infect Immun 68: 2215-2223.

19. Chang SP, Case SE, Gosnell WL, Hashimoto A, Kramer KJ, et al. (1996) A recombinant baculovirus 42-kilodalton C-terminal fragment of Plasmodium falciparum merozoite surface protein 1 protects Aotus monkeys against malaria. Infect Immun 64: 253-261.

20. Stowers AW, Cioce V, Shimp RL, Lawson M, Hui G, et al. (2001) Efficacy of two alternate vaccines based on Plasmodium falciparum merozoite surface protein 1 in an Aotus challenge trial. Infect Immun 69: 1536-1546.

21. Hirunpetcharat C, Tian JH, Kaslow DC, van Rooijen N, Kumar S, et al. (1997) Complete protective immunity induced in mice by immunization with the 19-kilodalton carboxyl-terminal fragment of the merozoite surface protein-1

(MSP1[19]) of Plasmodium yoelii expressed in Saccharomyces cerevisiae: correlation of protection with antigen-specific antibody titer, but not with effector CD4+ T cells. J Immunol 159: 3400-3411.

22. Ogutu BR, Apollo OJ, McKinney D, Okoth W, Siangla J, et al. (2009) Blood stage malaria vaccine eliciting high antigen-specific antibody concentrations confers no protection to young children in Western Kenya. PLoS One 4: e4708.
23. Angov E, Bergman-Leitner ES, Duncan EH, Brent-Kirk A, McCasland M, et al. (2007) Measurement of antibody fine specificities induced by malaria vaccine FMP1/ASO2A from a pediatric phase 2B trial in western Kenya. . American Journal of Tropical Medicine and Hygiene 77 Abstract 12.
24. Malkin E, Long CA, Stowers AW, Zou L, Singh S, et al. (2007) Phase 1 study of two merozoite surface protein 1 (MSP1(42)) vaccines for Plasmodium falciparum malaria. PLoS Clin Trials 2: e12.
25. Ellis RD, Martin LB, Shaffer D, Long CA, Miura K, et al. (2010) Phase 1 trial of the Plasmodium falciparum blood stage vaccine MSP1(42)-C1/Alhydrogel with and without CPG 7909 in malaria naive adults. PLoS One 5: e8787.
26. Stoute JA, Gombe J, Withers MR, Siangla J, McKinney D, et al. (2007) Phase 1 randomized double-blind safety and immunogenicity trial of Plasmodium falciparum malaria merozoite surface protein FMP1 vaccine, adjuvanted with AS02A, in adults in western Kenya. Vaccine 25: 176-184.
27. Lee EA, Flanagan KL, Minigo G, Reece WH, Bailey R, et al. (2006) Dimorphic Plasmodium falciparum merozoite surface protein-1 epitopes turn off memory T cells and interfere with T cell priming. Eur J Immunol 36: 1168-1178.
28. Lee EA, Flanagan KL, Odhiambo K, Reece WH, Potter C, et al. (2001) Identification of frequently recognized dimorphic T-cell epitopes in plasmodium falciparum merozoite surface protein-1 in West and East

Africans: lack of correlation of immune recognition and allelic prevalence. Am J Trop Med Hyg 64: 194-203.

29. Udhayakumar V, Anyona D, Kariuki S, Shi YP, Bloland PB, et al. (1995) Identification of T and B cell epitopes recognized by humans in the C-terminal 42-kDa domain of the Plasmodium falciparum merozoite surface protein (MSP)-1. J Immunol 154: 6022-6030.

30. Malhotra I, Wamachi AN, Mungai PL, Mzungu E, Koech D, et al. (2008) Fine specificity of neonatal lymphocytes to an abundant malaria blood-stage antigen: epitope mapping of Plasmodium falciparum MSP1(33). J Immunol 180: 3383-3390.

31. Tian JH, Miller LH, Kaslow DC, Ahlers J, Good MF, et al. (1996) Genetic regulation of protective immune response in congenic strains of mice vaccinated with a subunit malaria vaccine. J Immunol 157: 1176-1183.

32. Hui GS, Gosnell WL, Case SE, Hashiro C, Nikaido C, et al. (1994) Immunogenicity of the C-terminal 19-kDa fragment of the Plasmodium falciparum merozoite surface protein 1 (MSP1), YMSP1(19) expressed in S. cerevisiae. J Immunol 153: 2544-2553.

33. Stanisic DI, Martin LB, Good MF (2003) The role of the 19-kDa region of merozoite surface protein 1 and whole-parasite-specific maternal antibodies in directing neonatal pups' responses to rodent malaria infection. J Immunol 171: 5461-5469.

34. Tian JH, Good MF, Hirunpetcharat C, Kumar S, Ling IT, et al. (1998) Definition of T cell epitopes within the 19 kDa carboxylterminal fragment of Plasmodium yoelii merozoite surface protein 1 (MSP1(19)) and their role in immunity to malaria. Parasite Immunol 20: 263-278.

35. Datta SK (1998) Production of pathogenic antibodies: cognate interactions between autoimmune T and B cells. Lupus 7: 591-596.

36. Milich DR (1988) T- and B-cell recognition of hepatitis B viral antigens. Immunol Today 9: 380-386.

37. Milich DR, McLachlan A, Moriarty A, Thornton GB (1987) A single 10-residue pre-S(1) peptide can prime T cell help for antibody production to multiple epitopes within the pre-S(1), pre-S(2), and S regions of HBsAg. J Immunol 138: 4457-4465.

38. Lanzavecchia A (1985) Antigen-specific interaction between T and B cells. Nature 314: 537-539.

39. Hui G, Hashimoto C (2007) Plasmodium falciparum anti-MSP1-19 antibodies induced by MSP1-42 and MSP1-19 based vaccines differed in specificity and parasite growth inhibition in terms of recognition of conserved versus variant epitopes. Vaccine 25: 948-956.

40. Chang SP, Hui GS, Kato A, Siddiqui WA (1989) Generalized immunological recognition of the major merozoite surface antigen (gp195) of Plasmodium falciparum. Proc Natl Acad Sci U S A 86: 6343-6347.

41. Yuen D, Leung WH, Cheung R, Hashimoto C, Ng SF, et al. (2007) Antigenicity and immunogenicity of the N-terminal 33-kDa processing fragment of the Plasmodium falciparum merozoite surface protein 1, MSP1: implications for vaccine development. Vaccine 25: 490-499.

42. Schneider I (1972) Cell lines derived from late embryonic stages of Drosophila melanogaster. J Embryol Exp Morphol 27: 353-365.

43. Culp JS, Johansen H, Hellmig B, Beck J, Matthews TJ, et al. (1991) Regulated expression allows high level production and secretion of HIV-1 gp120 envelope glycoprotein in Drosophila Schneider cells. Biotechnology (N Y) 9: 173-177.

44. Singh H, Raghava GP (2001) ProPred: prediction of HLA-DR binding sites. Bioinformatics 17: 1236-1237.

45. Chang SP, Gibson HL, Lee-Ng CT, Barr PJ, Hui GS (1992) A carboxyl-terminal fragment of Plasmodium falciparum gp195 expressed by a recombinant baculovirus induces antibodies that completely inhibit parasite growth. J Immunol 149: 548-555.

46. Hui GS, Hashimoto AC, Nikaido CM, Choi J, Chang SP (1994) Induction of antibodies to the Plasmodium falciparum merozoite surface protein-1 (MSP1) by cross-priming with heterologous MSP1s. J Immunol 153: 1195-1201.

47. Hui G, Hashimoto C (2007) The requirement of CD80, CD86, and ICAM-1 on the ability of adjuvant formulations to potentiate antibody responses to a Plasmodium falciparum blood-stage vaccine. Vaccine 25: 8549-8556.

48. Leung WH, Meng ZQ, Hui G, Ho WK (2004) Expression of an immunologically reactive merozoite surface protein (MSP-1(42)) in E. coli. Biochim Biophys Acta 1675: 62-70.

49. Pang AL, Hashimoto CN, Tam LQ, Meng ZQ, Hui GS, et al. (2002) In vivo expression and immunological studies of the 42-kilodalton carboxyl-terminal processing fragment of Plasmodium falciparum merozoite surface protein 1 in the baculovirus-silkworm system. Infect Immun 70: 2772-2779.

50. Nagata M, Wong T, Clements D, Hui G (2007) Plasmodium falciparum: immunization with MSP1-42 induced non-inhibitory antibodies that have no blocking activities but enhanced the potency of inhibitory anti-MSP1-42 antibodies. Exp Parasitol 115: 403-408.

51. Siddiqui WA, Tam LQ, Kramer KJ, Hui GS, Case SE, et al. (1987) Merozoite surface coat precursor protein completely protects Aotus monkeys against Plasmodium falciparum malaria. Proc Natl Acad Sci U S A 84: 3014-3018.

52. McBride JS, Heidrich HG (1987) Fragments of the polymorphic Mr 185,000 glycoprotein from the surface of isolated Plasmodium falciparum merozoites form an antigenic complex. Mol Biochem Parasitol 23: 71-84.

53. Hui G, Choe D, Hashimoto C (2008) Biological activities of anti-merozoite surface protein-1 antibodies induced by adjuvant-assisted immunizations in mice with different immune gene knockouts. Clin Vaccine Immunol 15: 1145-1150.

54. Hui GS, Siddiqui WA (1987) Serum from Pf195 protected Aotus monkeys inhibit Plasmodium falciparum growth in vitro. Exp Parasitol 64: 519-522.

55. Ahlborg N, Ling IT, Holder AA, Riley EM (2000) Linkage of exogenous T-cell epitopes to the 19-kilodalton region of Plasmodium yoelii merozoite surface protein 1 (MSP1(19)) can enhance protective immunity against malaria and modulate the immunoglobulin subclass response to MSP1(19). Infect Immun 68: 2102-2109.

56. Wipasa J, Hirunpetcharat C, Mahakunkijcharoen Y, Xu H, Elliott S, et al. (2002) Identification of T cell epitopes on the 33-kDa fragment of Plasmodium yoelii merozoite surface protein 1 and their antibody-independent protective role in immunity to blood stage malaria. J Immunol 169: 944-951.

57. Draper SJ, Goodman AL, Biswas S, Forbes EK, Moore AC, et al. (2009) Recombinant viral vaccines expressing merozoite surface protein-1 induce antibody- and T cell-mediated multistage protection against malaria. Cell Host Microbe 5: 95-105.

58. Sette A, Moutaftsi M, Moyron-Quiroz J, McCausland MM, Davies DH, et al. (2008) Selective CD4+ T cell help for antibody responses to a large viral pathogen: deterministic linkage of specificities. Immunity 28: 847-858.

59. Egan AF, Burghaus P, Druilhe P, Holder AA, Riley EM (1999) Human antibodies to the 19kDa C-terminal fragment of Plasmodium falciparum merozoite surface protein 1 inhibit parasite growth in vitro. Parasite Immunology 21: 133-139.

60. O'Donnell RA, Koning-Ward TF, Burt RA, Bockarie M, Reeder JC, et al. (2001) Antibodies against merozoite surface protein (MSP)-1(19) are a major

component of the invasion-inhibitory response in individuals immune to malaria. Journal of Experimental Medicine 193: 1403-1412.

61. Perraut R, Marrama L, Diouf B, Sokhna C, Tall A, et al. (2005) Antibodies to the conserved C-terminal domain of the Plasmodium falciparum merozoite surface protein 1 and to the merozoite extract and their relationship with in vitro inhibitory antibodies and protection against clinical malaria in a Senegalese village. Journal of Infectious Diseases 191: 264-271.
62. John CC, O'Donnell RA, Sumba PO, Moormann AM, Koning-Ward TF, et al. (2004) Evidence that invasion-inhibitory antibodies specific for the 19-kDa fragment of merozoite surface protein-1 (MSP-1 19) can play a protective role against blood-stage Plasmodium falciparum infection in individuals in a malaria endemic area of Africa. The Journal of Immunology 173: 666-672.
63. Murhandarwati EE, Wang L, Black CG, Nhan DH, Richie TL, et al. (2009) Inhibitory antibodies specific for the 19-kilodalton fragment of merozoite surface protein 1 do not correlate with delayed appearance of infection with Plasmodium falciparum in semi-immune individuals in Vietnam. Infect Immun 77: 4510-4517.
64. Murhandarwati EE, Wang L, de Silva HD, Ma C, Plebanski M, et al. (2010) Growth-inhibitory antibodies are not necessary for protective immunity to malaria infection. Infect Immun 78: 680-687.
65. McIntosh RS, Shi J, Jennings RM, Chappel JC, de Koning-Ward TF, et al. (2007) The importance of human FcgammaRI in mediating protection to malaria. PLoS Pathog 3: e72.
66. Bouharoun-Tayoun H, Oeuvray C, Lunel F, Druilhe P (1995) Mechanisms underlying the monocyte-mediated antibody-dependent killing of Plasmodium falciparum asexual blood stages. J Exp Med 182: 409-418.

67. Goodman AL, Epp C, Moss D, Holder AA, Wilson JM, et al. (2010) New candidate vaccines against blood-stage Plasmodium falciparum malaria: prime-boost immunization regimens incorporating human and simian adenoviral vectors and poxviral vectors expressing an optimized antigen based on merozoite surface protein 1. Infect Immun 78: 4601-4612.

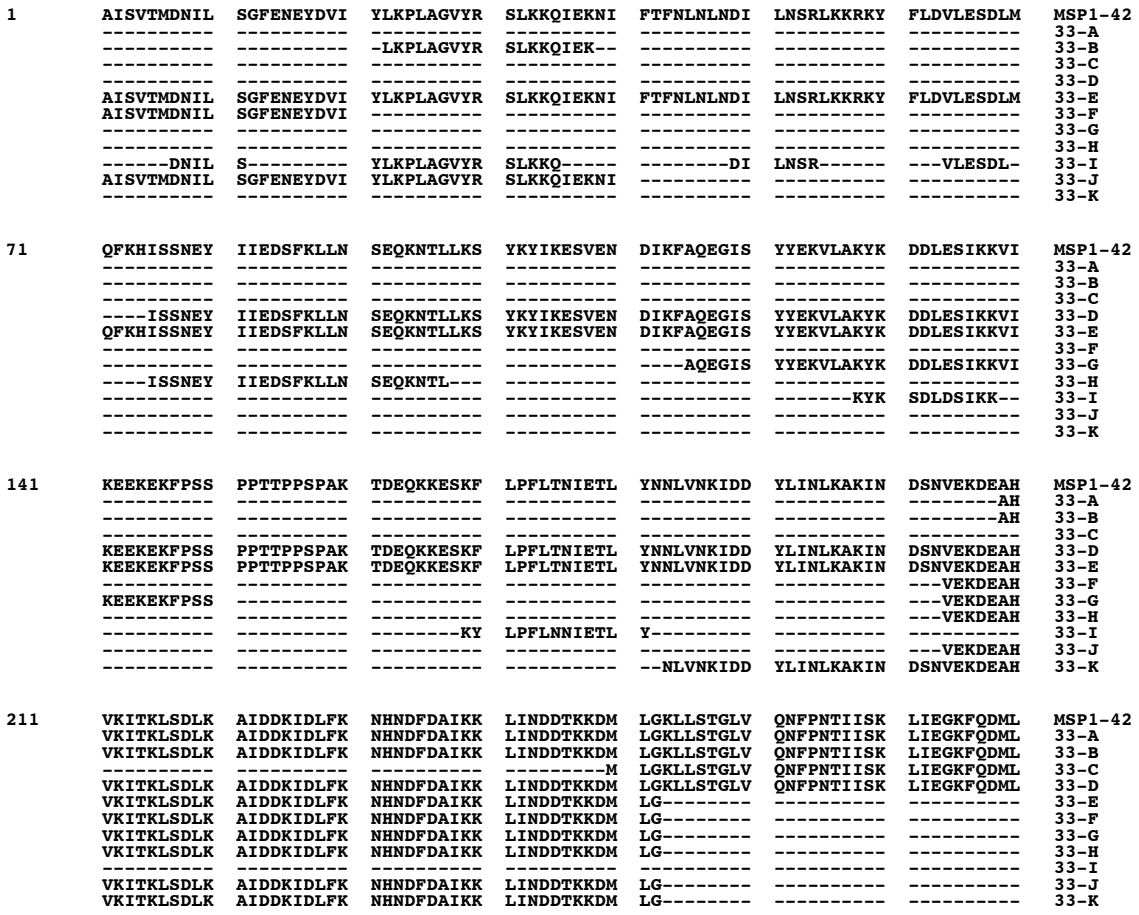

Figure 1.1 Aligned amino acid sequences of the eleven MSP1 C-terminal subunit protein constructs compared to MSP1-42. All constructs contain the MSP1-19 fragment (not shown) at the C-terminal end.

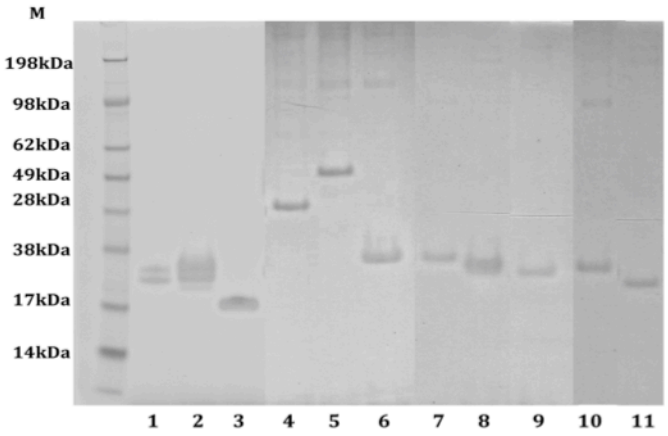

Figure 1.2 SDS-PAGE of the eleven purified S2 cell expressed recombinant MSP1 C-terminal subunit proteins. Expected molecular sizes of each construct are in parenthesis. Lane 1: Construct 33-A (19kDa); Lane 2: Construct 33-B (21kDa); Lane 3: Construct 33-C (14kDa); Lane 4: Construct 33-D (29kDa); Lane 5: Construct 33-E (32kDa); Lane 6: Construct 33-F (39kDa); Lane 7: Construct 33-G (21kDa); Lane 8: Construct 33-H (19kDa); Lane 9: Construct 33-I (17kDa); Lane 10: Construct 33-J (21kDa); Lane 11: Construct 33-K (19kDa).

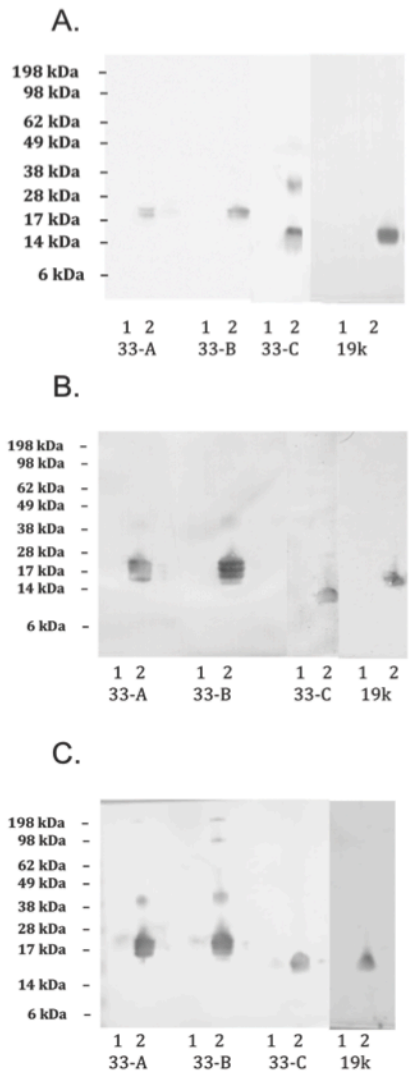

Figure 1.3 MSP1 C-terminal subunit proteins posses disulfide sensitive conformation. Immunoblots of recombinant proteins separated under reducing (lanes 1) and non-reducing (lanes 2) conditions and probed with conformational sensitive anti-MSP1-19 monoclonal antibodies. Panel A: Construct 33-A – 33-C and MSP1-19 probed with mAb 12.8; Panel B: Constructs 33-A – 33-C and MSP1-19 probed with mAb 2.2; and Panel C: Constructs 33-A – 33-C and MSP1-19 probed with mAb 5.2 [47,48].

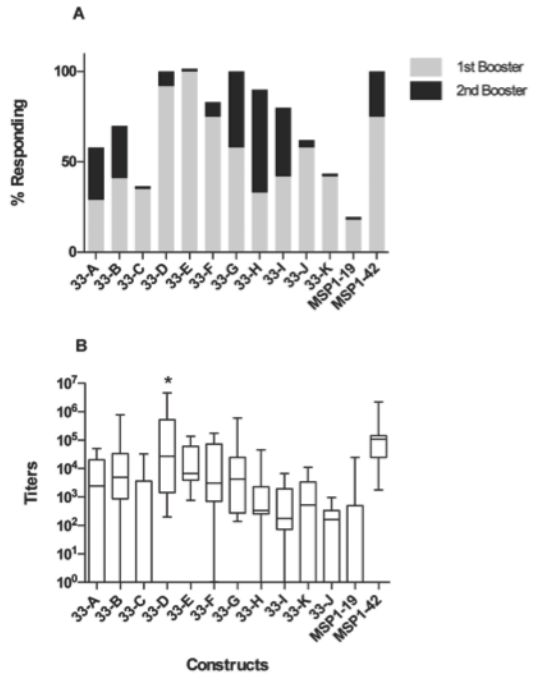

Figure 1.4 ELISA antibody responses against MSP1-19 in Swiss Webster mice immunized with recombinant MSP1 C-terminal proteins. Panel A, percent responsiveness of mice immunized with Constructs 33-A – 33-K after the first booster injection (grey) and after the second booster injection (black). Panel B, antibody titers of mice vaccinated with Constructs 33-A – 33-K. Results of tertiary bleeds are shown. Horizontal bars indicate mean antibody titers. ANOVA ($p<0.05$) indicated that the levels of antibody titers differed among groups. Asterisk indicates a significant difference (Turkey post-hoc test, $p<0.05$) between Construct 33-D and all other vaccination groups.

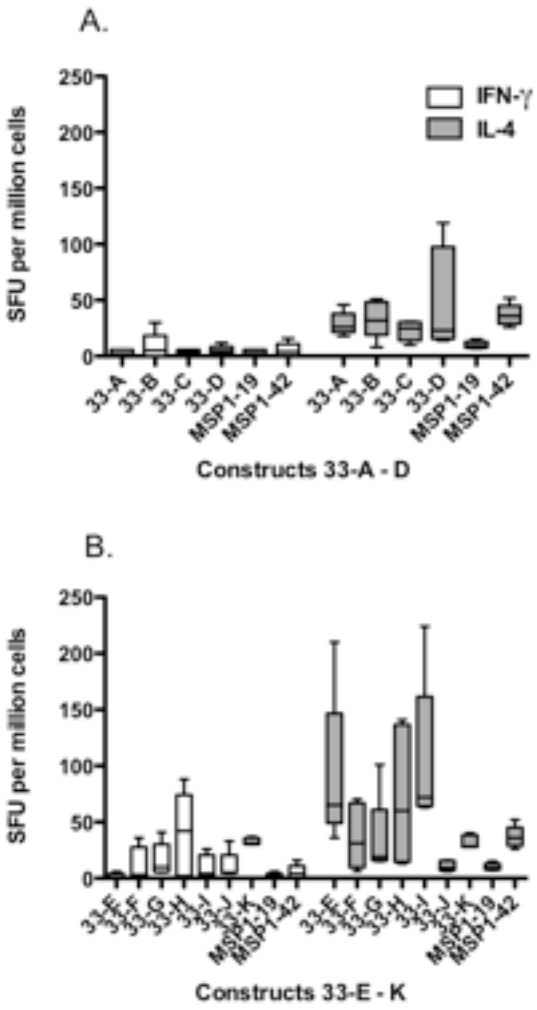

Figure 1.5 Induction of MSP1-specific IL-4 (grey bars) and IFN-γ (white bars) responses, as determined by ELISPOT, in mice immunized with recombinant MSP1 C—terminal proteins. Panel A: Constructs 33-A – 33-D; Panel B: Constructs 33-E – 33-K. Horizontal bars indicate mean SFU. Logistic Regression for Repeated Measures indicated that IFNγ levels were significantly higher ($p<0.05$) in Construct 33-E – 33-K compared to Construct 33-A – 33-D. No significant difference was found when comparing IL-4 levels. Mouse splenocytes were harvested 21 days after the last immunization.

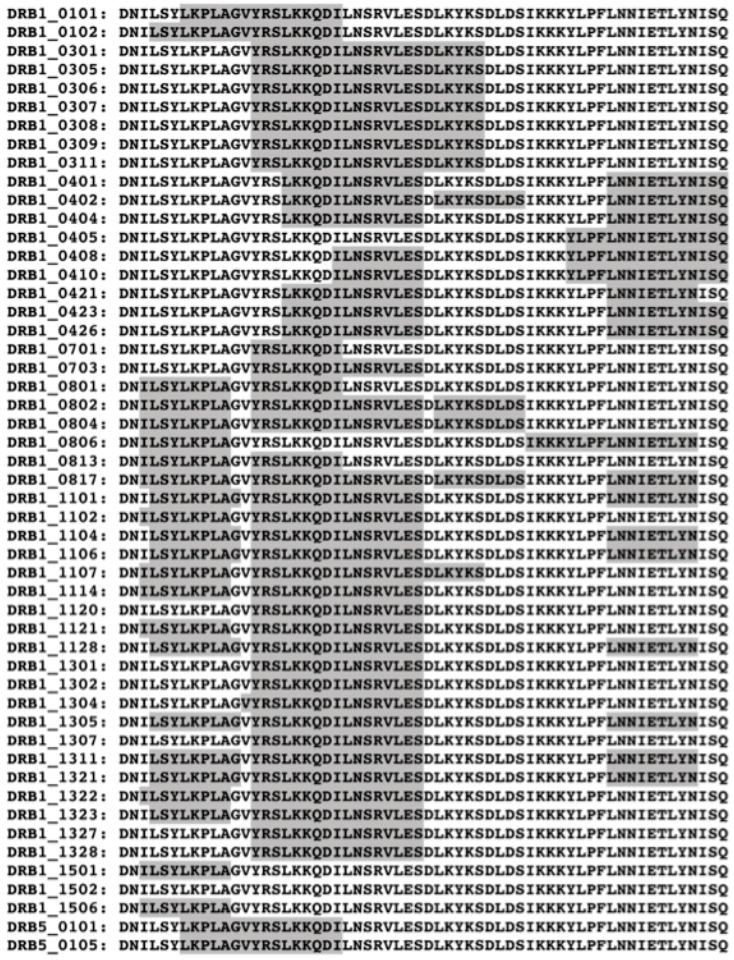

Figure 1.6 Class II epitope prediction of the sequence of Construct 33-I by computer algorithm (Propred). Grey shaded sequences represent motifs that may bind to Class II molecules.

Table 1.1 Sequence and location of previously identified and predicted T cell epitopes in truncated Constructs 33-A - 33-K

	MSP1-33 Amino Acid Position N-base #	Amino Acid Sequence
	Identified T cell epitopes	
1	3-19	SVTMDNILSGFENEYDV
2	22-38	LKPLAGVYRSLKKQIEK
3	37-54	EKNIFTFNLNLNDILNSR
4	81-95	IIEDSFKLLNSEQKN
5	118-134	GISYYEKVLAKYKDDLE
6	127-145	AKYKDDLESIKKVIKEEKE
7	175-191	TNIETLYNNLVNKIDDY
8	190-202	DYLINLKAKINDS
9	210-223	HVKITKLSDLKAID
10	225-244	KIDLFKNHNDFDAIKKLIND
11	252-270	GKLLSTGLVQNFPNTIISK
12	257-275	TGLVQNFPNTIISKLIEGK
13	263-275	FPNTIISKLIEGKFQDML
	Predicted T cell epitopes	
14	22-30	LKPLAGVYR
15	69, 128-135	LKYKSDLDS
16	170-178	YLPFLNNIE
17	9-11, 21-26	ILSYLKPLA
18	29-35, 49-50	YRSLKKQDI
19	174-181	LNNIETLY
20	32-35, 49-53	LKKQDILNS
21	65-69, 128-131	LESDLKYKS
22	177-181	IETLY
23	50-54, 64-67	ILNSRVLES
24	19-37	VIYLKPLAGVYRSLKKQIE
25	43-56	FNLNLNDILNSRLK
26	69-85	LMQFKHISSNEYIIEDS
27	170-189	FLPFLTNIETLYNNLVNKID
28	180-201	LYNNLVNKIDDYLINLKAKIND

Table 1.2 Primer Sequences for the Construction of Recombinant MSP1 C-terminal Constructs

Construct	MSP1-33 (Amino Acid Position, N ➔ C)	Primers/Oligonucleotides
33-A	209-280	F: acgtacggatccgttggcggtggtaccGCACATGTTAAAATAACTAAAC
		R: agtacaatctcgagttactaACTGCAGAAAATACCATCGAAAAGTG
33-B	22-38	F: aaagttggcggtggtaccGCACATGTTAAAATAACTAAAC
		R: agtacaatctcgagttactaACTGCAGAAAATACCATCGAAAAGTG
	209-280	F: acgtacggatccgttggcggtggtaccGCACATGTTAAAATAACTAAAC
		R: agtacaatctcgagttactaACTGCAGAAAATACCATCGAAAAGTG
33-C	250-280	F: acgtacggatccgttggcggtggtaccATGCTTGGCAAATTACTTAG
		R: agtacaatctcgagttactaACTGCAGAAAATACCATCGAAAAGTG
33-D	76-280	F: tagcggatccACACTTTTAAAAAGTTACAAA
		R: agtacaatctcgagttactaACTGCAGAAAATACCATCGAAAAGTG
33-E	1-252	F: gtcgactagtatgGCAATATCTGTCACAATGGAT
		R: gctacggccatggcggcggcggcggTTCGTATAGAAAAAAGCA
33-F	1-20	F: actagtatgGCAATATCTGTCACAATGGATAATATCCTCTCAGGAT TTGAAAATGAATATGATGTTATAggcggcggc
		R:ctaggcggcggcggATATTGTAGTATAAGTAAAAGTTTAGGACTCT CCTATAATAGGTAACACTGTCTATAACGGTAT
	204-252	F: atcgactagtggcggcggcggatccggcGTTGAAAAAGATGAAGCACAT
		R: gctacggccatggcggcggcggcggTTCGTATAGAAAAAAGCA
33-G	115-150	F: gtcgactagtatgGCACAGGAAGGTATAAGTTAT
		R: gctacggcctaggcggcggcggACTACTACCCTTGAAGAGGAA
	204-252	F: atcgactagtggcggcggcggatccggcGTTGAAAAAGATGAAGCACAT
		R: gctacggccatggcggcggcggcggTTCGTATAGAAAAAAGCA
33-H	75-97	F:CTAGTATGATATCCTCAAATGAATACATTATTGAAGATTCATTT AAATTATTGAATTCAGAACAAAAAAACACACTTGGCGGCGGCG
		R:ctaggTTCACACAAAAAAACAAGACTTAAGTTATTAAATTTACTT AGAAGTTATTACATAAGTAAACTCCTATA
	204-252	F: atcgactagtggcggcggcggatccggcGTTGAAAAAGATGAAGCACAT
		R: gctacggccatggcggcggcggcggTTCGTATAGAAAAAAGCA
33-I	7-11	GATAATATCCTCTCA
	21-36	TATTTAAAACCCTTTAGCTGGAGTATATAGAAGCTTAAAAAAACAAATT
	51-55	TTAAATTCACGTCTT
	64-69	GTATTAGAATCTGATTTA
	128-137	AAATATAAGGATGATTTAGAATCAATTAAA
	159-180	GCAAAAACAGACGAACAAAAGAAGGAAAGTAAGTTCCTTCCATT TTTAACAAACATTGAGACCTTA
33-J	1-40	F:actagtatgGCAATATCTGTCACAATGGATAATATCCTCTCAGGATT TGAAAATGAATATGATGTTATA
		R: gctacggcctaggcggcggcggTACAAAAAAAGTTAAACAAAA
	204-252	F: atcgactagtggcggcggcggatccggcGTTGAAAAAGATGAAGCACAT
		R: gctacggccatggcggcggcggcggTTCGTATAGAAAAAAGCA
33-K	183-252	F: actagtatgAACTTAGTTAATAAAATTGACGATTACTTAATT
		R: gctacggccatggcggcggcggcggTTCGTATAGAAAAAAGCA

Table 1.3 In vitro Parasite Growth Inhibition of Rabbit Antibodies Generated by Recombinant MSP1 C-terminal Subunit Proteins

Rabbit Sera (4th Bleeds)		% Parasite Growth Inhibition[a]	Reciprocal ELISA Antibody Titers			
			MSP1-42	Mean (Rbt#1-3±SD) [b]	MSP1-19	Mean (Rbt#1-3±SD) [b]
Anti-33-A[d]	Rbt #1	75%	624,000	482,000±131,538	93,000	43,000±37,233
	Rbt #2	37%	361,000		23,000	
	Rbt #3	24%	498,000		36,000	
Anti-33-B	Rbt #1	66%	27,000	101,000±109,610	161,000	139,000±20,133
	Rbt #2	26%	156,000		137,000	
	Rbt #3	0%	245,000		121,000	
Anti-33-C	Rbt #1	10%	2,490,000	1,440,000±814,338	254,000	365,000±122,111
	Rbt #2	32%	948,000		385,000	
	Rbt #3	22%	1,265,000		498,000	
Anti-33-D[c]	Rbt #1	58%	93,000	218,000±450,617	43,000	146,000±269,367
	Rbt #2	58%	125,000		133,000	
	Rbt #3	94%	889,000		548,000	
Anti-33-E	Rbt #1	31%	79,000	340,000±2,957,000	27,000	111,000±1,026,000
	Rbt #2	71%	113,000		28,000	
	Rbt #3	53%	5,218,000		1,804,000	
Anti-33-F[d]	Rbt #1	56%	137,000	55,000±59,355	117,000	74,000±41,053
	Rbt #2	0%	54,000		93,000	
	Rbt #3	0%	22,000		37,000	
Anti-33-G[d]	Rbt #1	0%	156,000	180,000±58,774	202,000	220,000±70,887
	Rbt #2	0%	253,000		172,000	
	Rbt #3	0%	22,000		307,000	
Anti-33-H[d]	Rbt #1	26%	110,000	169,000±61,101	223,000	214,000±21,362
	Rbt #2	56%	190,000		190,000	
	Rbt #3	0%	230,000		230,000	
Anti-33-I[c,d]	Rbt #1	85%	125,000	133,000±11,150	109,000	109,000±11,015
	Rbt #2	78%	146,000		121,000	
	Rbt #3	66%	129,000		99,000	
Anti-MSP1-42	Rbt #1	60%	1,252,000	1,198,000±162,263	140,000	179,000±105,510
	Rbt #2	0%	1,024,000		317,000	
	Rbt #3	56%	1,338,000		129,000	

[a]Mean of two growth inhibition assays

[b]Geometric mean and standard deviation of antibody titers

[c] Fisher Exact Test, $p<0.05$

[d] Construct titer significantly lower then MSP1-42 (33-A (p=0.0021), 33-D (p=0.0195), 33-F (p=0.0002), 33-G (p=0.0004), 33-H (p=0.0003), 33-I (p=0.0003)

Table 1.4 Anti-Construct 33-C Antibodies Interfere with Inhibitory Anti-MSP1-42 Antibodies

Serum Samples	% Parasite Growth Inhibition
MSP1-42 Inhibitory Serum #1	
alone	86%
+Normal Rabbit Serum	85%
+Anti-Construct 33-C Serum#1	59%
+Anti-Construct 33-C Serum#2	73%
MSP1-42 Inhibitory Serum #2	
alone	93%
+ Normal Rabbit Serum	91%
+Anti-Construct 33-C Serum#1	73%
+Anti-Construct 33-C Serum#2	89%

Chapter 2

Title: Antibody and T Cell Responses in Reciprocal Prime-boost Studies with Full-length and Truncated Merozoite Surface Protein 1 C-terminal Subunit Proteins

Authors: Kae Pusic, Sophie Kobuch, Danielle Clements, George Hui

University of Hawaii, School of Medicine, Department of Tropical Medicine, Honolulu, HI, USA

Short title: Reciprocal Prime-boost Studies with MSP1-42 and truncated MSP-42

Abstract

Background: The Merozoite Surface Protein 1-42 (MSP1-42) is one of the most studied malaria subunit vaccine candidates. The N-terminal fragment of MSP1-42, MSP1-33, has been found to possess a number of T helper epitopes which influence antibody responses toward the C-terminal region of MSP1, MSP1-19. Two recombinant protein subunits consisting of T helper epitope regions of MSP1-33 expressed in tandem with MSP1-19 were previously found to be more effective than the full-length MSP1-42 at eliciting robust immune responses. Here, we studied the immunogenicity of these two truncated recombinant proteins, Constructs D and I, in the context of recognition by immune responses induced by full length native MSP1-42 in order to gauge the effects of priming with MSP1-42 on immune responses induced by the truncated antigens.

Methods: Reciprocal cross priming/boosting studies were carried out in outbred Swiss Webster mice. Accordingly, mice were either primed with Construct D or with Construct I and boosted with full-length MSP1-42. Complementarily, mice primed with MSP1-42 mice were boosted with either Construct D or Construct I. These groups of mice were evaluated for antibody (MSP1-19 specific) and T cell immunogenicity.

Results: Both Constructs D and I were effective when used either as the priming antigen followed by boosting with MSP-42, or as the boosting antigen following priming with full length MSP1-42. Additionally, Construct I, consisting of only conserved MSP1-33 sequences fused to MSP1-19, was equally well recognized by homologous and heterologous allelic forms of MSP1-42.

Conclusions: Results indicated that these truncated forms of MSP1-42 can maintain or enhance their immunogenicity in populations exposed to native MSP1-42, and further suggest that field deployment of vaccines based on these construct designs in malaria endemic areas may provide a greater degree of efficacy.

Introduction

Efforts to develop a blood-stage vaccine for malaria have focused on a number of antigens [1, 2], among them is the Merozoite Surface Protein 1 (MSP-1), one of the major proteins found on the surface of invading merozoites. MSP-1 undergoes two sequential proteolytic cleavages during the blood stage development of the parasite [3, 4]. It is first cleaved into four fragments: 83kDa, 30kDa, 38kDa, and 42kDa. Subsequently, the C-terminal 42kDa fragment, MSP1-42, is further cleaved to yield 19 kDa (MSP1-19) and 33 kDa fragments (MSP1-33) [4]. During merozoite invasion the C-terminal MSP1-19 remains attached to the parasite's surface membrane and is carried into the erythrocyte; whereas MSP1-33 is released into the blood plasma [5]. It has been shown that MSP-1 has two dimorphic forms within the MSP1-42 molecule [6]. The MSP1-33 region is comprised of mostly allelic sequences where as MSP1-19 is mostly conserved [7].

Both MSP1-42 and MSP1-19 have shown potential as subunit vaccines in rodent and monkey models [8-12]. Passive transfer of anti-MSP1-42 or anti-MSP1-19 monoclonal antibodies have been found to protect against malaria, and appear to do so via inhibition of merozoite invasion and/or by merozoite opsonization [13]. Anti-MSP1-42/MSP1-19 antibodies have been shown to correlate with naturally acquired immunity in several epidemiological studies [14-18]

Studies on MSP1-33 have identified a number of T cell epitopes [19-21]. It has been suggested that T cell epitopes on MSP1-33 provide cognate helper function for the production of an anti-MSP1-19 antibody response [20-25]. In a recent study, we examined the potential role of T cell epitopes found in MSP1-33 to enhance the immunogenicity of MSP1-42 based vaccines. The immunogenicity of eleven constructs consisting of different combinations of MSP1-33 specific T cell epitopes linked to MSP1-19 was assessed. The results from this study demonstrated that different T cell epitopes in MSP1-33 induce positive or negative effects on the

induction of inhibitory antibodies and provided insight into how anti-MSP1-19 antibody responses can be modulated during vaccination and natural infections [26]. The study identified two truncated MSP1-42 constructs, Construct D and Construct I, that demonstrated greater vaccine potential than the full length MSP1-42 because they were able to produce a broad immune responsiveness and induce highly inhibitory antibodies [26]. Construct D represents an N-terminal truncation of the MSP1-33 region and is comprised of allelic and conserved regions of MSP1-33. While Construct I consists of only conserved sequences of MSP1-33 which have been linked together. Since both constructs represent truncated versions of MSP1-42 it is important to evaluate their immunogenicity in the context immune responses to full length MSP1-42. This is especially important since Construct I is comprised of short conserved sequences fused in tandem [26].

To this end, we evaluated the antibody and T cell immunogenicity of Constructs D and I when given as a boosting or priming immunogen in mice that were previously primed or subsequently immunized with full-length MSP1-42. Outbred SW mice were subjected to different prime/boost immunization regimens using the truncated constructs and full-length MSP1-42 (Table 4.1). Results demonstrate that both truncated constructs were highly immunogenic in terms of producing antibodies and T cell responses. More importantly is that a heterologous-homologous prime/boost regimen with the two allelic forms of MSP1-42 did not impact the immunogenicity of Construct I. In contrast, the immunogenicity of Construct D was significantly diminished when the heterologous MSP1-42 (FVO) allele was used.

Material and Methods

Mice strains

Outbred Swiss Webster (SW) mice (female, 6-8 weeks old) were obtained from Charles River Laboratory (Wilmington, MA). Cr: NIH(S)-nu/nu mice (female, 6 weeks old) were obtained from NCI Frederick (Frederick, Maryland). The use of mice was approved by the University of Hawaii's Institutional Animal Care and Use Committee.

Recombinant MSP1-42 subunit proteins and full length MSP1-42

Two truncated versions of MSP1-42 (Construct D and Construct I) were previously designed based on *P. falciparum* FUP strain [26] and expressed in *Drosophila* cells [27] and purified by affinity chromatography (Figure 2.1) [28]. These recombinant MSP1-42 derivatives have been shown to maintain correct conformation and induce parasite growth inhibitory antibodies in multiple animal models [26]. Full-length MSP1-42 of both allelic forms (FUP and FVO) were also expressed in *Drosophila* cells [27] and purified by affinity chromatography (Figure 2.1) [28]. MSP1-33 (FUP) was also cloned and expressed in *Drosophila* cells. The MSP1-33 was also purified by affinity chromatography [28].

Prime-Boost Vaccinations

SW mice were immunized with different combinations of the truncated MSP1-42 subunits and full-length MSP1-42 proteins. The combinations used for immunizations are outlined in Table 2.1 and Table 2.2. SW mice were divided into fifteen groups of six and were primed via the i.p. route with either 10 ug/dose of recombinant subunit protein or full-length protein emulsified in Freund's complete adjuvant (CFA). Mice were then boosted 14 days later, with either 10 ug/dose of truncated MSP1-42 subunits or full-length MSP1-42 emulsified in Freund's incomplete

adjuvant (IFA) depending on the formulation received for each group's primary injection (Table 2.1 and Table 2.2). Sera were obtained 21 days later through tail bleeds and mice were sacrificed for T cell analysis.

Cr: NIH(S)-nu/nu mice were divided into two vaccination groups. Both were primed with 10ug/dose of MSP1-42(FUP) emulsified in CFA via the i.p. route. Mice were then boosted 14 days later, one group received 10ug/dose of MSP1-42(FUP) and the other received 10ug/dose of MSP1-42(FVO), both emulsified in IFA. Sera were obtained 21 days later through tail bleeds.

MSP1-specific antibodies

Mouse sera were assayed for anti-MSP1-19 antibody by direct binding ELISAs as previously described [29]. MSP1-19 antigen was obtained from previous studies and was used for coating ELISA plates [23]. MSP1-19 was expressed in yeast and produced based on *P. falciparum* FUP strain [23]. Briefly, 96-well ELISA plates (Costar, Acton, MA) were coated with the appropriate test antigen at a concentration of 0.4µg/mL. Plates were then blocked with 1% Bovine Serum Albumin (BSA) in Borate Buffered Saline (BBS). Test sera were serially diluted in 1% BSA/0.5% yeast extract/BBS and then incubated for 60 minutes in the antigen-coated ELISA wells. Wells were washed seven times with High Salt Borate Buffered Saline (HSBBS) and incubated for 60 minutes with horseradish peroxidase conjugated anti-mouse IgG only antibodies (H & L chain specific, Kirkgaard and Perry Laboratories, Gaithersburg, MD) at a dilution of 1:2000. Wells were subsequently washed as above and color development was made using the peroxidase substrates, H_2O_2 and 2.2'-azinobis (3-ethylbenzthiazolinesulfonic acid)/ABTS (Kirkgaard and Perry Laboratories, Gaithersburg, MD). Optical density (O.D.) was determined at 405 nm and endpoint titers were calculated and graphed using Sigma Plot 10. End point titers were

calculated using the serum dilutions that gave an O.D. of 0.2, which is greater than 4 fold of background O.D. absorbance obtained using normal mouse serum.

ELISPOT Assays

ELISPOT assays of splenocytes from prime-boost immunized mice were performed according to methods previously described [30]. Briefly, ninety-six well PVDF plates (Millipore Inc., Bedford, MA) were coated with 10 ug/ml of the monoclonal antibody (mAb) against IFN-γ (R4-642) and 5 ug/ml of mAb against IL-4 (11B11) (BD Biosciences, San Diego, CA), and incubated overnight at room temperature. Plates were washed with Phosphate Buffered Saline (PBS) and blocked with 10% fetal bovine serum in DMEM for 60 minutes. Mouse spleens were harvested and single cell suspensions of splenocytes were prepared as previously described [26]. Purified splenocytes were plated at $0.5x10^6$, $0.25x10^6$, and $0.125x10^6$ cells per well and rMSP1 (4 ug/ml) was added to each well as the stimulating antigen. Positive control wells were incubated with 5 ng/ml of phorbol myristate acetate (PMA) and 1 ng/ml of ionomycin. Plates were incubated at 37º C in 5% CO_2 for 48 hours. Wells were washed and incubated with biotinylated mAb against IFN-γ at 2 µg/ml (XMG1.2), or mAbs against IL-4 at 1 µg/ml (BVD6-24G2) (BD, Biosciences, San Diego, CA), followed by the addition of peroxidase conjugated streptavidin (Kirkgaard and Perry Laboratories, Gaithersburg, MD) at a dilution of 1:800. Spots were developed with a solution consisting of 3,3'-diaminobenzidine tetrahydrochloride (DAB) (Sigma-Aldrich St. Louis, MO, 1mg/ml) and 30% H_2O_2 (Sigma-Aldrich St. Louis, MO) and enumerated microscopically. Data were presented as spot-forming-units (SFU) per million of isolated splenocytes.

Data handling and statistics

Sigma Plot 10® and GraphPadPrism 4® were used to calculate end point titers. The Student t-test was used to determine significant differences in antibody titers amongst the different test groups. Cytokine responses (ELISPOT) in mice induced by the different test groups were analyzed either by Student t-test (GraphPadPrism4). A $p<0.05$ was considered statistically significant.

Results

T-dependent antibody response in prime/boost immunizations with truncated and full-length MSP1-42 proteins

To asses the role of T-cells in MSP1-19 specific antibody responses, Nu/Nu mice which were primed with full length MSP1-42 (FUP) and then boosted with either the homologous MSP1-42 or the heterologous MSP1-42 (FVO) allele. No MSP1-19 or MSP1-42 specific antibodies were detected in both groups of mice (data not shown). As the Nu/Nu mice are incapable of providing T-cell help, the lack of anti-MSP1-19 antibody responses indicates that the MSP1-19 specific antibody responses induced by the prime/boost immunization regimens in SW mice (Table 2.2 and Figure 2.4) are entirely T cell dependent.

Reciprocal prime boost immunizations with truncated MSP1-42 proteins and full-length MSP1-42 induced MSP1-19 specific antibodies

Outbred SW mice were tested for their ability to respond to and mount an antibody response against MSP-19 to determine if the truncated MSP1-42 constructs, D and I, can act as a priming and/or boosting antigens. When Construct D or I were used as a priming antigen and boosted with the full-length MSP1-42 (Figure 2.2A), the degree of responsiveness was similar to or better than those observed when mice were primed and boosted with the same construct (Figure 2.2A). Moreover, the percent responsiveness in mice primed with both constructs were much higher than when mice were primed and boosted with full-length MSP1-42, as seen with Construct D (D-D and D-MSP1-42; 100% and 67% response respectively)(Figure 2.2A). Antibody titers of the responders in each vaccination group were similar; with the only significant difference observed between the vaccinated group, D-D and D-MSP1-42 ($p=0.038$) (Figure 2.2A).

When reciprocal immunization regimen were performed using Construct D as the boosting antigen in mice previously primed with the full-length MSP1-42 (Figure 2.2B), the response rate was only 50% as compared to the 100% responsiveness when mice were primed and boosted with Construct D (Figure 2.2B). In comparison, boosting with Construct I induced the same response rate 50% regardless of whether the full length MSP1-42 or Construct I was used as the priming antigen (Figure 2.2B). There were no significant differences in the antibody titers of the responders among the vaccination groups (Figure 2.2B).

Antigen specific T cell responses in reciprocal prime boost immunizations with truncated and full-length MSP1-42 proteins

To asses the T cell responses, splenocytes from mice immunized with the various prime/boost combinations were stimulated *in vitro* with the same antigen used for boosting and analyzed by IL-4/IFN-γ ELISPOTS (Figure 2.3). Priming with either of the truncated MSP1-42 proteins was found to induce a predominant IL-4 response (Figure 2.3A). This preferential IL-4 response seen here had no influence on IgG isotype expression (data not shown). A significant difference in IL-4 was only observed between immunization group D-D and D-MSP1-42 ($p=0.046$) (Figure 2.3A). There was no significant difference in the levels of IFN-γ produced between vaccination groups.

Priming with the full-length MSP1-42 and boosting with either Construct D or I induced an equal or more effective response as compared to priming and boosting with the same truncated construct (Figure 2.3B). Moreover, boosting with either truncated recombinant proteins induced a more balanced IL-4/IFN-γ response (Figure 2.3B) than when these truncated constructs were used as a priming antigen (Figure 2.3A).

MSP1-42 allelic effects on prime/boost immunizations with truncated and full-length MSP1-42 proteins

Secondary sera and splenocytes from immunized SW mice primed with Construct D, Construct I, full-length MSP1-42, or MSP1-33 and boosted with either the homologous or heterologous allele of the full length MSP1-42 (Table 2.2) were tested for antibodies specific for MSP1-19 and antigen specific T cells, respectively. When boosted with heterologous MSP1-42 allele, Construct D and I both induced a greater number of responders, 83% and 100% respectively, than when boosted with the homologous MSP1-42 allele (Figure 2.4A). The two truncated MSP1-42 constructs had contrasting results regarding antibody levels. Mice primed with Construct D had lower antibody titers when boosted with heterologous MSP1-42 allele ($p=0.044$) as compared to boosting with the homologous allele; whereas, mice primed with Construct I had higher titers when boosted with the heterologous MSP1-42 allele; however the difference was not statistically significant (Figure 2.4A).

T cell responses were also analyzed for these immunization groups (Table 2.2). Similar to the antibody response, heterologous MSP1-42 was more efficient in boosting T cell response than the homologous MSP1-42 allele (I-MSP1-42 versus I-MSP1-42(FVO) $p=0.0132$), with the exception of boosting IL-4 response in Construct D (D-MSP1-42 versus D-MSP1-42(FVO) $p=0.0001$)(Figure 2.4B). The IL-4 responses resulted from boosting with homologous and heterologous alleles followed the same trend as the antibody responses observed in the same immunization experiments (Figure 2.4A and B).

Mice primed with full-length MSP1-42 and MSP1-33 were boosted with the homologous or heterologous MSP1-42 allele, T cell responses induced by boosting with the heterologous MSP1-42 allele (FVO) did not produce measureable T cell responses as determined by ELISPOTs, with the exception of when MSP1-42 was boosted with MSP1-42(FVO)($p=0.007$, Figure 2.4B). In comparison, all groups

primed with Construct D or I and then boosted with the heterologous MSP1-42 allele induced measurable T cell responses by ELISPOT assays (Figure 2.4B).

Discussion

Previous studies have demonstrated that different T cell helper epitopes on MSP1-33 are able to exert positive or negative influences on the development of anti-MSP1-19 antibody responses and the induction of MSP1 inhibitory antibodies [26]. The data presented here demonstrates that the production of a MSP1-19 specific antibody response was entirely T cell dependent, as Nu/Nu mice did not develop detectable antibody responses. This further highlights the importance of T cell responses for the induction of MSP1 specific antibodies. In recent studies it was shown that two truncated MSP1-42 constructs that present different sets of T cell epitopes derived from the MSP1-33 region, Construct D and I, were able to produce a broad immune responsiveness and induce high levels of parasite growth inhibitory antibodies [26]. They were also shown to have greater vaccine potential than the full length MSP1-42 [26]. Since both constructs represent non-naturally occurring truncations or and fusions of individual segments of MSP1-33 [26], it is important to evaluate their immunogenicity in the context of recognition by immune responses to MSP1-42. As the MSP1-42 represents the native protein seen in natural infections, evaluation of cross prime/boost experiments utilizing the truncated MSP1-42 subunits and MSP-42 will allow for the potential immunological effects of the truncated MSP1-42 subunits to be gauged when deployed in populations expose to malaria.

Ideally, a MSP1-42 based vaccine should be able to elicit protective responses in naïve individuals traveling to areas of malaria transmission as well as in malaria exposed subjects who reside in endemic areas. In this regard, our reciprocal prime/boost study provides encouraging evidence the two truncated MSP1-42 antigens may be effective in both scenarios. Both truncated constructs were able to be recognized by native MSP1-42 when used as a priming antigen, inducing similar or higher vaccine responsiveness; similar or higher MSP1-19 specific antibodies

(Figure 3); and antigen specific T cell responses (Figure 2.4) as the control groups that were primed and boosted with MSP1-42. When both constructs were used as a booster antigen, they were able to recognize previously primed immune responses to native MSP1-42 by enhancing or boosting MSP1-19 specific antibodies (Figure 2.3) and T cell responses (Figure 2.4). However, in terms of responsiveness, only Construct I was able to produce similar levels of immune responsiveness as the controls. In addition, Construct I was also able to induce similar immune responsiveness as when boosted with its homologous self. Thus, Construct I may be a more effective immunogen as it elicits a more generalized response. Since Construct I possesses only conserved sequences of MSP1-33, the immunogenicity of the conserved T epitopes contained in these sequences may be equivalent in MSP1-42 and Construct I immunized mice. Previous studies indicated that these conserved epitopes may bind to multiple HLA alleles [26]; thus it is not surprising that a high degree of responsiveness was observed in the prime/boost regimen with Construct I and MSP1-42. It is also possible that Construct I is composed of T epitope regions which are relatively non-immunodominant but are less MHC restrictive. For Construct D, it may preferentially produce T cells specific for non-conserved epitopes. In this case, full length MSP1-42 priming may produce a larger repertoire of T epitopes not fully encompassed by the truncated Construct D resulting in the inability of Construct D to expand all of the primed T cells during boosting, which leads to diminished immunogenicity. On the other hand, T cells produced by Construct D priming will be readily expanded by full length MSP1-42 boosting, resulting in higher responsiveness.

Prime/boost immunizations with the truncated constructs preferentially induced IL-4 production from antigen stimulated splenocytes, suggestive of TH2 responses. While the role of TH1/TH2 responses in MSP1-42 specific immunity has not been established, protective immunity induced by MSP1-42 is clearly antibody

dependent which would benefit from a TH2 biased immune environment. In addition, TH2 cytokines may interact with B cells to induce antibody responses.

Although our prime/boost immunizations with the truncated constructs and full length MSP1-42 do not fully represent antigen exposure during live infections, they provide well controlled studies to test the reciprocal influence of immunogenicity by the two truncated MSP1-42 subunits. From the results, there is positive evidence that the immunogenicity of the truncated MSP1-42 vaccines can be enhanced or sustained with different sequences of exposure to native MSP1-42. The results indirectly suggest that deployment of the candidate vaccines in malaria endemic areas will be effective.

Another challenge of malaria vaccine design is the often observed strain specific immunity against the parasites. Some of the vaccines currently in development are more effective at protecting infections by a homologous parasite strain [31-33]. As natural infections by malaria can arise from genetically heterogeneous parasite populations, the phenomenon of strain-specific protective immunity is a major hindrance to the development of effective malaria vaccines. In this light, it is encouraging to observe that the immunogenicity of Construct I was unaffected in a heterologous-allelic prime/boost regimen. As mentioned above, Construct I may consist of non-immunodominant T cell epitopes that are less MHC restrictive, thus when boosting with heterologous MSP1-42 there is an increase in percent responders.

Heterologous-allelic prime/boost immunizations with the full-length MSP1-42s (ie. FUP/FVO), as a reference group, were more immunogenic and induced higher IL-4 and IFN-γ responses as compared to all other immunization groups. This however may be due to the possibility that the full-length protein is more antigenic than the truncated constructs, and/or conserved T epitopes are more readily generated in the context of the full length MSP1-42. This is supported by the fact that significantly

higher IFN-g responses were observed in the MSP1-42-MSP1-42(FVO) immunizations, and to a lesser extent in the MSP1-42-MSP1-42 group was in conjunction with higher IL-4 responses (Figure 2.4). Furthermore, conserved T epitopes within the full length MSP1-42 may be more readily generated during heterologous boosting, and at least some of them may have higher propensity to produce IFN-γ. Finally, it will be important to validate the present findings in carefully controlled studies using human reagents in appropriate malaria exposure settings.

References

1. Vekemans J, Ballou WR: Plasmodium falciparum malaria vaccines in development. Expert Rev Vaccines 2008, 7(2):223-240.
2. Richards JS, Beeson JG: The future for blood-stage vaccines against malaria. Immunol Cell Biol 2009, 87(5):377-390.
3. Holder AA, Freeman RR: The three major antigens on the surface of Plasmodium falciparum merozoites are derived from a single high molecular weight precursor. J Exp Med 1984, 160(2):624-629.
4. Holder AA, Lockyer MJ, Odink KG, Sandhu JS, Riveros-Moreno V, Nicholls SC, Hillman Y, Davey LS, Tizard ML, Schwarz RT et al: Primary structure of the precursor to the three major surface antigens of Plasmodium falciparum merozoites. Nature 1985, 317(6034):270-273.
5. Blackman MJ, Ling IT, Nicholls SC, Holder AA: Proteolytic processing of the Plasmodium falciparum merozoite surface protein-1 produces a membrane-bound fragment containing two epidermal growth factor-like domains. Mol Biochem Parasitol 1991, 49(1):29-33.
6. Tanabe K, Mackay M, Goman M, Scaife JG: Allelic dimorphism in a surface antigen gene of the malaria parasite Plasmodium falciparum. J Mol Biol 1987, 195(2):273-287.
7. Yuen D, Leung WH, Cheung R, Hashimoto C, Ng SF, Ho W, Hui G: Antigenicity and immunogenicity of the N-terminal 33-kDa processing fragment of the Plasmodium falciparum merozoite surface protein 1, MSP1: implications for vaccine development. Vaccine 2007, 25(3):490-499.
8. Singh S, Miura K, Zhou H, Muratova O, Keegan B, Miles A, Martin LB, Saul AJ, Miller LH, Long CA: Immunity to recombinant plasmodium falciparum merozoite surface protein 1 (MSP1): protection in Aotus nancymai monkeys

strongly correlates with anti-MSP1 antibody titer and in vitro parasite-inhibitory activity. Infect Immun 2006, 74(8):4573-4580.

9. Kumar S, Collins W, Egan A, Yadava A, Garraud O, Blackman MJ, Guevara Patino JA, Diggs C, Kaslow DC: Immunogenicity and efficacy in aotus monkeys of four recombinant Plasmodium falciparum vaccines in multiple adjuvant formulations based on the 19-kilodalton C terminus of merozoite surface protein 1. Infect Immun 2000, 68(4):2215-2223.

10. Chang SP, Case SE, Gosnell WL, Hashimoto A, Kramer KJ, Tam LQ, Hashiro CQ, Nikaido CM, Gibson HL, Lee-Ng CT et al: A recombinant baculovirus 42-kilodalton C-terminal fragment of Plasmodium falciparum merozoite surface protein 1 protects Aotus monkeys against malaria. Infect Immun 1996, 64(1):253-261.

11. Stowers AW, Cioce V, Shimp RL, Lawson M, Hui G, Muratova O, Kaslow DC, Robinson R, Long CA, Miller LH: Efficacy of two alternate vaccines based on Plasmodium falciparum merozoite surface protein 1 in an Aotus challenge trial. Infect Immun 2001, 69(3):1536-1546.

12. Hirunpetcharat C, Tian JH, Kaslow DC, van Rooijen N, Kumar S, Berzofsky JA, Miller LH, Good MF: Complete protective immunity induced in mice by immunization with the 19-kilodalton carboxyl-terminal fragment of the merozoite surface protein-1 (MSP1[19]) of Plasmodium yoelii expressed in Saccharomyces cerevisiae: correlation of protection with antigen-specific antibody titer, but not with effector CD4+ T cells. J Immunol 1997, 159(7):3400-3411.

13. McIntosh RS, Shi J, Jennings RM, Chappel JC, de Koning-Ward TF, Smith T, Green J, van Egmond M, Leusen JH, Lazarou M et al: The importance of human FcgammaRI in mediating protection to malaria. PLoS Pathog 2007, 3(5):e72.

14. al-Yaman F, Genton B, Kramer KJ, Chang SP, Hui GS, Baisor M, Alpers MP: Assessment of the role of naturally acquired antibody levels to Plasmodium falciparum merozoite surface protein-1 in protecting Papua New Guinean children from malaria morbidity. Am J Trop Med Hyg 1996, 54(5):443-448.

15. John CC, O'Donnell RA, Sumba PO, Moormann AM, Koning-Ward TF, King CL, Kazura JW, Crabb BS: Evidence that invasion-inhibitory antibodies specific for the 19-kDa fragment of merozoite surface protein-1 (MSP-1 19) can play a protective role against blood-stage Plasmodium falciparum infection in individuals in a malaria endemic area of Africa. The Journal of Immunology 2004, 173(1):666-672.

16. Perraut R, Marrama L, Diouf B, Sokhna C, Tall A, Nabeth P, Trape JF, Longacre S, Mercereau-Puijalon O: Antibodies to the conserved C-terminal domain of the Plasmodium falciparum merozoite surface protein 1 and to the merozoite extract and their relationship with in vitro inhibitory antibodies and protection against clinical malaria in a Senegalese village. Journal of Infectious Diseases 2005, 191(2):264-271.

17. Egan AF, Burghaus P, Druilhe P, Holder AA, Riley EM: Human antibodies to the 19kDa C-terminal fragment of Plasmodium falciparum merozoite surface protein 1 inhibit parasite growth in vitro. Parasite Immunology 1999, 21(3):133-139.

18. O'Donnell RA, Koning-Ward TF, Burt RA, Bockarie M, Reeder JC, Cowman AF, Crabb BS: Antibodies against merozoite surface protein (MSP)-1(19) are a major component of the invasion-inhibitory response in individuals immune to malaria. Journal of Experimental Medicine 2001, 193(12):1403-1412.

19. Lee EA, Flanagan KL, Odhiambo K, Reece WH, Potter C, Bailey R, Marsh K, Pinder M, Hill AV, Plebanski M: Identification of frequently recognized dimorphic T-cell epitopes in plasmodium falciparum merozoite surface

protein-1 in West and East Africans: lack of correlation of immune recognition and allelic prevalence. Am J Trop Med Hyg 2001, 64(3-4):194-203.

20. Udhayakumar V, Anyona D, Kariuki S, Shi YP, Bloland PB, Branch OH, Weiss W, Nahlen BL, Kaslow DC, Lal AA: Identification of T and B cell epitopes recognized by humans in the C-terminal 42-kDa domain of the Plasmodium falciparum merozoite surface protein (MSP)-1. J Immunol 1995, 154(11):6022-6030.

21. Malhotra I, Wamachi AN, Mungai PL, Mzungu E, Koech D, Muchiri E, Moormann AM, King CL: Fine specificity of neonatal lymphocytes to an abundant malaria blood-stage antigen: epitope mapping of Plasmodium falciparum MSP1(33). J Immunol 2008, 180(5):3383-3390.

22. Tian JH, Miller LH, Kaslow DC, Ahlers J, Good MF, Alling DW, Berzofsky JA, Kumar S: Genetic regulation of protective immune response in congenic strains of mice vaccinated with a subunit malaria vaccine. J Immunol 1996, 157(3):1176-1183.

23. Hui GS, Gosnell WL, Case SE, Hashiro C, Nikaido C, Hashimoto A, Kaslow DC: Immunogenicity of the C-terminal 19-kDa fragment of the Plasmodium falciparum merozoite surface protein 1 (MSP1), YMSP1(19) expressed in S. cerevisiae. J Immunol 1994, 153(6):2544-2553.

24. Stanisic DI, Martin LB, Good MF: The role of the 19-kDa region of merozoite surface protein 1 and whole-parasite-specific maternal antibodies in directing neonatal pups' responses to rodent malaria infection. J Immunol 2003, 171(10):5461-5469.

25. Tian JH, Good MF, Hirunpetcharat C, Kumar S, Ling IT, Jackson D, Cooper J, Lukszo J, Coligan J, Ahlers J et al: Definition of T cell epitopes within the 19 kDa carboxylterminal fragment of Plasmodium yoelii merozoite surface

protein 1 (MSP1(19)) and their role in immunity to malaria. Parasite Immunol 1998, 20(6):263-278.

26. Pusic KM, Hashimoto CN, Lehrer A, Aniya C, Clements DE, Hui GS: T cell epitope regions of the P. falciparum MSP1-33 critically influence immune responses and in vitro efficacy of MSP1-42 vaccines. PLoS One 2011, 6(9):e24782.

27. Schneider I: Cell lines derived from late embryonic stages of Drosophila melanogaster. J Embryol Exp Morphol 1972, 27(2):353-365.

28. Chang SP, Gibson HL, Lee-Ng CT, Barr PJ, Hui GS: A carboxyl-terminal fragment of Plasmodium falciparum gp195 expressed by a recombinant baculovirus induces antibodies that completely inhibit parasite growth. J Immunol 1992, 149(2):548-555.

29. Chang SP, Hui GS, Kato A, Siddiqui WA: Generalized immunological recognition of the major merozoite surface antigen (gp195) of Plasmodium falciparum. Proc Natl Acad Sci U S A 1989, 86(16):6343-6347.

30. Hui G, Hashimoto C: The requirement of CD80, CD86, and ICAM-1 on the ability of adjuvant formulations to potentiate antibody responses to a Plasmodium falciparum blood-stage vaccine. Vaccine 2007, 25(51):8549-8556.

31. Renia L, Ling IT, Marussig M, Miltgen F, Holder AA, Mazier D: Immunization with a recombinant C-terminal fragment of Plasmodium yoelii merozoite surface protein 1 protects mice against homologous but not heterologous P. yoelii sporozoite challenge. Infect Immun 1997, 65(11):4419-4423.

32. Ouattara A, Mu J, Takala-Harrison S, Saye R, Sagara I, Dicko A, Niangaly A, Duan J, Ellis RD, Miller LH et al: Lack of allele-specific efficacy of a bivalent AMA1 malaria vaccine. Malar J 2010, 9:175.

33. Lyon JA, Angov E, Fay MP, Sullivan JS, Girourd AS, Robinson SJ, Bergmann-Leitner ES, Duncan EH, Darko CA, Collins WE et al: Protection induced by Plasmodium falciparum MSP1(42) is strain-specific, antigen and adjuvant dependent, and correlates with antibody responses. PLoS One 2008, 3(7):e2830.

```
1     AISVT*MDNI LSGFENEYDV IYLKPLAGVY RSLKKQIEKN IFTFNLNLND  MSP1-42(FUP)
      AVTPSVIDNI LSKIENEYEV LYLKPLAGVY RSLKKQLENN VMTFNVNVKD  MSP1-42(FVO)
      ---------- ---------- ---------- ---------- ----------  Construct D
      -------DNI LS-------- -YLKPLAGVY RSLKKQ---- ---------D  Construct I

51    ILNSRLKKRK YFLDVLESDL MQFKHISSNE YIIEDSFKLL NSEQKNILLK  MSP1-42(FUP)
      ILNSRFNKRE NFKNVLESDL IPYKDLTSSN YVVKDPYKFL NKEKRDKFLS  MSP1-42(FVO)
      ---------- ---------- -----ISSNE YIIEDSFKLL NSEQKNILLK  Construct D
      ILNSR----- ----VLESDL ---------- ---------- ----------  Construct I

101   SYKYIKESVE NDIKFAQEGI SYYEKVLAKY KDDLESIKKV IKEEKEKFPS  MSP1-42(FUP)
      SYNYIKDSID TDINFANDVL GYYKILSEKY KSDLDSIKKY IN********  MSP1-42(FVO)
      SYKYIKESVE NDIKFAQEGI SYYEKVLAKY KDDLESIKKV IKEEKEKFPS  Construct D
      ---------- ---------- --------KY YSDLDSIKK- ----------  Construct I

151   SPPTTPPSPA KTDEQKKESK FLPFLTNIET LYNNLVNKID DYLINLKAKI  MSP1-42(FUP)
      ********** **DKQGENEK YLPFLNNIET LYKTVNDKID LFVIHLEAKV  MSP1-42(FVO)
      SPPTTPPSPA KTDEQKKESK FLPFLTNIET LYNNLVNKID DYLINLKAKI  Construct D
      ---------- ---------K YLPFLNNIET LY-------- ----------  Construct I

201   NDCNVEKDEA HVKITKLSDL KAIDDKIDLF KNTNDFEAIK KLINDDTKKD  MSP1-42(FUP)
      LNYTYEKSNV EVKIKELNYL KTIQDKLADF KKNNNFVGIA DLSTDYNHNN  MSP1-42(FVO)
      NDCNVEKDEA HVKITKLSDL KAIDDKIDLF KNTNDFEAIK KLINDDTKKD  Construct D
      ---------- ---------- ---------- ---------- ----------  Construct I

251   MLGKLLSTGL V*QIFPNTII SKLIEGKFQD ML                     MSP1-42(FUP)
      LLTKFLSTGM VFENLAKTVL SNLLDGNLQG ML                     MSP1-42(FVO)
      MLGKLLSTGL V*QIFPNTII SKLIEGKFQD ML                     Construct D
      ---------- ---------- ---------- --                     Construct I
```

Figure 2.1 Aligned amino acid sequence of the two truncated MSP1-42 protein constructs compared to MSP1-42. Both truncated constructs contain the MSP1-19 fragment (not shown) at the C-terminal end. Amino acid sequences of both allelic versions of MSP1-42, FUP and FVO, are shown.

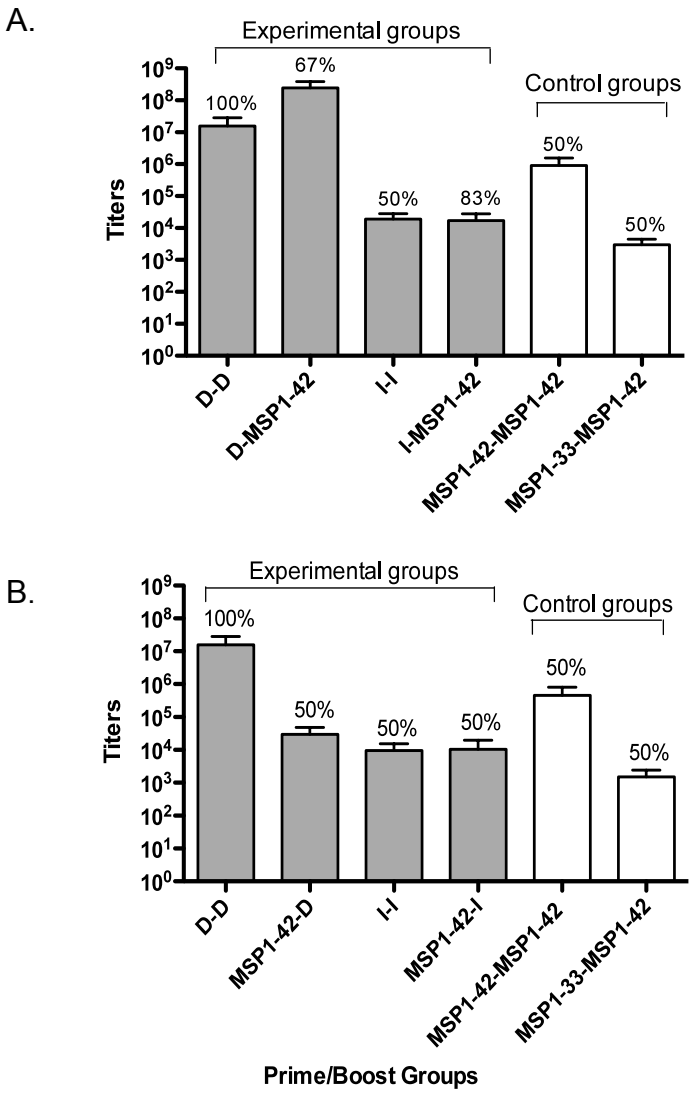

Figure 2.2 Antibody responses against MSP1-19 in reciprocal prime/boost immunizations in SW mice. Panel A, antibody titers of mice primed with Construct D or I and boosted with MSP1-42. Panel B, antibody titers of mice primed with MSP1-42 and boosted with Construct D or I. Grey bars represent the experimental groups where clear bars represent reference groups. Percent responsiveness is shown above each bar for the different immunization groups. Results of tertiary bleeds are shown.

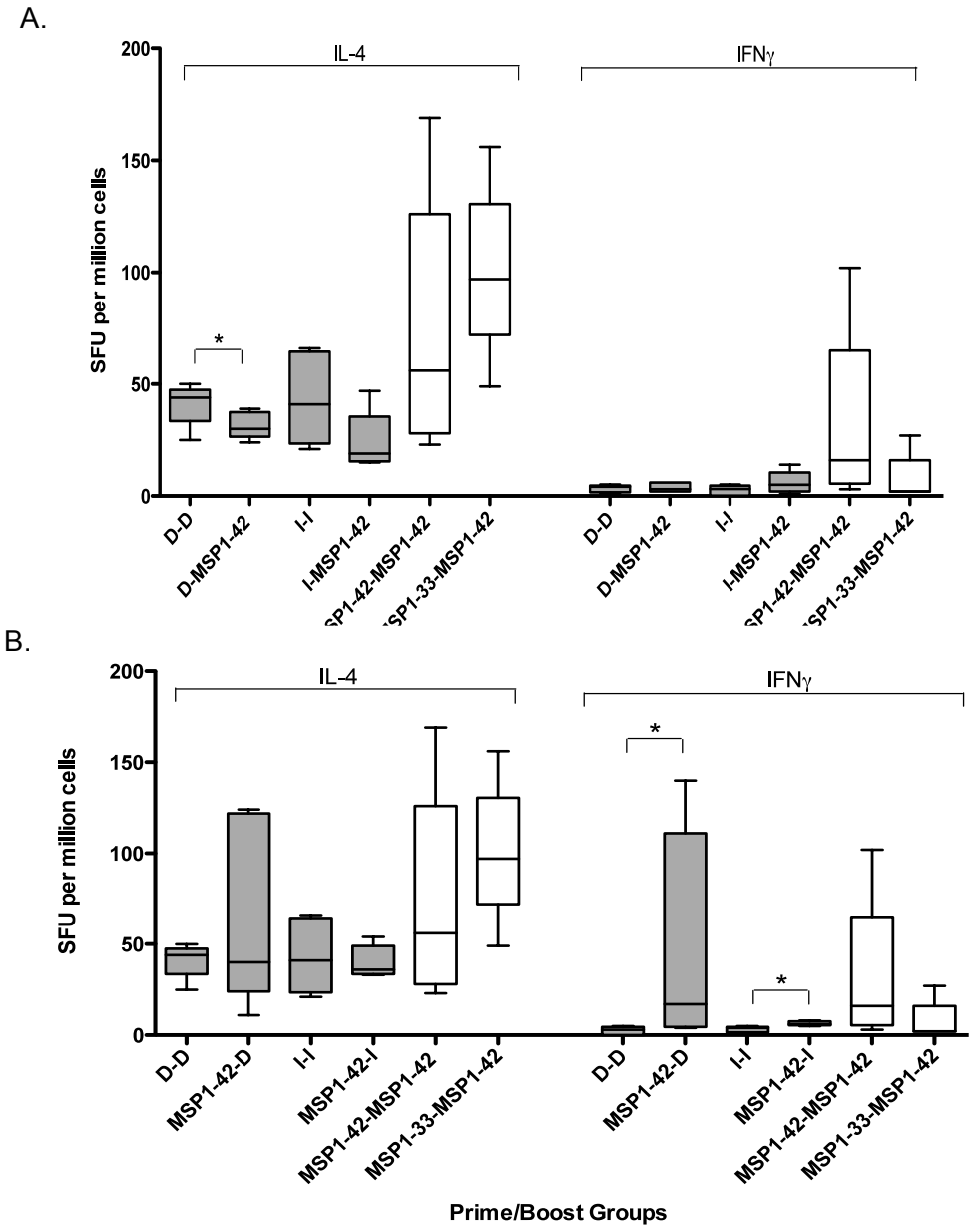

Figure 2.3 Induction of antigen-specific T cell responses in reciprocal prime/boost immunized mice. As determined my ELISPOT, Panel A: IL4/IFNγ responses in mice primed with Construct D or I and boosted with MSP1-42, Panel B: IL4/IFNγ responses in mice primed with MSP1-42 and boosted with Construct D or I. Grey bars represent the experimental groups where clear bars represent reference groups. Horizontal bars indicate mean SFU. Asterisks indicate a significant difference between groups (Mann-Whitney test, $p<0.05$).

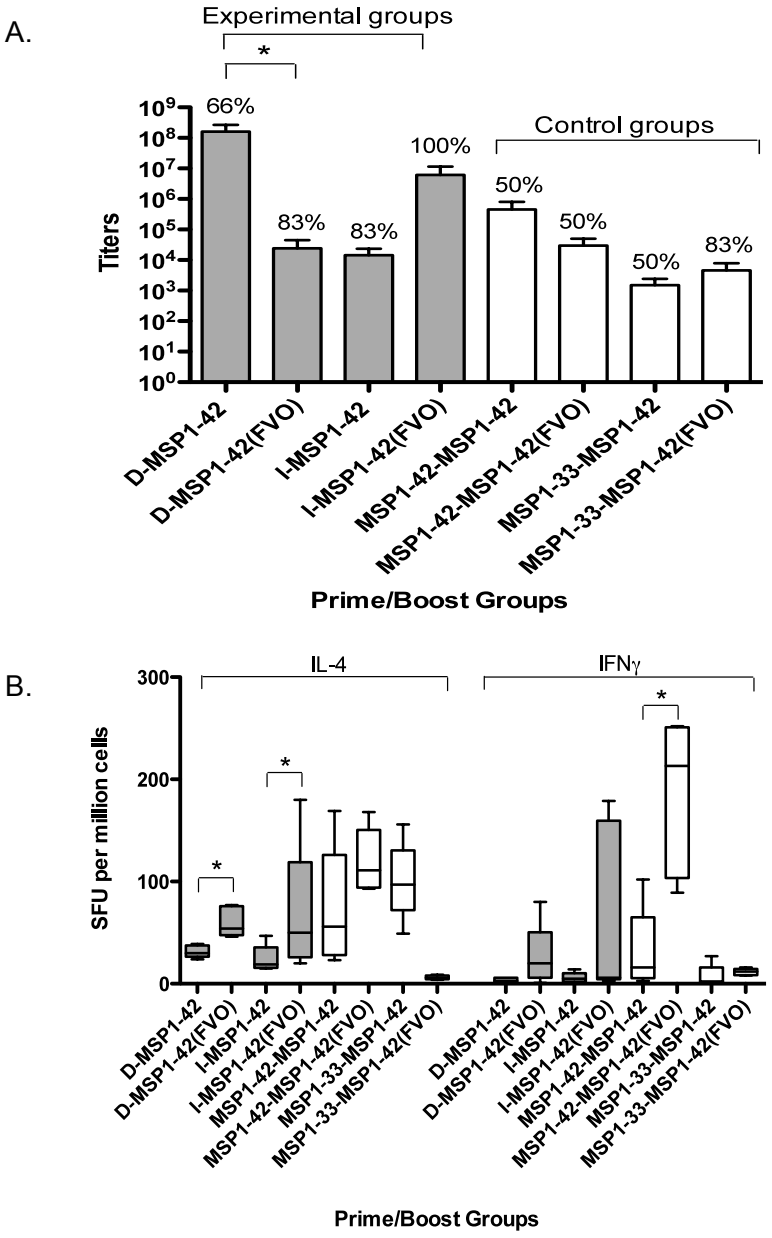

Figure 2.4 MSP1-42 allelic effects, as determined by antibody and T cell responses, in prime/boost immunizations in mice. Panel A, antibody titers of mice primed with Construct D or I and boosted with either homologous (FUP) or heterologous (FVO) MSP1-42 allele (grey bars). Clear bars represent control groups also boosted with both MSP1-42 alleles. Percent responsiveness are shown above each immunization group. Panel B, antigen specific T cell response, IL-4 and IFN-γ levels, in the same immunization groups as Panel A. Horizontal bars indicate mean SFU and asterisks indicate a significant difference between groups (Mann-Whitney test, $p<0.05$).

Table 2.1 Summary of Prime/Boost Immunizations with rMSP1 proteins		
Immunization Regimens	Priming	Boost
1	rMSP1(D)	rMSP1(D)
2	rMSP1(D)	MSP1-42
3	MSP1-42	rMSP1(D)
4	rMSP1(I)	rMSP1(I)
5	rMSP1(I)	MSP1-42
6	MSP1-42	rMSP1(I)
7(control)	MSP1-42	MSP1-42
8(control)	MSP1-33	MSP1-42

Table 2.2 Summary of Homologous vs. Heterologous Prime/Boost Immunizations

Immunization Regimens	Priming	Boost
1	rMSP1(D)	MSP1-42
2	rMSP1(D)	MSP1-42(FVO)
3	rMSP1(I)	MSP1-42
4	rMSP1(I)	MSP1-42(FVO)
5	MSP1-42	MSP1-42
6	MSP1-42	MSP1-42(FVO)
7	MSP1-42(FVO)	MSP1-42
8	MSP1-33	MSP1-42
9	MSP1-33	MSP1-42(FVO)

Chapter 3

Title: Conserved Merozoite Surface Protein 1-33 Sequences can Efficiently Prime Antibody and T Cell Help Responses Directed Towards the Merozoite Surface Protein 1-42

Authors: Kae Pusic, Mahdi Belcaid, Danielle Clements, George Hui

University of Hawaii, School of Medicine, Department of Tropical Medicine, Honolulu, HI, USA

Short title: Conserved MSP1-33 Sequences Efficient in Priming Immune Response to Malaria Antigen

Abstract

The N-terminal 33 kDa fragment of the *P. falciparum* Merozoite Surface Protein 1-42, MSP1-33, contains T helper epitopes that have been previously shown to positively or negatively influence the development of anti-MSP1-19 antibody responses. Additionally, a truncated MSP1-42 subunit (Construct I) consisting of only conserved sequences of MSP1-33 fused in tandem to MSP1-19 has been shown to a induce a more robust and broader immune response than the recombinant MSP1-42 subunit. Here, we further analyzed Construct I to examine the ability of the T cell epitopes contained in this truncated version of MSP1-42 via T cell responses. Re-examination of Construct I identified ten putative T cell epitopes, four of which represent native MSP1-33 epitopes and six that are the result of the fusion of the conserved blocks. Synthetic peptides corresponding to each of the putative T cell epitopes and tested in outbred mice for their ability to prime T helper responses that can be recalled by native MSP1-42 for the production of anti-MSP1-19 antibodies. In this manner, four T cell epitopes that efficiently enhanced anti-MSP1-19 antibody responses and antigen specific T cells when boosted with MSP1-42 were identified. These results provide the basis for further refinement of Construct I as a more effective and rationally designed MSP1 C-terminal malaria vaccine.

Introduction

The *P. falciparum* Merozoite Surface Protein 1 (MSP-1) is one of the major proteins found on the surface of the invading merozoite [1]. The C-terminal fragment of MSP1, MSP1-42, is a leading candidate for a malaria blood-stage vaccine [1]. MSP1-42 specific protection against malaria is primarily antibody mediated [2,3,4,5,6] and antibodies against this antigen have been correlated with naturally acquired immunity in several epidemiological studies [2,3,6,7]. In this light, MSP1-42 specific T helper responses will have an important role in the production of protective antibodies. Within MSP1-42, the majority of T epitopes are located at the N-terminal 33kDa processing fragment ie. MSP1-33 [8,9,10], and this region is comprised of mostly semi-conserved, allelic sequences [11].

In a previous study, the potential of T cell epitopes of MSP1-33 to enhance the immunogenicity of MSP1-42 based vaccines was examined [12]. The study evaluated the immunogenicity of eleven constructs consisting of varying combinations of MSP1-33 segments known to contain T cell epitopes fused to MSP1-19. It was determined that T cell epitopes on MSP1-33 are able to provide a cognate helper function for the production of anti-MSP1-19 antibody responses [12]. Most importantly, different T cell helper epitopes exert either positive or negative effects on the production of parasite inhibitory antibodies [12]. These results suggests that the full-length MSP1-42 may not be an ideal vaccine candidate because it consists of a full complement of T cell epitopes; some of which, if dominantly recognized may skew responses toward the production of non-inhibitory antibodies. Thus, a more effective MSP1-42 vaccine would consist of only those T cell helper epitopes which efficiently provide help for protective or inhibitory antibody responses.

In the same study, two truncated MSP1-42 constructs which show greater vaccine potential than the full-length MSP1-42 were identified [12]. One of these

constructs, Construct I, is a fusion of conserved segements of MSP1-33 (56 amino acids in length) expressed in tandem with MSP1-19 [12]. Computer algorithm analysis of this fusion segment reveals potential T cell epitope sequences, which collectively are capable of binding to all major HLA Class II molecules [12]. This strongly suggests a broad vaccine responsiveness to Construct I.

We performed a follow up study to further evaluate the immunogenicity of this construct in the context of recognition by immune responses to full-length MSP1-42 (Chapter 2). Construct I was found to be highly immunogenic, inducing both antibody and T cell responses when used as a priming or boosting antigen This finding is of significance since Construct I possesses artificially fused MSP1-33 sequences, and its ability to be recognized by T cells induced by full-length, naïve MSP1-42 is key for successful vaccine deployment in malaria exposed populations.

Since the MSP1-42 protein exists in two allelic forms [13,14], it is important to asses the potential of Construct I to induce a cross-reactive T cell response to both heterologous and homologous MSP1-42 alleles. Indeed, in an allelic prime/boost regimen using Construct I and the full length MSP1-42 alleles, the immunogenicity of Construct I did not increase or decrease (Chapter 2). Based on these promising results, the present study is aimed to further analyze and study all putative T helper epitopes within Construct I in an effort to further refine the vaccine construct. To this end, we identified putative T cell epitopes on Construct I and synthesized peptides corresponding to the identified epitopes. The contribution of the individual peptides to influence the antibody immunogenicity of MSP1-19 was assessed. Specifically, outbred Swiss Webster mice were used to examine the ability of these putative T cell epitopes to provide help that can be recalled by MSP1-42 for induction of antigen specific antibody and T cell responses. Results indicate that only a few of these T cell epitopes can contribute helper function and help broaden vaccine responsiveness. These data provide the basis for further refinement of

MSP1-42 based vaccines that are not only broadly immunogenic in genetically diverse populations, but are also parasite strain transcending.

Material and Methods

Mouse strain

Female and male outbred Swiss Webster (SW) mice, 6-8 weeks of age, were purchased from Taconic Farms (New York, NY) and Simonsen (Santa Clara, CA) and were cross bred in house. The Female progeny (6-8 weeks old) were used in all vaccination experiments. The use of mice for this study was approved by the University of Hawaii's Institutional Animal Care and Use Committee.

Recombinant MSP1-42 subunit protein and full length MSP1-42

A truncated, recombinant MSP1-42, refer to as Construct I, was previously designed based on the *P. falciparum* FUP/FVO gene sequence [12], expressed in *Drosophila* cells [15] and purified by affinity chromatography (Figure 3.1A)[16]. Construct I has been shown to be capable of inducing parasite growth inhibitory antibodies in animal models [12]. Full-length MSP1-42 (FUP) was also expressed in *Drosophila* cells [15] and purified by affinity chromatography [16]. The amino acid sequences and alignment of these proteins are shown in Figure 3.1A.

Peptides representing putative T cell epitopes

The region of the truncated MSP1-42 overlapping with the original MSP1-33 sequence, Construct I, was analyzed for potential T epitopes using the computer algorithm Propred (http://www.imtech.res.in/raghava/propred/index.html). TEN putative T epitopes were identified (Figure 3.1B). Four of the putative epitopes identified in Construct I can be found on the native N-terminal MSP1-33 sequences. The remaining six epitopes are the result of the fusion of the conserved sequence blocks that make up Construct I and thus they do not occur in MSP1-42 (Figure 3.1). All ten putative epitopes were synthesized as linear peptides (United Peptide,

Rockville MD). Peptide purity was 95 to 98%, as determined by high pressure liquid chromatography (HPLC) and amino acid composition was confirmed.

Peptide vaccinations

Swiss Webster (SW) mice were divided into ten groups (10 mice/group) for immunization with each peptide. In each group, all mice were immunized with two doses of peptide (25 µg in100 µl PBS). Five mice within each group received a third boost of MSP1-42 (5 µg in 100 µl) while the other five received a third dose of Construct I (5 µg in100 µl). All antigens were emulsified in CFA for the first immunization and IFA for the two boosts. Two control groups were immunized with sterile PBS+CFA for the first two immunizations with one group receiving MSP1-42 and the other receiving Construct I for the third immunization. Immunizations were given 21 days apart and mice were bled once, 14 days after the third immunization. Twenty-one days after the third immunization mice were sacrificed and their spleens were harvested for further experimentation.

MSP1-specific antibodies

Mouse sera were assayed for anti-MSP1 antibody (MSP1-19) by direct binding ELISAs as previously described [17]. MSP1-19 was expressed in yeast and produced based on the *P. falciparum* FUP sequence [18]. MSP1-19 antigen was obtained from previous studies and was used to coat ELISA plates. Briefly, 96-well ELISA plates (Costar, Acton, MA) were coated with the appropriate test antigen at a concentration of 0.4µg/mL. Plates were then blocked with 1% Bovine Serum Albumin (BSA) in Borate Buffered Saline (BBS). Test sera were serially diluted in 1% BSA/0.5% yeast extract/BBS, added to the antigen-coated wells, and then incubated for 60 minutes. Wells were washed seven times with High Salt Borate Buffered Saline (HSBBS) and incubated for 60 minutes with horseradish peroxidase conjugated anti-mouse IgG

only antibodies (H & L chain specific, Kirkgaard and Perry Laboratories, Gaithersburg, MD) at a dilution of 1:2000. Wells were subsequently washed as above and enzymatic activity was measured using the peroxidase substrates, H_2O_2 and 2.2'-azinobis (3-ethylbenzthiazolinesulfonic acid)/ABTS (Kirkgaard and Perry Laboratories, Gaithersburg, MD). Optical density (O.D.) was determined at 405 nm and endpoint titers were calculated and graphed using Sigma Plot 10. End point titers were calculated using the serum dilutions giving an O.D. of 0.2, which is 4-fold greater than the background absorbance obtained using normal mouse serum.

ELISPOT Assay

ELISPOT assays of splenocytes from immunized mice were performed according to methods previously described [19]. Briefly, 96-well PVDF plates (Millipore Inc., Bedford, MA) were coated with 10 ug/ml of the monoclonal antibody (mAb) against IFN-γ (R4-642) and 5 ug/ml of mAb against IL-4 (11B11) (BD Biosciences, San Diego, CA), and incubated overnight at room temperature. Plates were washed with Phosphate Buffered Saline (PBS) and blocked with 10% fetal bovine serum in DMEM for 60 minutes. Mouse spleens were harvested and single cell suspensions of splenocytes were prepared as previously described [19]. Purified splenocytes were plated as duplicates at $0.5x10^6$, $0.25x10^6$, and $0.125x10^6$ cells per well and rMSP1 (4 ug/ml) or peptide (0.2ug/ml) was added to each well as the stimulating antigen. For peptide stimulation three different concentrations (0.125 µg/ml, 0.25 µg/ml, 2.5 µg/ml) were first tested to find the optimal dose. Positive control wells were incubated with 5 ng/ml of phorbol myristate acetate (PMA) and 1 ng/ml of ionomycin. Plates were incubated at 37º C in 5% CO_2 for 48 hours. Wells were washed and incubated with biotinylated mAb against IFN-γ at 2 µg/ml (XMG1.2), or mAbs against IL-4 at 1 µg/ml (BVD6-24G2) (BD, Biosciences, San Diego, CA), followed by the addition of peroxidase conjugated streptavidin (Kirkgaard and Perry

Laboratories, Gaithersburg, MD) at a dilution of 1:800. Spots were developed with a solution consisting of 3,3'-diaminobenzidine tetrahydrochloride (DAB) (Sigma-Aldrich St. Louis, MO, 1 mg/ml) and 30% H_2O_2 (Sigma-Aldrich St. Louis, MO) and enumerated microscopically. Data were presented as spot-forming-units (SFU) per million of isolated splenocytes.

Cross-Reactive Peptides

Putative T cell epitopes created from the junctional fusion of the MSP1-33 fragments on Construct I were aligned against the full length MSP1-42 sequence, using the Water program from the EMBOSS suite [20] in order to identify potential crossreactive T epitopes on native MSP1-42 . Alignments were performed based on four key features of the amino acids: conservative substitution, charge and polarity, hydrophobicity, and surface exposure [21]. Each of these features was assigned an impact factor of 4 through 1 consecutively and in descending priority [21]. Thus, each sequence alignment received a compound score, which is the numeric sum of the impact factors of the four features outlined above. Each alignment starting from the best compound score (higher the score better the alignment) was masked from the sequence by replacing that portion of amino acids with an "X" and then re-aligned to finding the next best alignment.

Data handling and statistics

Sigma Plot 10® and GraphPadPrism 4® were used to calculate end point antibody titers. The Student t-test was used to determine significant differences in antibody titers amongst the different test groups. Cytokine responses (ELISPOT) in mice induced by the different test groups were analyzed by Student t-test (GraphPadPrism4). A p value <0.05 was considered statistically significant.

Results

Recognition of Putative T Cell Epitopes by Construct I Primed Mice

Primed splenocytes from mice immunized with Construct I or MSP1-42 were isolated and stimulated *in vitro* with each of the ten putative T cell epitope peptides and analyzed by ELISPOTS for IL-4 and IFNγ production (Figure 3.2). Construct I immunized mice induced a predominant IFNγ response as the IL-4 responses were very low when stimulated with all ten peptides, whereas MSP1-42 immunized mice induced low levels of IFNγ and modest levels of IL-4 (Figure 3.2). However, the IL-4 and IFNγ levels from MSP1-42 immunized mice were not higher than the native controls (data not shown). Thus, only Construct I immunized mice were able to recognize all ten peptides and mount robust peptide specific T cell responses (Figure 3.2).

Immunogenicity of Putative T Cell Epitopes in Mice

Tertiary sera from SW mice immunized with two doses of peptide (putative T cell epitopes) and boosted with either Construct I (Figure 3.3A) or full length MSP1-42 (Figure 3.3B) were tested for antibodies specific for MSP1-19. In this manner, the ability of each of the ten putative T cell epitopes to act as a priming antigen in order to address their helper function for an antibody response to Construct I as well as to evaluate their ability to induce a T cell population that could provide help during the immune response to full length MSP1-42.

Five out of ten peptides were able to prime for anti-MSP1-19 antibody responses when boosted with either Construct I (peptide #1, 5, 7, 9, and 10) or the full length MSP1-42 (peptide #1, 2, 5, 8, and 9). Three peptides, #1, 5, and 9, were able to prime for antibody response when boosted with either Construct I or MSP1-42 (Figure 3.3). Only peptide #1 is found on an individual block on native

MSP1-33 sequence, whereas two of the peptides, #5 and #9, are comprised of junctional sequences formed by the fusion of two blocks of MSP1-33 sequence. In general, peptide priming followed by boosting with full length MSP1-42 had higher response rate than boosting with Construct I, ranging from 40% to 100% (Figure 3.3). Peptides #1 and #9 both induced a 100% response rate when boosted with MSP1-42 (Figure 3.3B) and peptide #5 induced the same 60% response rate regardless of the boosting antigen (Figure 3.3). Antibody titers for most of the vaccination groups were similar; with the only group showing a significant increase being those immunized with peptide #9 and peptide #2 and boosted with full length MSP1-42 ($p=0.0285$)(Figure 3.3B).

Antigen Specific T cell Responses in Putative T cell Epitope Immunizations

Splenocytes from mice immunized each of the ten peptide and boosted with either construct I or MSP1-42 were stimulated *in vitro* with either Construct I or MSP1-42 and analyzed by IL-4/IFN-γ ELISPOTS (Figure 3.4). Splenocytes from mice immunized with two doses of peptides and a boost of Construct I were stimulated with Construct I (Figure 3.4A); and those from mice receiving two doses of peptide and a boost of full-length MSP1-42 were stimulated with MSP1-42 (Figure 3.4B). In general, immunization/priming with peptides induced stronger IL-4 responses than IFNγ responses irrespective of the stimulating antigen used (Figure 3.4). Significant differences were observed among the immunization groups when comparing both IL-4 and IFNγ responses (Figure 3.4). Mice primed with peptides #1, 2, 3, 5, 6, 7, 8, and 9 showed significant increases in IL-4 responses when boosted with Construct I (respective p values are 0.004, 0.004, 0.031, 0.004, 0.006, 0.004, 0.004, and 0.004) as compared to the Control group that received two doses of CFA adjuvant alone and a boost with Construct I. Similarly, significant increases in IFNγ responses were observed for peptides #1 and 2 in comparison to the Control group (p values:

0.006 and 0.029; respectively) (Figure 3.4A). In mice that were primed with peptides and subsequently boosted with full length MSP1-42, significant increases in IL-4 responses were observed for peptides #1, 3, 5, 8, and 9, when compared to the Control group (respective p values are 0.004, 0.007, 0.0159, and 0.004) (Figure 3.4B). Priming with peptides #1 and 2 significantly enhanced IFNγ responses when boosted with MSP1-42 (p values: 0.006 and 0.006, respectively) (Figure 3.4B). There was no correlation between ELISPOT results and anti-MSP1-19 specific antibody responses (Figure 3.3) for each peptide immunization.

Potential Cross Reactive peptides of T cell epitopes on Construct I

Peptides #5, 8, and 9 which represent putative T cell epitopes that resulted from the fusion of MSP1-33 sequence blocks and which do not occur in the native MSP1-42 sequence, were analyzed for homology against the MSP1-42 sequence. A crossreactive sequence for peptide #5, ISYYEKVLA (A), was identified with a score of 15.0 (Figure 3.5). Peptide #8 had three cross reactive peptides: ILNSRLKKRK (B), KLLNSEQKNILLKS (C), and NTIISKLIEGK (D) with corresponding scores of 26.0, 14.5, 12.0; respectively. Four potential cross reactive sequences were identified for peptide #9: ILNSRLKKRKY (E), VLESDLMQFKHI (F), SVENDIKFAQ (G), and YYEKVLAKYKDD (H), with scores of 15.0, 21.0, 22.0, and 12.0; respectively (Figure 3.5). Higher compounded score values indicate the better match of all four factors in the alignment. Thus, peptide #8 and #9 had the highest scoring crossreactive MSP1-42 sequences, ranging from 21.0 to 26.0.

Discussion

Construct I, a truncated MSP1-42 construct consisting of only conserved allelic sequences of MSP1-33 fused in tandem to MSP1-19 has been shown to potentially be a more efficacious vaccine than the full length MSP1-42 [12]. Construct I elicits broad immune responsiveness in outbred animals and induces potent parasite growth inhibitory antibodies [12]. Construct I has also been shown to be highly immunogenic in inducing MSP1-19 specific antibodies and T cell responses when used either as a priming or boosting antigen in reciprocal prime/boost studies with native MSP1-42 (Chapter 2). Moreover, its immunogenicity was unaffected and highly crossreactive with the heterologous MSP1-42 allele in prime/boost studies (Chapter 2). These promising data provided strong impetus and foundation to analyze these T cell epitopes of Construct I, particularly in relationship to their roles in helper functions. Since it has been previously demonstrated that there is a critical influence of these MSP1-33 specific T epitopes on anti-MSP1-19 antibody responses, detailed mapping of T helper epitopes will allow for further rationale design of MSP1-42 vaccines.

Based on computer algorithm prediction, ten putative T cell epitopes were identified on Construct I. These epitopes were made up of native and junctional sequences within the tandemly fused T epitope blocks. When mice immunized with Construct I and full length MSP1-42 were analyzed for their ability to recognize the ten putative T cell epitopes, only those mice immunized with Construct I were able to mount a T cell response. It is possible that no response was seen with the MSP1-42 immunized mice because these mice were hyper-immunized with full length MSP1-42. When tested for their ability to prime for T helper responses that can be recalled by both the full length MSP1-42 and Construct I for the production of anti-MSP1-19 antibodies, three peptides, Peptide #1, 5 and 9, were found to be effective (Figure 3.3). The data suggests that the T epitopes defined by the three peptide sequences

are crossreactive between MSP1-42 and Construct I, and are likely responsible for the efficient priming or boosting of MSP1-42 responses by Construct I as previously observed (Chapter 2). Peptides #1 and 9 were also able to prime for the highest response rate and the highest MSP1-19 specific antibody titers when boosted with MSP1-42 (Figure 3.3B). Of note is the ability of Peptide 2 and 8 to prime for antibody responses in MSP1-42 boosted mice, but not Construct I boosted mice. The two epitopes are not less immunogenic since they were able to prime for T cell responses in Construct I and MSP1-42 boosted mice (Figure 3.4). It is possible that the phenotypes of Peptide 1 and 8 specific T cells generated by MSP1-42 and Construct I were different, with only those from MSP1-42 immunization having the ability to provide helper function. We have not ruled out the possibility that these two peptides may have homology with epitope sequences in MSP1-42 thereby inducing these observed populations of T helper cells.

Results of ELISPOT assays of peptide primed and Construct I or MSP1-42 boosted mice showed that more peptides were able to prime for T cell responses with IL-4 or IFN-γ production, than prime for antibody responses (Figure 3.3 and Figure 3.4). There were no correlation observed between antibody and T cell responses. Peptides 3 and 6 exclusively primed for T cell IL-4 responses but not antibody production in either Construct I or MSP1-42 immunization. Thus, T epitope characterization by measurement of in vitro antigen-specific restimulation did not correlate with their ability to enhance antibody responses. It is possible that the splenocytes utilized for examining T cell responses here may not sufficiently represent T helper cell populations slated for interaction with antigen specific B cells. Other populations of T cells, such as those in the draining lymph nodes need to be similarly examined. Additionally, a more detailed phenotypic investigation of the T cells induced by these peptide immunizations may provide insight into the nature of the contributions of these epitopes' to B and T cell immunogenicity.

Compilation of results from our antibody and T cell studies have identified four out of the ten predicted T epitopes as being able to efficiently prime T helper response and induce broad percent responsiveness: peptide #1, #5, #8, and #9. Peptides #5, #8, and #9 are all junctional T cell epitopes which do not naturally occur in the full length MSP1-42 sequence but yet they were found to contribute T helper function with broad antibody responsiveness. Hence, these peptides were further analyzed by computer algorithms for potential homology between itself and the full length native MSP1-42. Indeed, amino acid sequences with high degree of structural and chemical similarities were found for all junctional T cell epitopes, which may explain for their ability to prime T cells that can be recalled by native MSP1-42 and induce a response. Peptides #8 and #9 have the most strongly aligned MSP1-42 sequences (Figure 3.5), which is based on sequences having six to seven common amino acids combined with a high factor of the four biochemical and structural features. Examination of the abilities of these putative crossreactive sequences to restimulate primed peptide responses will be an important next step. Once their crossreactivities are confirmed these epitopes can be further tested for their ability to enhance antibody immunogenicity to MSP1-19. Crossreactive sequences found to have better immunogenicity, as compared to the original peptides, may be incorporated in vaccine design.

Future studies will be needed to further validate the vaccine potential of these newly identified T cell epitopes. For example, it will be necessary to evaluate if these T cell epitopes from Construct I are immunogenic in malaria exposed individuals. More specifically, if human T cells specific for these epitopes can in fact provide helper function and induce protective antibody responses. Down selection of these epitopes based on their function will enable rational modifications of this candidate MSP1-42 vaccine to further improve potency and efficacy.

References

1. Holder AA, Guevara Patino JA, Uthaipibull C, Syed SE, Ling IT, et al. (1999) Merozoite surface protein 1, immune evasion, and vaccines against asexual blood stage malaria. Parassitologia 41: 409-414.
2. al-Yaman F, Genton B, Kramer KJ, Chang SP, Hui GS, et al. (1996) Assessment of the role of naturally acquired antibody levels to Plasmodium falciparum merozoite surface protein-1 in protecting Papua New Guinean children from malaria morbidity. Am J Trop Med Hyg 54: 443-448.
3. John CC, O'Donnell RA, Sumba PO, Moormann AM, Koning-Ward TF, et al. (2004) Evidence that invasion-inhibitory antibodies specific for the 19-kDa fragment of merozoite surface protein-1 (MSP-1 19) can play a protective role against blood-stage Plasmodium falciparum infection in individuals in a malaria endemic area of Africa. The Journal of Immunology 173: 666-672.
4. Perraut R, Marrama L, Diouf B, Sokhna C, Tall A, et al. (2005) Antibodies to the conserved C-terminal domain of the Plasmodium falciparum merozoite surface protein 1 and to the merozoite extract and their relationship with in vitro inhibitory antibodies and protection against clinical malaria in a Senegalese village. Journal of Infectious Diseases 191: 264-271.
5. Egan AF, Blackman MJ, Kaslow DC (2000) Vaccine efficacy of recombinant Plasmodium falciparum merozoite surface protein 1 in malaria-naive, -exposed, and/or -rechallenged Aotus vociferans monkeys. Infect Immun 68: 1418-1427.
6. Egan AF, Burghaus P, Druilhe P, Holder AA, Riley EM (1999) Human antibodies to the 19kDa C-terminal fragment of Plasmodium falciparum merozoite surface protein 1 inhibit parasite growth in vitro. Parasite Immunology 21: 133-139.

7. O'Donnell RA, Koning-Ward TF, Burt RA, Bockarie M, Reeder JC, et al. (2001) Antibodies against merozoite surface protein (MSP)-1(19) are a major component of the invasion-inhibitory response in individuals immune to malaria. Journal of Experimental Medicine 193: 1403-1412.

8. Udhayakumar V, Anyona D, Kariuki S, Shi YP, Bloland PB, et al. (1995) Identification of T and B cell epitopes recognized by humans in the C-terminal 42-kDa domain of the Plasmodium falciparum merozoite surface protein (MSP)-1. J Immunol 154: 6022-6030.

9. Lee EA, Flanagan KL, Odhiambo K, Reece WH, Potter C, et al. (2001) Identification of frequently recognized dimorphic T-cell epitopes in plasmodium falciparum merozoite surface protein-1 in West and East Africans: lack of correlation of immune recognition and allelic prevalence. Am J Trop Med Hyg 64: 194-203.

10. Malhotra I, Wamachi AN, Mungai PL, Mzungu E, Koech D, et al. (2008) Fine specificity of neonatal lymphocytes to an abundant malaria blood-stage antigen: epitope mapping of Plasmodium falciparum MSP1(33). J Immunol 180: 3383-3390.

11. Yuen D, Leung WH, Cheung R, Hashimoto C, Ng SF, et al. (2007) Antigenicity and immunogenicity of the N-terminal 33-kDa processing fragment of the Plasmodium falciparum merozoite surface protein 1, MSP1: implications for vaccine development. Vaccine 25: 490-499.

12. Pusic KM, Hashimoto CN, Lehrer A, Aniya C, Clements DE, et al. (2011) T cell epitope regions of the P. falciparum MSP1-33 critically influence immune responses and in vitro efficacy of MSP1-42 vaccines. PLoS One 6: e24782.

13. Tanabe K, Mackay M, Goman M, Scaife JG (1987) Allelic dimorphism in a surface antigen gene of the malaria parasite Plasmodium falciparum. J Mol Biol 195: 273-287.

14. Miller LH, Roberts T, Shahabuddin M, McCutchan TF (1993) Analysis of sequence diversity in the Plasmodium falciparum merozoite surface protein-1 (MSP-1). Mol Biochem Parasitol 59: 1-14.

15. Schneider I (1972) Cell lines derived from late embryonic stages of Drosophila melanogaster. J Embryol Exp Morphol 27: 353-365.

16. Chang SP, Gibson HL, Lee-Ng CT, Barr PJ, Hui GS (1992) A carboxyl-terminal fragment of Plasmodium falciparum gp195 expressed by a recombinant baculovirus induces antibodies that completely inhibit parasite growth. J Immunol 149: 548-555.

17. Chang SP, Hui GS, Kato A, Siddiqui WA (1989) Generalized immunological recognition of the major merozoite surface antigen (gp195) of Plasmodium falciparum. Proc Natl Acad Sci U S A 86: 6343-6347.

18. Hui GS, Gosnell WL, Case SE, Hashiro C, Nikaido C, et al. (1994) Immunogenicity of the C-terminal 19-kDa fragment of the Plasmodium falciparum merozoite surface protein 1 (MSP1), YMSP1(19) expressed in S. cerevisiae. J Immunol 153: 2544-2553.

19. Hui G, Hashimoto C (2007) The requirement of CD80, CD86, and ICAM-1 on the ability of adjuvant formulations to potentiate antibody responses to a Plasmodium falciparum blood-stage vaccine. Vaccine 25: 8549-8556.

20. Rice P, Longden I, Bleasby A (2000) EMBOSS: the European Molecular Biology Open Software Suite. Trends Genet 16: 276-277.

21. Wu CHaM, J.W. (2000) Neural networks and genome informatics: Elsevier Science.

Figure 3.1 Aligned amino acid sequence of truncated MSP1-42 subunit protein and its putative T cell epitopes. Panel A, amino acid sequence or Construct I compared to full-length MSP1-42. Construct contains MSP1-19 fragment at C-terminal end (not shown). Panel B, amino acid sequence of Construct I with the ten aligning putative T cell epitope sequences. Putative T cell epitopes found on individual blocks on MSP1-33 are shown in red and those found on junctional sequences are shown in blue. Beginning amino acids of MSP1-19 are highlighted in yellow.

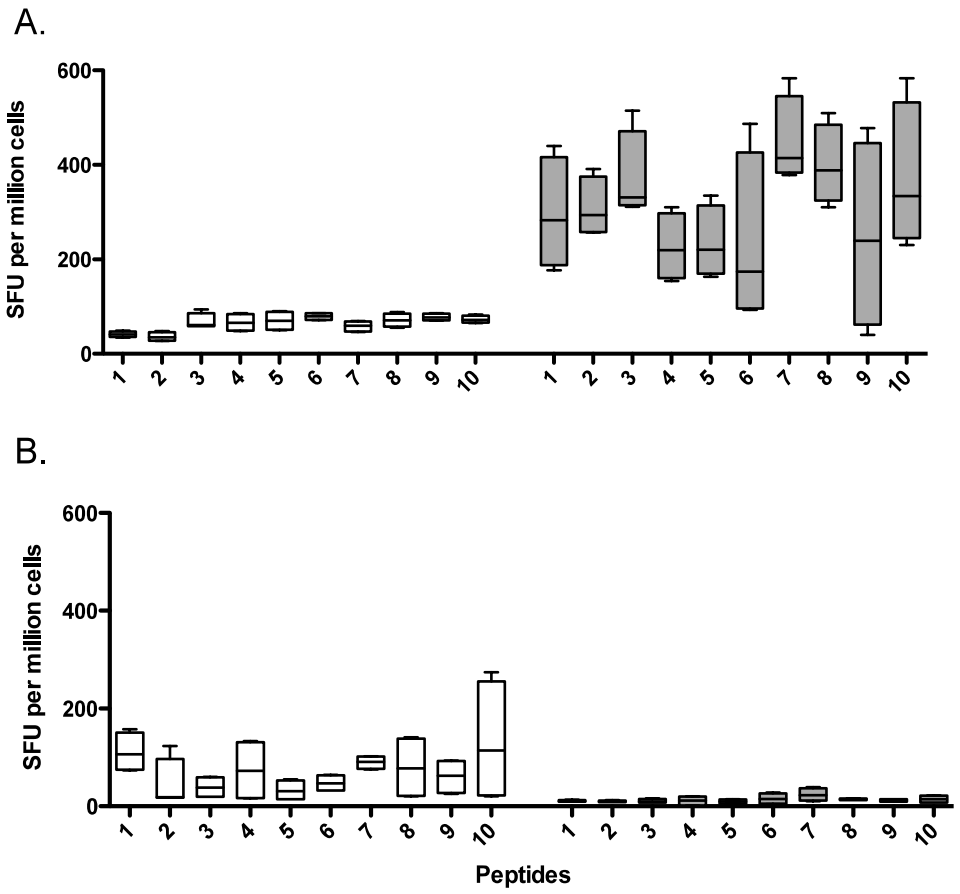

Figure 3.2 Induction of peptide specific IL-4 (white bars) and IFNγ (grey bars) responses in Construct I primed mice. Splenocytes from mice immunized with Construct I (Panel A) or MSP1-42 (Panel B) were stimulated with ten putative T cell epitope peptides. Horizontal bars indicate mean SFU. Clear bars represent IL-4 responses and grey bars represent IFNγ responses. No significant differences in Panel A and B were found when comparing to naïve control stimulated with respective peptides (data not shown).

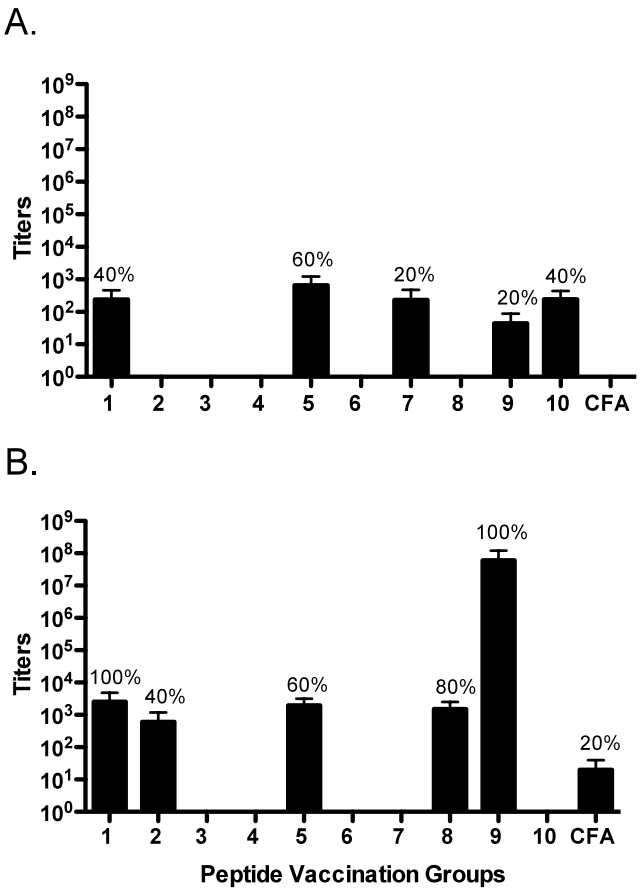

Figure 3.3 ELISA antibody responses against MSP1-19 in Swiss Webster mice immunized with putative T cell epitiope peptides. Mice were immunized with two does of peptide (1-10) and boost with either Construct I (Panel A) or MSP1-42 (Panel B). Results of tertiary bleeds are shown. Percent responders from each immunization group is noted above each bar.

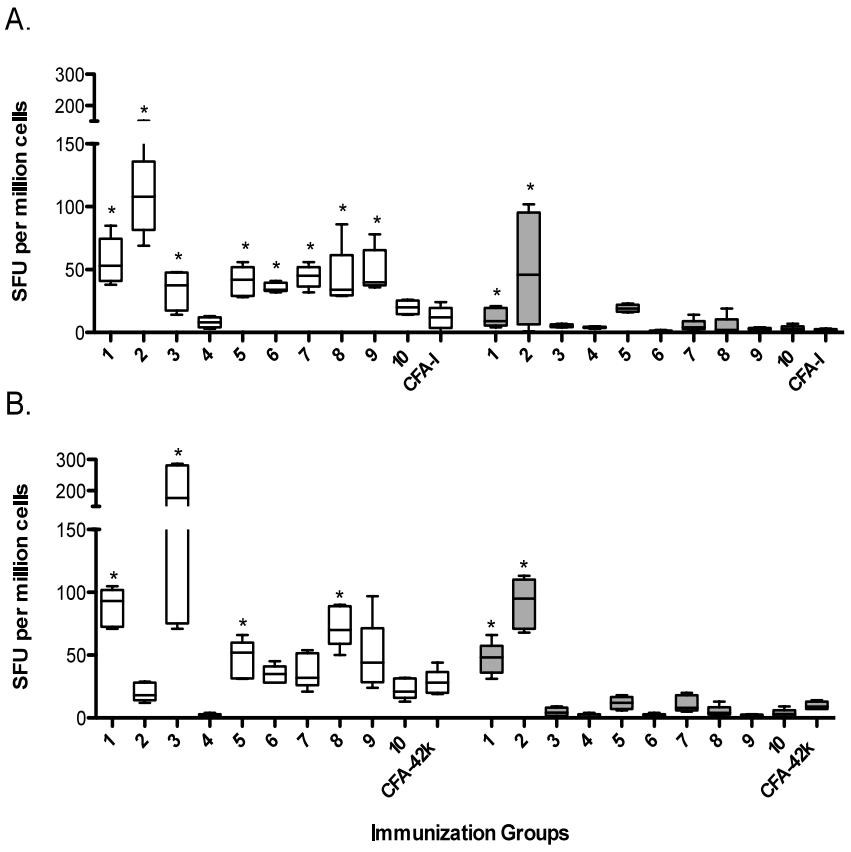

Figure 3.4 Antigen-specific T cell response in putative T cell immunized Swiss Webster mice. Splenocytes were measured for their IL4 (white bars) and IFNγ (grey bars) responses to re-stimulation with either Construct I (Panel A) or MSP1-42 (Panel B). Horizontal bars indicate mean SFU. Asterisks indicate significantly higher levels of IL4 or IFNγ (Mann-Whitney test, $p<0.05$) in a number of immunizations groups compared to control CFA.

```
1     AISVTMDNIL SGFENEYDVI YLKPLAGVYR SLKKQIEKNI FTFNLNLNDI  MSP1-42(FUP)
      ---------- ---------- ---------- ---------- ----------  Cross-Reactive #5
      ---------- ---------- ---------- ---------- ---------I  Cross-Reactive #8
      ---------- ---------- ---------- ---------- ---------I  Cross-Reactive #9

51    LNSRLKKRKY FLDVLESDLM QFKHISSNEY IIEDSFKLLN SEQKNILLKS  MSP1-42(FUP)
      ---------- ---------- ---------- ---------- ----------  Cross-Reactive #5
      LNSRLKKRK- ---------- ---------- ------KLLN SEQKNILLKS  Cross-Reactive #8
      LNSRLKKRKY ---VLESDLM QFKHI----- ---------- ----------  Cross-Reactive #9

101   YKYIKESVEN DIKFAQEGIS YYEKVLAKYK DDLESIKKVI KEEKEKFPSS  MSP1-42(FUP)
      ---------- --------IS YYEKVLA--- ---------- ----------  Cross-Reactive #5
      ---------- ---------- ---------- ---------- ----------  Cross-Reactive #8
      ------SVEN DIKFAQ---- YYEKVLAKYK DD-------- ----------  Cross-Reactive #9

151   PPTTPPSPAK TDEQKKESKF LPFLTNIETL YNNLVNKIDD YLINLKAKIN  MSP1-42(FUP)
      ---------- ---------- ---------- ---------- ----------  Cross-Reactive #5
      ---------- ---------- ---------- ---------- ----------  Cross-Reactive #8
      ---------- ---------- ---------- ---------- ----------  Cross-Reactive #9

201   DCNVEKDEAH VKITKLSDLK AIDDKIDLFK NTNDFEAIKK LINDDTKKDM  MSP1-42(FUP)
      ---------- ---------- ---------- ---------- ----------  Cross-Reactive #5
      ---------- ---------- ---------- ---------- ----------  Cross-Reactive #8
      ---------- ---------- ---------- ---------- ----------  Cross-Reactive #9

251   LGKLLSTGLV QIFPNTIISK LIEGKFQDML                        MSP1-42(FUP)
      ---------- ---------- ---------- ---------- ----------  Cross-Reactive #5
      ---------- ----NTIISK LIEGK----- ---------- ----------  Cross-Reactive #8
      ---------- ---------- ---------- ---------- ----------  Cross-Reactive #9
```

Cross-Reactive Peptides	Scores
A) ISYYEKVLA	15.0
B) ILNSRLKKRK	26.0
C) KLLNSEQKNILLKS	14.5
D) NTIISKLIEGK	12.0
E) ILNSRLKKRKY	15.0
F) VLESDLMQFKHI	21.0
G) SVENDIKFAQ	22.0
H) YYEKVLAKYKDD	12.0

Figure 3.5 Sequence of potential crossreactive peptides of Construct I T cell epitopes. Panel A, aligned amino acid sequence of potential crossreactive peptides to Construct I T cell epitopes #5 (red), 8 (blue), and 9 (green) against MSP1-42. Identified via EMBOSS. Panel B, crossreactive peptides and their corresponding compound scores. Scores are compilation of impact factors of four features based on biochemical and structural characteristics.

Chapter 4

Title: Blood Stage Merozoite Surface Protein Conjugated to Nanoparticles Induce Potent Parasite Inhibitory Antibodies

Running Title

Nanoparticle -based MSP1 Vaccine

Kae Pusic[a], Hengyi Xu[b], Andrew Stridiron[a], Zoraida Aguilar[b], Andrew Wang[b], George Hui[a]*

[a]*University of Hawaii, School of Medicine, Department of Tropical Medicine, Honolulu, HI, USA*[1] [b]*Oceannanotech LLC, Springdale, AR, USA*

rMSP1: recombinant truncated MSP1-42 malaria vaccine antigen (Construct I)

Pusic, K.; Xu, H.; Stridiron, A.; Aguilar, Z.; Wang, A.; Hui, G., Blood stage merozoite surface protein conjugated to nanoparticles induce potent parasite inhibitory antibodies. *Vaccine* **2011,** *29*, 8898-908.

Abstract

In this proof-of-concept study we report the use of <15nm inorganic nanoparticles as a vaccine delivery system for a blood stage malaria vaccine. The recombinant malarial antigen, Merozoite Surface Protein 1 (rMSP1) of *P. falciparum* served as the model vaccine. The rMSP1 was covalently conjugated to polymer-coated quantum dot CdSe/ZnS nanoparticles (QDs) via surface carboxyl groups, forming rMSP1-QDs. Anti-MSP1 antibody responses induced by rMSP1-QDs were found to have 2 to 3 log higher titers than those obtained with rMSP1 administered with the conventional adjuvants, Montanide ISA51 and CFA. Moreover, the immune responsiveness and the induction of parasite inhibitory antibodies were significantly superior in mice injected with rMSP1-QDs. The rMSP1-QDs delivered via intra-peritoneal (i.p.), intra-muscular (i.m.), and subcutaneous (s.c.) routes were equally efficacious. The high level of immunogenicity exhibited by the rMSP1-QDs was achieved without further addition of other adjuvant components. Bone marrow derived dendritic cells were shown to efficiently take up the nanoparticles leading to their activation and the expression/secretion of key cytokines, suggesting that this may be a mode of action for the enhanced immunogenicity. This study provides promising results for the use of water soluble, inorganic nanoparticles (<15nm) as potent vehicles/platforms to enhance the immunogenicity of polypeptide antigens in adjuvant-free immunizations.

Key Words: Adjuvant, Malaria Vaccine, Nanoparticles, Dendritic Cells, Inhibitory Antibodies

Introduction

A major obstacle in the development of subunit recombinant and peptide vaccines is the availability of adjuvants that can induce robust immune responses. The development of human blood stage malaria vaccines is a good example. One such vaccine is the *Plasmodium falciparum* Merozoite Surface Protein 1-42 (MSP1-42) [1-5]. MSP1-42 is a surface protein found on the invading merozoites of the erythrocytic stage [6, 7]. Vaccinations with MSP1-42 in animal models have demonstrated strong protection with the use of strong oil-water emulsion adjuvants such as Freund's Complete Adjuvant [1, 3-5, 8]. Parasite inhibitory antibodies specific for MSP1-42 are protective and correlate with clinical immunity [3, 4, 9-13]. Despite clear demonstration of protective immunity in animal models, a clinical trial using MSP1-42 showed no significant efficacy [14]. The inability of the MSP1-42 vaccine formulations to induce protection in clinical trials could be attributed to very low levels (titers) of parasite inhibitory antibodies [14, 15]. Two Phase 1 trials of MSP1-42 using Alum and Alum+CPG adjuvants also induced low levels of inhibitory antibodies [16, 17]. The failure to elicit protective immunity and/or high levels of parasite inhibitory antibodies in these clinical trials may be attributed partially to the choice of adjuvants (ASO2A, CPG and Alum) [14, 16-18]. Currently, there are limited numbers of adjuvants that are registered for human use; not only for malaria vaccines but also for vaccines against other infectious diseases. Alternative strategies need to be explored and developed to enhance vaccine immunogenicity. One such strategy is the use of particle-mediated delivery systems such as micro- or nanoparticles [19-23]. The types of particles currently being evaluated are lipid polymers (eg. PLGA, PGA, PLA) particles [24-27]; Virus-Like Particles (VLPs) [28, 29]; Immune Stimulating Complexes (ISCOMS) [30, 31]; chitosans [32-34]; and inorganic particles [35]. More recently, Self-Assembling, Polypeptide-based

Nanoparticles (SAPN) have also been tested as a delivery platform for a peptide sporozoite malaria vaccine [36].

In this study, we focused on the use of the semiconductor nanoparticles, Quantum Dots (QDs), as an alternative vaccine delivery platform. QDs are small (<15nm) inorganic nanoparticles with a crystal shell of alternating cationic and anionic layers, which in this case is CdSe/ZnS [37-39]. QDs are non-immunogenic, stable, and when coated with an organic layer allow for an array of proteins, DNA, and other biomolecules to be conjugated to their surfaces [37-39]. Because of their small size and surface modification, QDs are highly soluble and behave as a true solution [40]. These characteristics may allow the particles to be rapidly dispersed *in vivo*, thereby readily reaching immunological sites and organs. Despite these advantages, the effectiveness of nanoparticles below 15 nm as vaccine delivery vehicles has not been thoroughly investigated. We used a recombinant truncated MSP1-42 malaria vaccine antigen, referred to herein as rMSP1 (Construct I)[41], as a model immunogen to evaluate nanoparticles below 15 nm as a vaccine delivery platform in adjuvant-free immunizations. Results demonstrate that rMSP1 conjugated to QDs (rMSP1-QD) was far superior to rMSP1 administered with CFA or with a clinically acceptable adjuvant, Montanide ISA51 in enhancing immunogenicity and efficacy. Our data provides promising proof-of-concept for the development of solid inorganic nanoparticles (<15 nm) as adjuvant-free vaccine delivery platforms.

Material and Methods

Mouse Strain.

Outbred Swiss Webster (SW) mice and C57Bl/6 mice (female, 6-8 weeks old) were obtained from Charles River Laboratory (Wilmington, MA). The use of mice was approved by the University of Hawaii's Institutional Animal Care and Use Committee.

Recombinant MSP1-42 (rMSP1).

A truncated version of MSP1-42 (Construct I) was expressed in *Drosophila* cells [41] and purified by affinity chromatography [42]. Figure 1A shows SDS-PAGE profile of the purified protein. This recombinant MSP1-42 (rMSP1) has been shown to induce parasite growth inhibitory antibodies [41].

Conjugation of rMSP1-42 to Quantum Dot Nanoparticles.

The rMSP1-QD conjugates were prepared using N-hydroxysulfosuccinimide sodium salt (sulfo-NHS) and 1-ethyl-3-(3-dimethylaminopropyl) carbodiimide (EDC) covalent coupling chemistry. In this method, QDs (4 uM) with surface carboxyl groups were activated by incubating with sulfo-NHS (molar ratio 2000:1) and EDC (molar ratio 2000:1) for 5 minutes in borate buffer, pH 7.4, after which 2 mg of rMSP1 was added, vortexed thoroughly, and reacted for 2 hours at room temperature. At the end of 2 hours, the reaction was quenched by adding 5 µl of Ocean's quenching buffer, a proprietary formulation in aqueous borate buffered solution at pH 9.5±0.1, and mixed for 10 minutes. The rMSP1-QD conjugates were stored at 4^{o}C for about 12 hours and purified by ultra-centrifugation at 60,000 rpm and 20°C for 30 minutes in order to separate and remove the unconjugated QDs from the supernatant.

The rMSP1-QD and unconjugated QDs were evaluated by agarose (1.5%) gel electrophoresis in Tris-Acetate-EDTA (TAE) buffer, pH 8.5. For each well, 20 µl of

the QD samples at 100 nM were mixed with 5 µl of 5XTAE loading buffer [5XTAE, 25% (v/v) glycerol and 0.25% (w/v) Orange-G at pH 8.5]. The gel was resolved at 100 V for 30 minutes (PowerPak Basic, Bio-Rad, USA) and then imaged with two exposures using a gel imaging system (Alpha Imager HP 2006, Alpha Innotech, USA).

Immunization of Mice with rMSP1-QD and rMSP1 with Conventional Adjuvants.

SW mice (6 per group) were immunized with rMSP1-QDs using the intra-peritoneal (i.p), intra-muscular (i.m.), and subcutaneous (s.c.) routes. Injection volume for the i.p. and s.c. routes was 100 ul/dose (16 µg of rMSP1/dose), and for the i.m route was 30 ul/dose (5 ug/dose). Mice were immunized 3 times at 21 days intervals. Mice were also immunized via i.p. with rMSP1 emulsified in either CFA/IFA or Montanide ISA51. The first immunization consisted of a sub-optimal dose of 2 µg antigen, followed by two booster injections at 21 days interval with an optimal dose of 5 µg [43]. Sera were obtained through tail bleeds on the 14th day after each immunization.

MSP1-specific Antibody Assays.

Mouse sera were assayed for anti-MSP1 antibodies (MSP1-19 specific) by direct binding ELISA as previously described [44]. The MSP1-19 used for coating ELISA plates was obtained from a previous study [45]. Plates were coated with MSP1-19 at a concentration of 0.4 µg/ml. Mouse sera were serial diluted in 1% yeast extract, 0.5% BSA in Borate Buffer Saline (BBS). Horseradish peroxidase conjugated goat anti-mouse antibodies (H & L chain specific) (Kirkgaard and Perry Laboratories, Gaithersburg, MD) were used as the secondary conjugate at a dilution of 1:2000. Color development was produced by using the peroxidase substrates, H_2O_2 and 2.2'-azinobis(3-ethylbenzthiazolinesulfonic acid)/ABTS (Kirkgaard and Perry Laboratories, Gaithersburg, MD). Optical density (O.D.) was determined at 405 nm. End point

titers were calculated using the serum dilutions that gave an O.D. reading of 0.2, which is greater than 4-fold of the background absorbance using pre-immune mouse serum samples.

Antigenicity of rMSP1 conjugated to QD nanoparticles as determined by ELISA

Following the same ELISA procedures described in the previous section, serial dilutions of rMSP1-QD and unconjugated QD nanoparticles were made and used for coating ELISA plates. The coated ELISA plates were incubated with mAb 5.2 [46] at a concentration of 0.2 µg/µl in 1% yeast extract, 0.5% BSA in BBS, followed by incubation with horseradish peroxidase conjugated goat anti-mouse antibodies. The O.D. readings for each serial dilution of rMSP1-QD and unconjugated QD were plotted and the levels of reactivity were compared to the standard ELISA reactivity of mAb 5.2 against unconjugated rMSP1.

Isotype-specific ELISAs.

The immunoglobulin isotypes of the anti-MSP1-19 specific antibodies were determined by isotype specific ELISAs as previously described [47]. Goat anti-mouse-IgG1 and IgG2a (Southern Biotechnology, Birmingham, AL) were used at a dilution of 1:4000. Optical density was determined at 405 nm and the O.D. ratios of IgG1/IgG2a were calculated.

IFN-γand IL-4 ELISPOT Assays.

ELISPOT assays of splenocytes from immunized mice were performed according to methods previously described [48]. Briefly, ninety-six well PVDF plates (Millipore Inc., Bedford, MA) were coated with 10 µg/ml of the monoclonal antibody (mAb) against IFN-γ (R4-642) and 5 µg/ml of mAb against IL-4 (11B11) (BD Biosciences, San Diego, CA), and incubated overnight at room temperature. Plates were washed

with Phosphate Buffered Saline (PBS) and blocked with 10% fetal bovine serum in DMEM for 60 minutes. Mouse spleens were harvested and single cell suspensions of splenocytes were prepared as previously described [48]. Purified splenocytes were plated at $0.5x10^6$, $0.25x10^6$, and $0.125x10^6$ cells per well and rMSP1 (4 µg/ml) was added to each well as the stimulating antigen. Positive control wells were incubated with 5 ng/ml of phorbol myristate acetate (PMA) and 1 ng/ml of ionomycin. Plates were incubated at 37º C in 5% CO_2 for 48 hours. Wells were washed and incubated with biotinylated mAb against IFN-γ at 2 µg/ml (XMG1.2), or mAbs against IL-4 at 1 µg/ml (BVD6-24G2) (BD, Biosciences, San Diego, CA), followed by the addition of peroxidase conjugated streptavidin (Kirkgaard and Perry Laboratories, Gaithersburg, MD) at a dilution of 1:800. Spots were developed with a solution consisting of 3,3'-diaminobenzidine tetrahydrochloride (DAB) (Sigma-Aldrich St. Louis, MO, 1mg/ml) and 30% H_2O_2 (Sigma-Aldrich St. Louis, MO) and enumerated microscopically. Data were presented as spot-forming units (SFU) per million of plated splenocytes.

In vitro Parasite Growth Inhibition Assay with Purified Mouse Serum Samples.
The ability of mouse sera generated from SW mice immunized with different rMSP1 formulations to inhibit parasite growth was determined using an *in vitro* assay [5, 45, 49, 50]. Immunoglobulins from pooled mouse serum samples from each group were purified as previously described [47] with modifications. Briefly, antibodies were purified by ammonium sulfate precipitation and followed by dialysis using an Amicon Ultra-10 Centrifugal Filter (Millipore, Billerica, MA) with a molecular weight cut off of 100 kDa. Purified antibodies were reconstituted to original serum volume with RPMI 1640. Inhibition assays were performed using sorbitol synchronized parasite cultures (3D7 strain) as described [45]. Synchronized parasite cultures at a starting parasitemia of 0.2% and 0.8% hematocrit were incubated in purified mouse antibodies at an equivalent of 20% serum concentration. Cultures were then

incubated for 72 hours with periodic mixing. Parasitemias of the parasite cultures were determined microscopically by Giemsa staining of thin blood smears. The degree of parasite growth inhibition was determined by comparing the parasitemias of cultures incubated in pre-immune antibodies as previously described [45, 49, 50].

Dendritic Cell Isolation and QD Uptake Assay.

Immature bone marrow dendritic cells (BMDC) were isolated from 12-14 week old C57Bl/6 mice as described [51]. Stromal cells were purified by passage through a cell strainer to remove bone and debris. Red blood cells were lysed using a RBC lysis buffer consisting of 0.15M NH_4Cl, 10mM $KHCO_3$, and 0.1mM EDTA. After washings, BMDCs were plated in 6-well plates (Cell Star, Monroe, NC) at a density of 10^6 cells/ml together with GM-CSF (Peprotech Inc, Rocky Hill, NJ) at a concentration of 20 ng/ml. After 24 hours, cell cultures were further incubated in RPMI 1640 with GM-CSF (20 ng/ml) for an additional 7 days. On day 7, BMDCs in suspension were removed and transferred to a new plate and these cells were used as the cell source for all subsequent experimentations [52].

Unconjugated QD nanoparticles were introduced at a final concentration of 4 uM to the 7-day old BMDC cultures, and incubated for 24 hours at 37°C. Cells were fixed with 1% paraformaldyhde (PFA) and labeled with goat anti-CD11c-PE antibodies (eBioscience, San Diego, CA), at a dilution of 1:2000, for identification and purity assessment. The cells were imaged using a fluorescent microscope (Olympus ix71) with a fluorescent cube containing the following filters: V-N41004 (ex560 and em585) and V-N41001 (ex480 and em535).

Dendritic Cell Activation by QDs.

Unconjugated QD nanoparticles (4 uM) were introduced to 7-day old BMDCs [52] for 24 hours at 37°C. The cells were harvested and washed twice with FACS buffer (PBS

with 2% FBS), fixed with 0.25% PFA for 10 minutes on ice, and stained with monoclonal antibodies to cell surface markers: (APC)-labeled anti-CD80, (PE)-labeled anti-MHC II, (AlexaFluor488)-labeled anti-CD11c (eBiosciences, San Diego, CA), and (PE-Cy7)-labeled anti-CD86 (Invitrogen, Carlsbad, CA). Cells were analyzed using the FACSAria flow cytometer with FACSDiva software (Becton Dickinson, San Jose, CA).

Cytokine Gene Expression by QD stimulated Dendritic Cells.

RNA was extracted from BMDCs (3 x 10^6 cells) at 0, 3, 6, and 12 hours after the addition of unconjugated QD (4 μM) or LPS (100 ng/ml), using the RNeasy Kit (Qiagen, Valencia, CA). RNA concentrations were measured and then the RNA samples were reverse transcribed in 50 μl reactions using the isc-ript cDNA synthesis kit (Bio-Rad, Hercules, CA) following manufacturer's protocol. Real-time PCR reactions using 1 μl of cDNA and iQ SYBR Green Supermix (Bio-Rad, Hercules, CA) were run on the MyiQ Single-Color Real Time Detection System (Bio-Rad, Hercules, CA). Both forward and reverse primers for TNF-α, TGF-β, IL-12, IL-6, IFN-γ, IL-1β were used at a 10 nM concentration (IDT, Coralville, Iowa). The primer sequences are listed in Table 4.1. Analysis of gene expression was performed using the RT^2 Profiler PCR Array Data Analysis (SABiosciences, http://pcrdataanalysis.sabiosciences.com/pcr/arrayanalysis.php). Briefly, each sample was normalized to an endogenous control, GAPDH, and the fold changes for each cytokine gene assayed was determined.

Multiplex Assay for Cytokines and Chemokines Detection.

The presence of cytokines and chemokines in the supernatants of the BMDCs stimulated with unconjugated QD nanoparticles or with LPS over a 12-hour period were measured using the Milliplex MAP Mouse Cytokine/Chemokine 32 plex assay

and Luminex 200 (Millipore Corp, Billerica, MA). The following cytokines/chemokines were simultaneously measured: Eotaxin, G-CSF, GM-CSF, IFN-γ, IL-10, IL-12 (p40), IL-12 (p70), IL-13, IL-15, IL-17, IL-1α, IL-1β, IL-2, IL-2, IL-4, IL-5, IL-6, IL-7, IL-9, IP-10, KC-like, LIF, LIX, M-CSF, MCP-1, MIG, MIP-1α, MIP-1β, MIP-2, RANTES, TNF-α, VEGF.

Data Handling and Statistics.

Sigma Plot 10 and GraphPadPrizm 4 were used to calculate the endpoint antibody titers. The Mann-Whitney test was used to determine significant differences in antibody titers and isotype ratios among the different test groups. Cytokine responses (ELISPOT) in mice were analyzed by Logistic Regression for Repeated Measures (IBM SPSS Statistics). A $p<0.05$ was considered statistically significant.

Results

Antigenicity of rMSP1-conjugated QD Nanoparticles.

The rMSP-1 conjugated QDs were tested to determine if the antigen was successfully conjugated to the nanoparticles, and whether the chemical conjugation processes affected the antigenicity of the rMSP1. Conjugated and unconjugated QDs were analyzed by agarose gel electrophoresis (Figure 4.1B). rMSP1-QDs (Lane 1) migrated as a single and higher molecular mass band, compared to the unconjugated QDs (Lane 2). This indicates that the conjugation process produced a homogeneous species of rMSP1-QDs. The antigenicity of rMSP1 was evaluated by examining the reactivity of the conformation dependent anti-MSP1-42 monoclonal antibody, mAb 5.2, with rMSP1-QD. The mAb 5.2 strongly recognized the rMSP1 conjugated to the QDs but not the unconjugated particles (Figure 4.1C). As a reference, an O.D. reading of 1.3 was observed with mAb 5.2 incubated with unconjugated rMSP1-42 at the plating concentration of 0.4 μg/ml. This suggests that the antigenicity of the rMSP1 antigen was preserved.

Immunogenicity of rMSP1-QD Nanoparticles.

The efficacy of QD nanoparticles in enhancing vaccine immunogenicity was compared with that of conventional adjuvants. Three groups of outbred SW mice were immunized via i.p. with rMSP1-QDs, rMSP1 formulated with CFA, and rMSP1 with ISA51. Immune sera were tested for antibodies against MSP1-19 by ELISA. Vaccine responders were defined as having an ELISA O.D. of >0.2 at a 1:50 serum dilution. This was above the O.D. values observed for pre-immune mouse sera. As shown in Figure 4.2A, rMSP1-QDs induced an antibody response in all mice after two immunizations, resulting in a 100% response rate. In comparison, only five out of ten mice immunized with ISA51 had detectable antibodies, resulting in a 50%

response rate (Figure 4.2B). All mice that received immunizations with CFA also responded, as shown in Figure 4.2B.

Comparison of antibody endpoint titers of the tertiary bleeds among the three vaccination groups shows that the rMSP1-QDs induced the highest mean antibody titer of $5.3x10^{-6}$ (Figure 4.2B); in contrast with the CFA formulation that induced a mean antibody titer of 2.9×10^{-4} ($p=0.012$) and with the ISA51 formulation that induced the lowest mean antibody titer of 1.9×10^{-3} ($p=0.001$). Thus, immunization of rMSP1-QDs produced antibody titers that were 2 to 3 log higher than the commonly used adjuvants, CFA and ISA51. Despite the high mean antibody titer observed with rMSP1-QD immunizations, there were high and low responders (Figure 4.2B) within the group of outbred mice as reflected in the broad range of endpoint titers.

Mice were also immunized with the rMSP1-QD via the i.m. and s.c routes. Analysis of the tertiary immune sera revealed that a 100% response rate was achieved with all three immunization routes (Figure 4.2C). The mean antibody titers induced by s.c. immunizations ($3.9x10^{-6}$) were comparable to i.p. immunizations ($5.3x10^{-6}$), while i.m. immunizations elicited the lowest mean antibody titer of $0.96x10^{-6}$ (Figure 4.2C). However, there were no statistically significant differences in antibody titers among the three routes.

IgG Isotype Response to MSP1-19.

Analyses of the MSP1-19 specific Ig sub-classes (IgG1/IgG2a ratios) in mice immunized with rMSP1-QD (i.p.), rMSP1-CFA (i.p.), and rMSP1-ISA51 (i.p.) showed no significant differences among these groups (Table 4.2). Comparison of mice immunized via i.p., i.m., and s.c. routes also showed no significant differences (Table 4.2). However, rMSP1-ISA51 induced a more polarized IgG1 response compared to other immunization groups that induced a more balanced IgG1/IgG2a response.

TH1/TH2 Response.

ELISPOT analyses of mice immunized with rMSP1-QDs via the i.p., i.m., and s.c. routes showed balanced responses in terms of IL-4 (Figure 4.3A) and IFN-γ (Figure 4.3B) production. In comparison, rMSP1 formulated with CFA and ISA51 predominantly induced IL-4 (Figure 4.3). Analysis by logistic regression for repeated measures (SPSS) showed no significant differences across all groups.

In vitro Parasite Growth Inhibitory Activity of Recombinant Anti-MSP1-42 Antibodies.

Purified mouse antibodies from all immunized groups were tested for their ability to inhibit parasite growth in vitro [47]. As shown in Table 2, the anti-MSP1-42 antibodies obtained from immunizations with rMSP1-QDs via the i.p., i.m., or s.c. route significantly inhibited parasite growth, with inhibition ranging from 73-81% (Table 4.3). None of the anti-MSP1-42 antibodies induced by rMSP1-CFA and rMSP1-ISA51 inhibited parasite growth by more than 50%, a level that is considered to be biologically significant [47, 53].

Dendritic Cell Uptake of QDs.

To better understand the mechanisms by which QDs may enhance immune responses, we studied QD interaction with dendritic cells in vitro. QDs (emitting at 540 nm) were introduced to 7-day old BMDC cultures and assayed for nanoparticle uptake. Figure 4.4 (A-C) shows that BMDCs (CD11c positive) actively internalized the QD nanoparticles. The portion of BMDCs with internalized QDs was approximately 92%.

Dendritic Cells are Activated by QDs.

Unconjugated QD nanoparticles were introduced to immature BMDC cultures and the degree of activation was measured by MHC II, CD80, and CD86 expression using flow cytometry. Unstimulated, QD-stimulated, and LPS-stimulated (positive control) dendritic cells were first measured for CD11c positivity and then were further gated for the MHC II, CD80, and CD86 activation markers. QD-stimulated, CD11c-positive (Figure 4.5A, Panel iv) dendritic cells were activated and showed increased expression of MHC II (Figure 4.5A, Panel v), CD80, and CD86 (Figure 4.5A, Panel vi). QD-stimulated dendritic cells had the highest percentage (42%) of positive MHC II markers compared to unstimulated (32%) and LPS-stimulated (38%) dendritic cells; however, these levels were not statistically significant (Figure 4.5B). The percentage of single positive CD80 and CD86 cells were statistically higher in QD-stimulated dendritic cells than in unstimulated dendritic cells, with a p value of 0.0172 and 0.0431 respectively (Figure 4.5B). Double positive CD80/CD86 expression was also significantly higher than in unstimulated dendritic cells ($p = 0.0086$). QD-stimulated dendritic cells induced similar levels of MHC II and double positive CD80/CD86 expression as the LPS-stimulated dendritic cells. However, significantly higher levels of CD80 were observed in QD-stimulated dendritic cells than in LPS-stimulated cells ($p = 0.007$), indicating that the QD nanoparticles were able to induce CD80 activation more efficiently than LPS (Figure 4.5B). Conversely, LPS-stimulated DCs expressed significantly higher CD86 levels than QD-stimulated DCs, ($p = 0.0312$) (Figure 4.5B).

QD Uptake Induces Cytokine/Chemokine Production by BMDCs.

Immature BMDCs exposed to unconjugated QD nanoparticles over a 12-hour period expressed cytokines vital for immune response activation/enhancement. By RT-PCR, QD nanoparticles significantly increased the production of the cytokines, TNF-α, IL-6, IFN-γ, IL-12, and TGF-β by more than twofold when compared to levels at 0 hour

(Figure 4.6A). QDs uptake primarily led to the increased expression of pro-inflammatory cytokines, TNF-α and IL-6 indicating that immunization with QDs can induce early inflammation similar to LPS stimulation (Figure 4.6). On the other hand, LPS-stimulated DCs produced a broader array of cytokines with significant fold increases in expression levels of all cytokines assayed, with the sole exception of TGF- β (Figure 4.6B).

To broaden our assay for cytokine/chemokine expression, a 32-plex Luminex assay was performed. BMDCs stimulated with unconjugated QD nanoparticles or with LPS secreted a number of cytokines (Figure 4.7) and chemokines (Figure 4.8) over a 12-hour period. Most notably, QD uptake/stimulation led to higher levels of production of the pro-inflammatory cytokines, IL-6, TNF-a, IL-1b, and IL-1a (Figure 4.7) in comparison to media alone. Gradual increases in the levels of these cytokines were observed over time in the QD-stimulated BMDC cultures (Figure 4.7). A number of chemokines were also produced in response to stimulation by unconjugated QDs (Figure 4.8). Among these, CCL3 and CCL4 were highly expressed and reached the same levels as LPS-stimulated BMDCs at 12 hours post-incubation.

Discussion

The main objective of this study was to investigate an alternative strategy to effectively deliver vaccines against malaria in order to enhance their immunogenicity and to show greater efficacy of the solid nanoparticles (<15 nm) over commonly used vaccine adjuvants. The results demonstrated the effectiveness of these inorganic nanoparticles for the delivery of a recombinant blood stage malaria vaccine.

One of the key findings from recombinant MSP1 delivered by the QD nanoparticles is the very high antibody titers that were induced in comparison to CFA and ISA51. The mean titers induced by rMSP1-QDs was two to three logs higher than those induced by CFA and ISA51. Moreover, these levels of antibodies were much higher than levels with any other adjuvants we have tested in previous studies with MSP1 vaccines [47, 54]. Results from antibody subclass determination and ELISPOTs showed that QD immunizations potentiated a balanced TH1/TH2 response. While the importance of TH1 versus TH2 response in anti-MSP1-mediated immunity has yet to be established, the balanced TH1/TH2 responses mediated by QDs may be important against other infectious diseases [55, 56].

Equally significant is the ability of rMSP1-QDs to elicit a 100% response rate in outbred mice, irrespective of immunization route. This level of generalized responsiveness could be achieved only with the very potent adjuvant, CFA. The low toxicity adjuvant, ISA51 induced only a 50% response rate (Figure 4.2). Of note is the requirement of two immunizations to induce the high level of responsiveness observed with rMSP1-QDs in the un-optimized study. Further optimization of the nanoparticle platform in terms of particle concentration, particle size, and surface coating may lead to the potentiation of similar levels of immunogenicity with a single immunization.

Studies have shown that the levels of parasite inhibitory anti-MSP1 antibodies correlate with immunity [9-13]. In this context, the rMSP1-QD exhibited potency far superior to the rMSP1-CFA and rMSP1-ISA51 formulations. Antibodies from rMSP1-QD immunized mouse sera were highly inhibitory against parasite growth (81%), while antibodies induced by CFA and ISA51 were completely ineffective. The high levels of parasite growth inhibition observed with the rMSP1-QD immunized sera, compared to those induced by rMSP1-CFA or rMSP1-ISA51, may or may not be due to higher overall antibody titers, as we have previously shown that the ability of anti-MSP1 antibodies to inhibit parasite growth does not correlate with antibody titers [46]. It is possible that as a group the rMSP1-QD immunization induced antibodies that are more focused on parasite inhibitory epitopes despite the fact that some of the animals in this group had lower antibody titers similar to those in the rMSP1-CFA group.

The route of immunization has been shown to play a role in the outcome of immune responses [21, 57]. Our results showed that rMSP1-QD elicited similar high antibody titers and parasite inhibitory antibodies when delivered via i.p., i.m., or s.c routes. Thus, the potency of this delivery platform was independent of immunization route. Future studies will investigate its effectiveness in non-parenteral routes, i.e. intra-nasal and oral administrations.

The significance of the QDs as a delivery platform lies in its ability to induce antibody and T cell responses without the addition of other adjuvants. However, it is possible that incorporation of adjuvants such as CpG and other TLR ligands to the nanoparticle delivery system could further increase its potency, which may allow for dose sparing administration of the conjugated vaccines.

Recently, self-assembling polypeptide-based nanoparticles (SAPNs) were reported as a delivery platform for a malaria sporozoite vaccine [36]. These SAPNs are highly effective for small peptide antigens but lack the capability to incorporate

large polypeptide antigens such as the MSP1-42 [36]. Another study using recombinant vault nanoparticles has shown efficacy in delivering recombinant proteins via the intra-nasal route [58]. Whether this platform is suitable for parenteral immunizations remains to be demonstrated. However, antigens bearing vault nanoparticles may break self-tolerance, producing self-reactive antibodies [58].

There has been very limited information on the effectiveness of solid inorganic nanoparticles (<15 nm) for the delivery of polypeptide antigens. An obstacle in the use of these nanoparticles as a delivery platform for biomolecules is that they are too rapidly cleared from the body [59, 60]. However, at sizes <15nm, the nanoparticle suspensions behave as true solutions and thus may readily disperse and penetrate tissues to reach key immunological sites [40]. These particles can be highly effective when they are readily taken up by antigen presenting cells (APCs), as shown by our particle uptake studies with bone marrow derived dendritic cells (Figure 4.4). Our dendritic cell activation studies have shown further that these nanoparticles had the ability to upregulate the key activation marker, CD80 on BMDCs (Figure 4.5). Additionally, nanoparticle-stimulated DCs expressed and secreted markedly high levels of pro-inflammatory cytokines (IL-6, IL-1a, TNF-a) and chemokines (CCL3, CCL4, CXCL1) necessary for efficient immune responses, especially toward a TH1-mediated immunity (Figures 4.6, 4.7, and 4.8). Based on the chemokines produced, stimulation of BMDCs by QDs would enhance the migratory characteristics of these immune cells which might result in more efficient antigen presentation and/or T cell activation. QDs were also able to induce production of some chemokines (CCL3/CCL4) at levels similar to those induced by LPS-stimulated BMDCs, indicating the potential of these nanoparticles to activate a strong immune response (Figure 4.8).

This study provides "proof of concept" for the utilization of water-soluble, solid inorganic nanoparticles (<15nm) as a vaccine vehicle/platform to enhance the

immunogenicity of antigens in adjuvant-free immunizations. These nanoparticles not only served as a delivery platform for protein antigens but could also activate key immune cells. To further increase the immunogenicity of this platform, other parameters may be studied or optimized. These include conjugation method, antigen orientation (either N-terminal or C-terminal conjugation), and antigen release characteristics. Concurrent with the present study, a toxicity evaluation was performed on the immunized mice by examining the plasma levels of Glu, BUN, Na, Cl, TCO_2, AnGap, Hct, Hb, pH, PCO_2, HCO_3, and BEecf; and by histological studies of kidney sections. Results showed no significant deviations in these laboratory values or in histological findings from non-immunized mice (data not shown). Although in vivo tests demonstrated no immediate toxic effects, these nanoparticles are not compatible for human use due to the presence of cadmium (Cd) in the particle core. The Cd toxicity in the QDs is contained by coating the core with a shell layer of ZnS, which is further coated with an amphiphilic polymer. Because of the possibility of eventual polymer and nanoparticle degradation, attempts are currently being made to develop cadmium free QD nanoparticles. We used the CdSe/ZnS QDs in this study because the main focus was to demonstrate as proof of principle that <15 nm solid nanoparticles can be used as an effective vaccine delivery platform. Furthermore, due to their high fluorescence, we have the advantage of being able to track the fate of these nanoparticles in vivo in order to help determine the mechanisms of immune enhancement for further optimization of the delivery platform. Similarly, we can also determine the mechanisms and rate of clearance of <15 nm solid nanoparticles for future safety and toxicity evaluations. In parallel, other investigations will determine whether similarly sized and surface-modified nanoparticles having other core compositions, such as Fe_2O_3, and Au, which are biocompatible and have been used in clinical studies and applications, will have immunogenicity profiles comparable to the CdSe nanoparticles.

Acknowledgments

We thank David Clements of Hawaii Biotech Inc for providing the MSP1 recombinant protein. We also thank Mazie Tsang and Natasha Cortez for their technical support. This work was supported by a grant from NIH/NIAID (A1076955) and NIH/NCRR COBRE(5P20RR018727-07). KPusic is supported by NIH/NIDDK (DK078386).

References

[1] Kumar S, Collins W, Egan A, Yadava A, Garraud O, Blackman MJ, et al. Immunogenicity and efficacy in aotus monkeys of four recombinant Plasmodium falciparum vaccines in multiple adjuvant formulations based on the 19-kilodalton C terminus of merozoite surface protein 1. Infection and Immunity 2000;68(4):2215-23.

[2] Holder AA, Guevara Patino JA, Uthaipibull C, Syed SE, Ling IT, Scott-Finnigan T, et al. Merozoite surface protein 1, immune evasion, and vaccines against asexual blood stage malaria. Parassitologia 1999;41(1-3):409.

[3] Singh S, Miura K, Zhou H, Muratova O, Keegan B, Miles A, et al. Immunity to Recombinant Plasmodium falciparum Merozoite Surface Protein 1 (MSP1): Protection in Aotus nancymai Monkeys Strongly Correlates with Anti-MSP1 Antibody Titer and In Vitro Parasite-Inhibitory Activity. Infection and Immunity 2006;74(8):4573.

[4] Chang SP, Case SE, Gosnell WL, Hashimoto A, Kramer KJ, Tam LQ, et al. A recombinant baculovirus 42-kilodalton C-terminal fragment of Plasmodium falciparum merozoite surface protein 1 protects Aotus monkeys against malaria. Infection and Immunity 1996;64(1):253.

[5] Stowers AW, Cioce V, Shimp RL, Lawson M, Hui G, Muratova O, et al. Efficacy of two alternate vaccines based on Plasmodium falciparum merozoite surface protein 1 in an Aotus challenge trial. Infection and Immunity 2001;69(3):1536.

[6] Holder AA, Blackman MJ, Burghaus PA, Chappel JA, Ling IT, McCallum-Deighton N, et al. A malaria merozoite surface protein (MSP1)-structure, processing and function. Memorias do Instituto Oswaldo Cruz 1992;87 Suppl 3:37.

[7] Holder AA, Freeman RR. The three major antigens on the surface of Plasmodium falciparum merozoites are derived from a single high molecular weight precursor. Journal of Experimental Medicine 1984;160(2):624-9.

[8] Burghaus PA, Wellde BT, Hall T, Richards RL, Egan AF, Riley EM, et al. Immunization of Aotus nancymai with recombinant C terminus of Plasmodium falciparum merozoite surface protein 1 in liposomes and alum adjuvant does not induce protection against a challenge infection. Infection and Immunity 1996;64(9):3614-9.

[9] Egan AF, Burghaus P, Druilhe P, Holder AA, Riley EM. Human antibodies to the 19kDa C-terminal fragment of Plasmodium falciparum merozoite surface protein 1 inhibit parasite growth in vitro. Parasite Immunology 1999;21(3):133.

[10] Al Yaman F, Genton B, Kramer KJ, Chang SP, Hui GS, Baisor M, et al. Assessment of the role of naturally acquired antibody levels to Plasmodium falciparum merozoite surface protein-1 in protecting Papua New Guinean children from malaria morbidity. American Journal of Tropical Medicine and Hygiene 1996;54(5):443-8.

[11] John CC, O'Donnell RA, Sumba PO, Moormann AM, de Koning-Ward TF, King CL, et al. Evidence that invasion-inhibitory antibodies specific for the 19-kDa fragment of merozoite surface protein-1 (MSP-1 19) can play a protective role against blood-stage Plasmodium falciparum infection in individuals in a malaria endemic area of Africa. J Immunol 2004 Jul 1;173(1):666-72.

[12] O'Donnell RA, Koning-Ward TF, Burt RA, Bockarie M, Reeder JC, Cowman AF, et al. Antibodies against merozoite surface protein (MSP)-1(19) are a major component of the invasion-inhibitory response in individuals immune to malaria. Journal of Experimental Medicine 2001;193(12):1403-12.

[13] Perraut R, Marrama L, Diouf B, Sokhna C, Tall A, Nabeth P, et al. Antibodies to the conserved C-terminal domain of the Plasmodium falciparum merozoite surface protein 1 and to the merozoite extract and their relationship with in vitro inhibitory antibodies and protection against clinical malaria in a Senegalese village. Journal of Infectious Diseases 2005;191(2):264-71.

[14] Ogutu BR, Apollo OJ, McKinney D, Okoth W, Siangla J, Dubovsky F, et al. Blood stage malaria vaccine eliciting high antigen-specific antibody concentrations confers no protection to young children in Western Kenya. PLoS One 2009;4(3):e4708.

[15] Angov E, Bergman-Leitner ES, Duncan EH, Brent-Kirk A, McCasland M, Mease R, et al. Measurement of antibody fine specificities induced by malaria vaccine FMP1/ASO2A from a pediatric phase 2B trial in western Kenya. . American Journal of Tropical Medicine and Hygiene 2007;77 (5 (Supplement)):Abstract 12.

[16] Ellis RD, Martin LB, Shaffer D, Long CA, Miura K, Fay MP, et al. Phase 1 trial of the Plasmodium falciparum blood stage vaccine MSP1(42)-C1/Alhydrogel with and without CPG 7909 in malaria naive adults. PLoS One;5(1):e8787.

[17] Malkin E, Long CA, Stowers AW, Zou L, Singh S, MacDonald NJ, et al. Phase 1 study of two merozoite surface protein 1 (MSP1(42)) vaccines for Plasmodium falciparum malaria. PLoSClinTrials 2007;2(4):e12.

[18] Stoute JA, Gombe J, Withers MR, Siangla J, McKinney D, Onyango M, et al. Phase 1 randomized double-blind safety and immunogenicity trial of Plasmodium falciparum malaria merozoite surface protein FMP1 vaccine, adjuvanted with AS02A, in adults in western Kenya. Vaccine 2007 Jan 2;25(1):176-84.

[19] O'Hagan DT, Singh M. Microparticles as vaccine adjuvants and delivery systems. Expert Rev Vaccines 2003 Apr;2(2):269-83.

[20] O'Hagan DT, Singh M, Ulmer JB. Microparticle-based technologies for vaccines. Methods 2006 Sep;40(1):10-9.

[21] Peek LJ, Middaugh CR, Berkland C. Nanotechnology in vaccine delivery. AdvDrug DelivRev 2008;60(8):915-28.

[22] Singh M, Chakrapani A, O'Hagan D. Nanoparticles and microparticles as vaccine-delivery systems. ExpertRevVaccines 2007;6(5):797-808.

[23] Bramwell VW, Perrie Y. Particulate delivery systems for vaccines. Crit RevTherDrug Carrier Syst 2005;22(2):151-214.

[24] Mundargi RC, Babu VR, Rangaswamy V, Patel P, Aminabhavi TM. Nano/micro technologies for delivering macromolecular therapeutics using poly(D,L-lactide-co-glycolide) and its derivatives. JControl Release 2008;125(3):193-209.

[25] Lu JM, Wang X, Marin-Muller C, Wang H, Lin PH, Yao Q, et al. Current advances in research and clinical applications of PLGA-based nanotechnology. ExpertRevMolDiagn 2009;9(4):325-41.

[26] Akagi T, Wang X, Uto T, Baba M, Akashi M. Protein direct delivery to dendritic cells using nanoparticles based on amphiphilic poly(amino acid) derivatives. Biomaterials 2007;28(23):3427-36.

[27] Shive MS, Anderson JM. Biodegradation and biocompatibility of PLA and PLGA microspheres. AdvDrug DelivRev 1997;28(1):5-24.

[28] Ludwig C, Wagner R. Virus-like particles-universal molecular toolboxes. CurrOpinBiotechnol 2007;18(6):537-45.

[29] Chackerian B. Virus-like particles: flexible platforms for vaccine development. ExpertRevVaccines 2007;6(3):381-90.

[30] Skene CD, Sutton P. Saponin-adjuvanted particulate vaccines for clinical use. Methods 2006;40(1):53-9.

[31] Sun HX, Xie Y, Ye YP. ISCOMs and ISCOMATRIX. Vaccine 2009;27(33):4388-401.

[32] Masotti A, Ortaggi G. Chitosan micro- and nanospheres: fabrication and applications for drug and DNA delivery. MiniRevMedChem 2009;9(4):463-9.

[33] van dLI, Verhoef JC, Borchard G, Junginger HE. Chitosan for mucosal vaccination. AdvDrug DelivRev 2001;52(2):139-44.

[34] Illum L, Jabbal-Gill I, Hinchcliffe M, Fisher AN, Davis SS. Chitosan as a novel nasal delivery system for vaccines. AdvDrug DelivRev 2001;51(1-3):81-96.

[35] Ueno Y, Futagawa H, Takagi Y, Ueno A, Mizushima Y. Drug-incorporating calcium carbonate nanoparticles for a new delivery system. JControl Release 2005;103(1):93-8.

[36] Kaba SA, Brando C, Guo Q, Mittelholzer C, Raman S, Tropel D, et al. A nonadjuvanted polypeptide nanoparticle vaccine confers long-lasting protection against rodent malaria. J Immunol 2009 Dec 1;183(11):7268-77.

[37] Xu H, Aguilar ZP, Su HP, Dixon JD, Wei H, Wang AY. Breast cancer cell imaging using semiconductor quantum dots. ECS Transactions 2009;25(11):69-77.

[38] Xu H, Aguilar ZP, Wang AY. Quantum dot based senors for proteins. ECS Transactions 2010;25(31):1-8.

[39] Xu H, Wei H, Aguilar ZP, Waldron JL, Wang AY. Application of semiconductor quantum dots for breast cancer cell sensing. IEEE 2009.

[40] Gao X, Cui Y, Levenson RM, Chung LW, Nie S. In vivo cancer targeting and imaging with semiconductor quantum dots. Nat Biotechnol 2004 Aug;22(8):969-76.

[41] Pusic, K. M.; Hashimoto, C. N.; Lehrer, A.; Aniya, C.; Clements, D. E.; Hui, G. S., T cell epitope regions of the P. falciparum MSP1-33 critically influence immune responses and in vitro efficacy of MSP1-42 vaccines. *PLoS One* **2011,** *6*, e24782.

[42] Chang SP, Gibson HL, Lee-Ng CT, Barr PJ, Hui GS. A carboxyl-terminal fragment of Plasmodium falciparum gp195 expressed by a recombinant baculovirus induces antibodies that completely inhibit parasite growth. Journal of Immunology 1992;149(2):548-55.

[43] Hui GS, Hashimoto AC, Nikaido CM, Choi J, Chang SP. Induction of antibodies to the Plasmodium falciparum merozoite surface protein-1 (MSP1) by cross-priming with heterologous MSP1s. J Immunol 1994 Aug 1;153(3):1195-201.

[44] Chang SP, Hui GS, Kato A, Siddiqui WA. Generalized immunological recognition of the major merozoite surface antigen (gp195) of Plasmodium falciparum. Proc Natl Acad Sci U S A 1989 Aug;86(16):6343-7.

[45] Hui GS, Gosnell WL, Case SE, Hashiro C, Nikaido C, Hashimoto A, et al. Immunogenicity of the C-terminal 19-kDa fragment of the Plasmodium falciparum merozoite surface protein 1 (MSP1), YMSP1(19) expressed in S. cerevisiae. J Immunol 1994 Sep 15;153(6):2544-53.

[46] Siddiqui WA, Tam LQ, Kramer KJ, Hui GS, Case SE, Yamaga KM, et al. Merozoite surface coat precursor protein completely protects Aotus monkeys against Plasmodium falciparum malaria. Proc Natl Acad Sci U S A 1987 May;84(9):3014-8.

[47] Hui G, Choe D, Hashimoto C. Biological activities of anti-merozoite surface protein-1 antibodies induced by adjuvant-assisted immunizations in mice with different immune gene knockouts. Clin Vaccine Immunol 2008 Aug;15(8):1145-50.

[48] Hui G, Hashimoto C. The requirement of CD80, CD86, and ICAM-1 on the ability of adjuvant formulations to potentiate antibody responses to a Plasmodium falciparum blood-stage vaccine. Vaccine 2007 Dec 12;25(51):8549-56.

[49] Leung WH, Meng ZQ, Hui G, Ho WK. Expression of an immunologically reactive merozoite surface protein (MSP-1(42)) in E. coli. Biochim Biophys Acta 2004 Nov 18;1675(1-3):62-70.

[50] Pang AL, Hashimoto CN, Tam LQ, Meng ZQ, Hui GS, Ho WK. In vivo expression and immunological studies of the 42-kilodalton carboxyl-terminal processing fragment of Plasmodium falciparum merozoite surface protein 1 in the baculovirus-silkworm system. Infect Immun 2002 Jun;70(6):2772-9.

[51] Inaba K, Inaba M, Romani N, Aya H, Deguchi M, Ikehara S, et al. Generation of large numbers of dendritic cells from mouse bone marrow cultures supplemented with granulocyte/macrophage colony-stimulating factor. J Exp Med 1992 Dec 1;176(6):1693-702.

[52] Szymczak WA, Deepe GS, Jr. Antigen-presenting dendritic cells rescue CD4-depleted CCR2-/- mice from lethal Histoplasma capsulatum infection. Infect Immun May;78(5):2125-37.

[53] Hui G, Hashimoto C. Plasmodium falciparum anti-MSP1-19 antibodies induced by MSP1-42 and MSP1-19 based vaccines differed in specificity and parasite growth inhibition in terms of recognition of conserved versus variant epitopes. Vaccine 2007 Jan 15;25(5):948-56.

[54] Hui GS, Hashimoto CN. Adjuvant formulations possess differing efficacy in the potentiation of antibody and cell mediated responses to a human malaria vaccine under selective immune genes knockout environment. Int Immunopharmacol 2008 Jul;8(7):1012-22.

[55] Quinnell RJ, Bethony J, Pritchard DI. The immunoepidemiology of human hookworm infection. Parasite Immunol 2004 Nov-Dec;26(11-12):443-54.

[56] Infante-Duarte C, Kamradt T. Th1/Th2 balance in infection. Springer Semin Immunopathol 1999;21(3):317-38.

[57] Shahiwala A, Vyas TK, Amiji MM. Nanocarriers for systemic and mucosal vaccine delivery. Recent Pat Drug DelivFormul 2007;1(1):1-9.

[58] Champion CI, Kickhoefer VA, Liu G, Moniz RJ, Freed AS, Bergmann LL, et al. A vault nanoparticle vaccine induces protective mucosal immunity. PLoS One 2009;4(4):e5409.

[59] Ferrari M. Cancer nanotechnology: opportunities and challenges. NatRevCancer 2005;5(3):161-71.

[60] Peer D, Karp JM, Hong S, Farokhzad OC, Margalit R, Langer R. Nanocarriers as an emerging platform for cancer therapy. NatNanotechnol 2007;2(12):751-60.

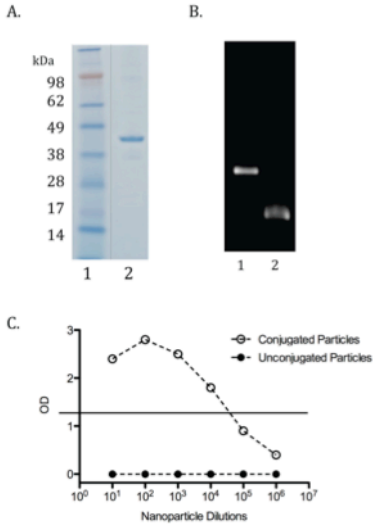

Figure 4.1 Purification, conjugation, and antigenicity analysis of rMSP1 protein to nanoparticles. Panel A, SDS-PAGE of purified recombinant C terminus MSP1 protein. Lane 1: Molecular Marker, Lane 2: Purified recombinant MSP1 (rMSP1). Panel B, 1% agarose gel electrophoresis of rMSP1 conjugated (Lane 1) and unconjugated QDs (Lane 2). Panel C, antigenicity of rMSP1 conjugated nanoparticles. ELISA titration curves of rMSP1 conjugated nanoparticles (open circles) and unconjugated nanoparticles (filled circles) against MSP1-42 specific monoclonal antibody, mAb 5.2. Straight line represents OD reading of mAb 5.2 binding to native MSP1-42 at coating concentration of 0.4 ug/ml.

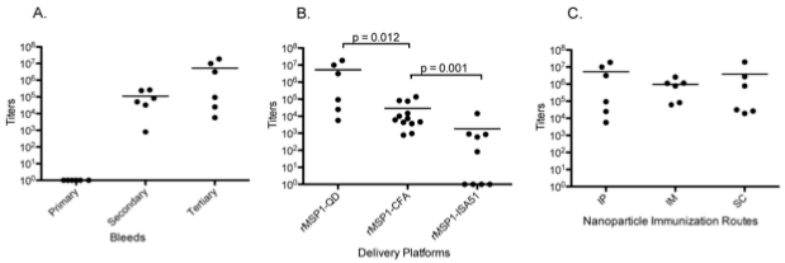

Figure 4.2 ELISA antibody response against MSP1-19 in SW mice immunized with recombinant MSP1. Panel A, antibody titers of mice vaccinated (IP) with rMSP1-QD. Results of primary, secondary, and tertiary bleeds are shown. Panel B, antibody titers of mice vaccinated with different adjuvant/delivery platforms (rMSP1-QD, rMSP1-CFA, and rMSP1-ISA51). Results of tertiary bleeds are shown. Panel C, antibody response in mice vaccinated with rMSP1-QD via different routes (i.p., i.m., and s.c.). Results of tertiary bleeds are shown. Horizontal bars indicate mean antibody titers. Significant differences in ELISA titers among vaccination groups are indicated with p-values (Mann-Whitney test).

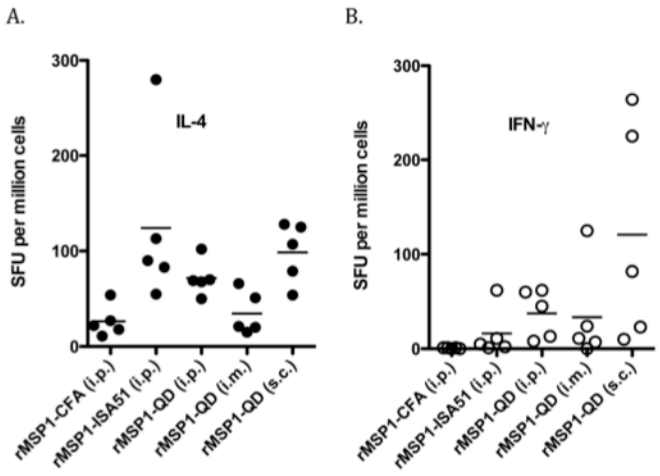

Figure 4.3 MSP1-specific IL-4 and IFN-γresponses induced by rMSP1-QD and other adjuvants. MSP1-specific IL-4 (Panel A) and IFN-γ (Panel B) responses, as determined by ELISPOT, in SW mice immunized with rMSP1 in five different adjuvant/delivery platforms. Horizontal bars indicate mean SFU. Mouse splenocytes were harvested 21 days after the last immunization.

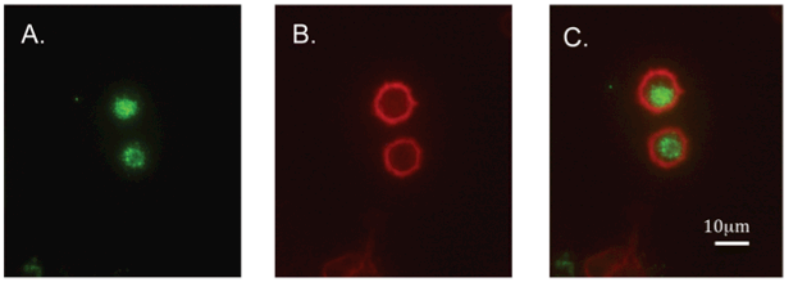

Figure 4.4 Uptake of QD nanoparticles by bone marrow derived dendritic cells (BMDC). Panel A, localization of QD particles (green) in BMDC cultured cells. Panel B, surface staining of the same BMDC cells with PE conjugated goat anti-mouse CD11c (red). Panel C, merged image of Panel A + B.

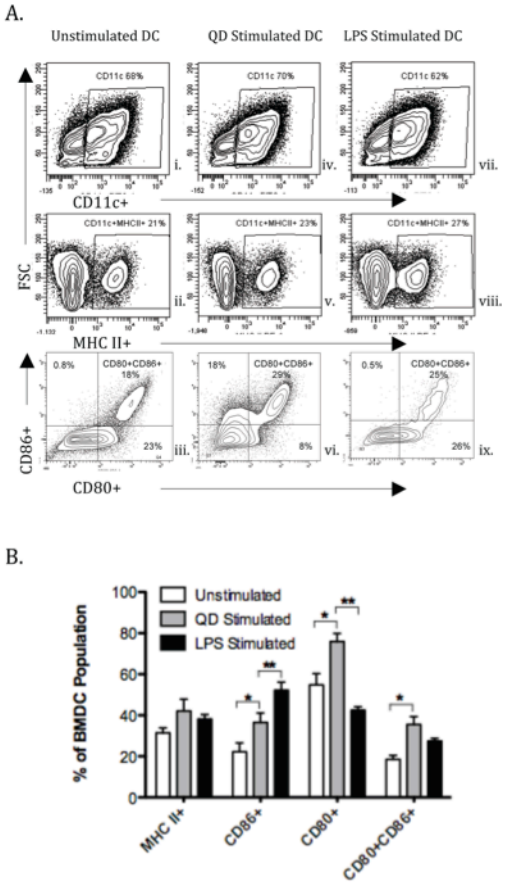

Figure 4.5 Activation of BMDCs by QD nanoparticles. Panel A, representative of one experiment in which BMDCs (1 x10^6 cells) were incubated with media alone, QD nanoparticles, or LPS at 37°C for 24 hours. Cells were stained for surface markers: CD11c-FITC, MHC II-PE, CD80-APC, and CD86-PE-Cy7 and analyzed using flow cytometry. Panel i. gated for CD11c+ BMDCs, Panel ii. & iii. are live gates of Panel i. and stained for MHC II, CD80, and CD86. Similarly, Panel v. and vi. are live gates of Panel iv.; and Panel viii and ix are live gates of Panel vii. Panel B, summary of three BMDC activation experiments. Significant differences were observed between unstimulated and QD-stimulated DCs (*) for the expression of CD86+ (p= 0.0431), CD80+ (p= 0.0172), and CD80+/CD86+ (p= 0.0086). Significant differences were also observed between QD-stimulated DCs and LPS-stimulated DCs (**) for the expression of CD86+ (p=0.0312) and CD80+ (p=0.0007).

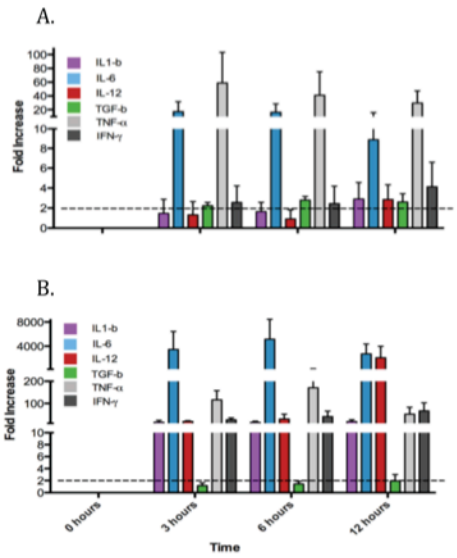

Figure 4.6 Cytokine expression by stimulated BMDCs. RT-PCR quantification of expression of six different cytokine genes in QD-stimulated dendritic cells (Panel A)and LPS-stimulated dendritic cells (Panel B) over a 12-hour period. Data were first normalized to GAPDH and fold changes were calculated based on "0 hour" samples.

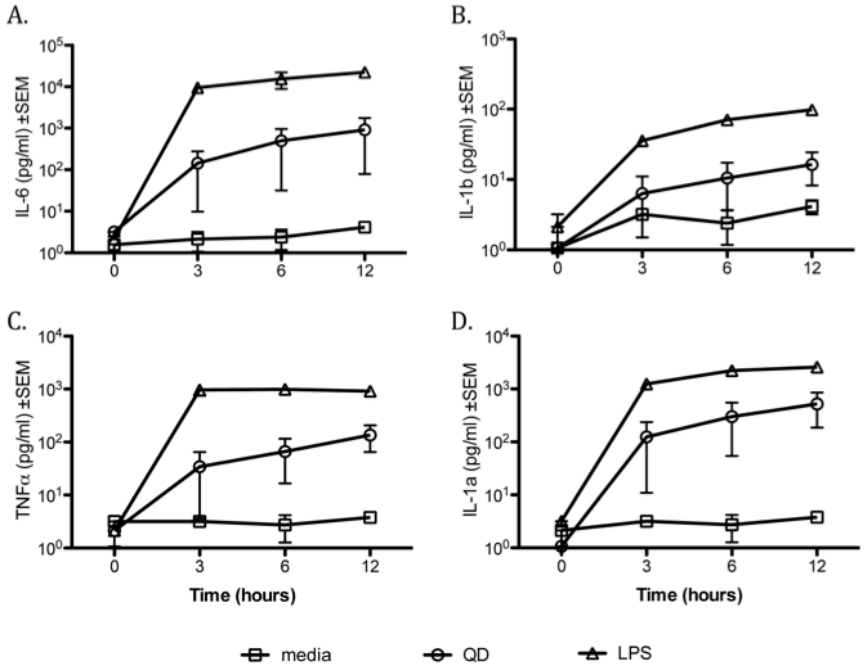

Figure 4.7 Cytokines production by stimulated BMDCs. BMDCs ($1x10^6$ cells)were incubated with media alone (open squares), QD nanoparticles (4uM) (open circles), or LPS (100 ng/ml) (open triangles). Culture supernatants were collected at 0, 3, 6, and 12 hours and cytokines IL-6 (A), IL-1b (B), TNF-α (C), and IL-1a (D) were measured by Luminex using the Milliplex MAP Mouse Cytokine/Chemokine 32 plex assay. Only the cytokines with highest expression detected are depicted here. Cell supernatants were measured in triplicates.

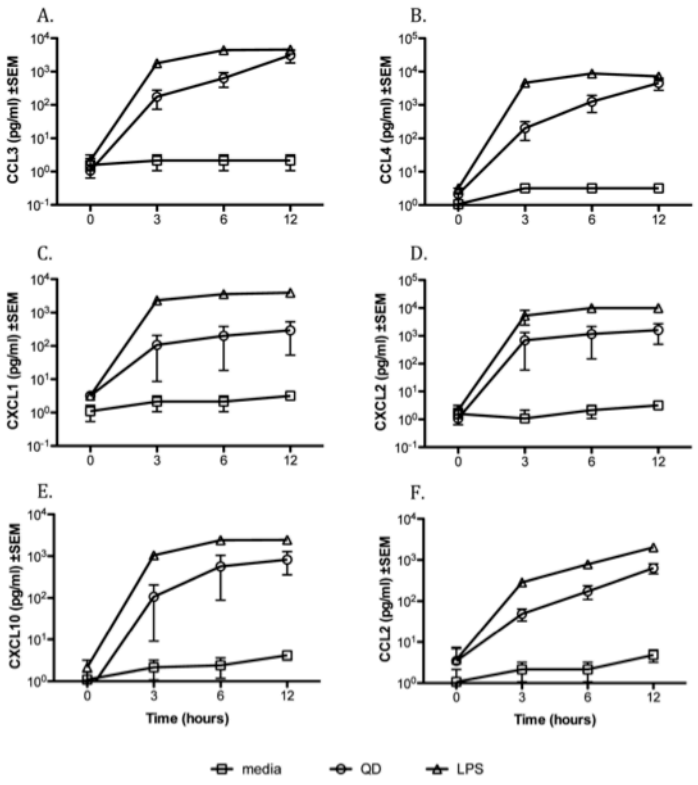

Figure 4.8 Chemokines production by stimulated BMDCs. BMDCs ($1x10^6$ cells)were incubated with media alone (open squares), QD nanoparticles (4 uM) (open circles), or LPS (100 ng/ml) (open triangles). Culture supernatants were collected at 0, 3, 6, and 12 hours and chemokines CCL3 (A), CCL4 (B), CXCL1 (C), CXCL2 (D), CXCL10 (E), and CCL2 (F) were measured by Luminex using the Milliplex MAP Mouse Cytokine/Chemokine 32 plex assay. Only the chemokines with highest expression detected are depicted here. Cell supernatants were measured in triplicates.

Table 4.1 Sequences of RT-PCR primers

Gene	GenBank Accession #	Primer*	Sequence (5' ➔ 3')
IL-1β	NM_008361	F	TGGAGAGTGTGGATCCCAAGCAAT
		R	ATGGTTTCTTGTGACCCTGAGCGA
IL-6	NM_031168	F	ATCCAGTTGCCTTCTTGGGACTGA
		R	TGGTACTCCAGAAGACCAGAGGAA
IL-12p40	NM_008352	F	ACCTGTGACACGCCTGAAGAAGAT
		R	AGAGACGCCATTCCACATGTCACT
TGF-β	M13177	F	TAAAGAGGTCACCCGCGTGCTAAT
		R	TTTGCTGTCACAAGAGCAGTGAGC
TNF-α	NM_008352	F	AGCTCAAACCCTGGTATGAACCCA
		R	AGTCCTTGATGGTGGTGCATGAGA
IFN-γ	XM_125899	F	TGCATCTTGGCTTTGCAGCTCTTC
		R	TGGGTTGTTGACCTCAAACTTGGC
GAPDH	M32599	F	TGTGATGGGTGTGAACCACGAGAA
		R	GAGCCCTTCCACAATGCCAAAGTT

* F, forward primer; R, reverse primer

Table 4.2 Immunoglobulin Isotype Specific Antibodies Against MSP1-19 in Mice Immunized with rMSP1 in Different Adjuvant/Delivery System[@]

Immunogen	IgG1	IgG2a	IgG1/IgG2a[†]*
rMSP1-QD (i.p.)	1.567±0.342	0.499±0.132	4.147±1.561
rMSP1-QD (i.m.)	1.431±0.114	0.667±0.217	3.161±0.882
rMSP1-QD (s.c.)	1.399±0.132	0.579±0.190	4.487±1.492
rMSP1-ISA51 (i.p.)	1.363±0.344	0.028±0.009	101.8±51.88
rMSP1-CFA (i.p.)	1.239±0.320	0.721±0.314	2.989±1.148

[@]Mean O.D.±SD are shown for IgG1 and IgG2a
[†]Mean mean ratio of O.Ds IgG1/IgG2a ±SD
*****Unpaired t test performed. Significantly different from the rest of the groups

Table 4.3 In vitro Parasite Growth Inhibition of Purified Mouse Anti-Mouse Antibodies

Pooled Mouse Purified Antibody (Tertiary Bleeds)	% Parasite growth inhibition@
rMSP1-QD (i.p.)	81%
rMSP1-QD (i.m.)	73%
rMSP1-QD (s.c.)	78%
rMSP1-CFA (i.p.)	17%
rMSP1-ISA51 (i.p.)	0%

@Mean of two growth inhibition assays

Chapter 5

Title: Iron Oxide Nanoparticles as a Delivery Platform for a Recombinant Protein Blood-Stage Malaria Vaccine

Authors: Kae Pusic[1]*, Zoraida Aguilar[2], Sophie Kobuch[1], Hong Xu[2], Mazie Tsang[1], Andrew Wang[2], George Hui[1]

[1]*University of Hawaii, School of Medicine, Department of Tropical Medicine, Honolulu, HI, USA*; [2]*Oceannanotech LLC, Springdale, AR, USA*

Short title: IO Nanoparticles as a Malaria Delivery Platform

rMSP1: recombinant truncated MSP1-42 malaria vaccine antigen (Construct I)

Abstract

Iron Oxide (IO) nanoparticles have been approved in a number of clinical applications. This study demonstrated the use of IO nanoparticles (<15nm) as a potent vaccine delivery platform to enhance the immunogenicity of antigens without additional adjuvants. A recombinant truncated Merozoite Surface Protein 1-42 malarial antigen (rMSP1), was used as the model vaccine conjugated to IO nanoparticles. rMSP1-IO was immunogenic in mice and its immunogenicity was equal to those obtained with rMSP1 administered with a clinically acceptable and commercially available adjuvant, Montanide ISA51. Aotus monkeys immunized with rMSP1-IO also achieved good immune responsiveness and induced significant levels of parasite inhibitory antibodies. There was no apparent local or systemic toxicity associated with IO immunization. Dendritic cells efficiently took up IO nanoparticles, which led to their activation and expression/secretion of co-stimulatory molecules, cytokines and chemokines. Thus, IO nanoparticles exhibit promise as an effective and safe platform to deliver recombinant protein vaccines.

Key Words: Nanoparticles, Malaria Vaccine, Adjuvant, Dendritic Cells

Introduction

Currently, there are very limited numbers of adjuvant formulations approved for use in vaccines, for example MF59 [1], alum [1], Montanide ISA51 [1], and ASO2A.[2] The development of new adjuvants has not kept pace with the increasing demand for their use in vaccine formulations. The fact that adjuvants often influence the quality of the immune responses in different ways [3] indicates that there is not a single adjuvant formulation that will be universally effective for all vaccines. Thus, new and alternative strategies need to be explored to expand the portfolio of vaccine adjuvants and delivery platforms. One potential strategy makes use of particle-mediated delivery systems such as micro and nanoparticles, in an attempt to try to improve immunogenicity through targeted antigen delivery and/or presentation. [4] Among such particles being evaluated are biodegradable polymers (eg. PLGA, PGA, PLA) [5-8]; virus-like particles (VLP) [9, 10]; Immune Stimulating Complexes (ISCOMS) [11, 12]; chitosans [13-15]; and inorganic particles. [16] Some vaccines, such as the Hepatitis B vaccine and the human papilloma virus vaccine, are already on the market utilizing the VLP technology. [17, 18] Other examples of experimental use of nanoparticles for vaccine delivery are: the Self-Assembling Polypeptide-based Nanoparticles (SAPN) for a peptide sporozoite malaria vaccine [19], nanolipoproteins for vaccines against West Nile Encephalitis [4], and poly(propylene sulfide) nanoparticles for intranasal delivery of peptide antigens to enhance mucosal immune responses. [20]

In a previous study, we investigated the use of <15 nm solid nanoparticles, Quantum Dot (QDs), as a vaccine delivery platform. QDs were found to be far superior in enhancing immunogenicity and efficacy for the recombinant subunit proteins tested than conventional adjuvants such as Freund's Complete Adjuvant and Montanide ISA51. Additionally, it was demonstrated that these QD nanoparticles were readily taken up by professional antigen presenting cells (ie. dendritic cells), which were then activated to express co-stimulatory molecules, and secrete pro-

inflammatory cytokines and chemokines. Despite these positive and promising results, QD nanoparticles are not compatible for human use due to the presence of cadmium (Cd) in the particle core. Hence, in this study we explored using a type of clinically acceptable nanoparticle, Iron Oxide (Fe_2O_3) as an alternative.

Iron oxide nanoparticles differing in size (15-180 nm) and surface modifications are currently employed in several medical applications. [21] Dextran-coated superparamagnetic iron oxide (SPIO) nanoparticles are used as MRI contrast agents. [22] Another SPIO particle of a smaller size is undergoing clinical trials for lymph node metastasis detection. [23] In addition to MRI agents, IO nanoparticles are being used for drug delivery/targeting and hyperthermia. [21] Other potential clinical applications of IO nanoparticles include cancer imaging, stem cell tracking, and monitoring of transplanted tissues. [21] Feraheme, a form of iron oxide nanoparticles, is FDA approved for the treatment of iron deficiency anemia in adult patients with chronic kidney diseases and is administered intravenously (IV).[24] The IOs being evaluated in this study are small (<15 nm), stable, behaves like a true solution and has an amphiphilic polymer coating. The surface layer contains carboxylate groups which are readily available for conjugation with proteins, peptides, and DNA. [25-27] Previous studies indicate that particle size is an important factor in determining the ability of the nanoparticles to achieve effective delivery of the payload. [28] Small particle sizes (<15 nm) may facilitate rapid dispersion and tissue penetration to reach immunological sites and organs. As we have demonstrated the effectiveness of QD (<15 nm) in vaccine delivery [29], we hypothesized that IO of similar size and surface characteristics will demonstrate comparable efficacy.

In this study we used a recombinant malaria vaccine antigen, *P. falciparum* Merozoite Surface Protein 1-42 (rMSP1), as a model immunogen to evaluate IO nanoparticles in an adjuvant-free vaccine delivery platform. The Merozoite Surface Protein 1-42 is found on the surface of the invading merozoites during the

erythrocytic stage of the malaria life cycle [30, 31], and is one of the most promising and most studied malaria vaccine candidates. [32-36] Protective immunity to malaria infections has been correlated with parasite inhibitory antibodies specific for MSP1-42. [34, 35, 37-41] The rMSP1 conjugated to IOs (rMSP1-IO) was used to immunize outbred mice, rabbits and Aotus monkeys. Results showed that rMSP1-IO was as effective in enhancing immunogenicity as rMSP1 administered with a clinically acceptable adjuvant, Montanide ISA51. Moreover, rMSP1-IO induced parasite inhibitory antibodies in more than one animal species. Preliminary toxicity studies in mice and monkeys showed no significant deviations from normal values. Lastly, we investigated the effects of IO uptake by dendritic cell and macrophages as the possible mode of action in enhancing vaccine induced immune responses. Therefore our results indicate that, IO nanoparticles represent a viable vaccine delivery platform for further clinical development.

Materials and Methods

Mouse, Rabbit, and Non-human Primates

Outbred Swiss Webster (SW) mice and C57Bl/6 mice (female, 6-8 weeks old) were obtained from Charles River Laboratory (Wilmington, MA). New Zealand White (NZW) rabbits (female, 8-10 lbs) were obtained from Western Oregon Rabbit Company (Philomath, Oregon). *Aotus lemurinus trivirgatus* karyotype II and III adult monkeys (one female and three males) were colony born and raised at the University of Hawaii's Non-human Primate Facility. Use of all animals was approved by the University of Hawaii's Institutional Animal Care and Use Committee.

Recombinant MSP1-42 (rMSP1)

A truncated version of MSP1-42 (rMSP1) was expressed in *Drosophila* cells [42] and purified by affinity chromatography. [43] Figure 1A shows SDS-PAGE profile of the purified protein. The rMSP1 has been shown to induce parasite inhibitory antibodies. [44]

Conjugation of rMSP1-42 to Iron Oxide Nanoparticles

The rMSP1-IO conjugates were prepared using N-hydroxysulfosuccinimide sodium salt (sulfo-NHS) and 1-ethyl-3-(3-dimethylaminopropyl) carbodiimide (EDC) covalent coupling chemistry. IOs with carboxyl groups on the surface (5 mg/ml) were activated by incubating with sulfo-NHS (molar ratio 2000:1) and EDC (molar ratio 2000:1) for 5 minutes in borate buffer, pH 5.5, after which the pH was adjusted to 8.0 and 2 mg of rMSP1 was added, vortexed thoroughly, and incubated for 2 h at room temperature. Following incubation, the reaction was quenched by adding 5 µl of Ocean NanoTech's quenching buffer, mixed, and incubated for 10 minutes at room temperature. The rMSP1-IO conjugates were then purified/separated by using a SuperMag Separator™ (OceanNanoTech, Springdale, AR) for 10-24 hours.

The rMSP1-IO conjugates and unconjugated IOs were evaluated by agarose (1.5%) gel electrophoresis in Tris-acetate-EDTA (TAE) buffer, pH 8.5. For each well, 20 µl of IO samples at 100 nM were mixed with 10% (v/v) glycerol. The gel was resolved at 100 V for 30 min (PowerPak Basic, Bio-Rad, USA) then imaged using a gel imaging system (Alpha Imager HP 2006, Alpha Innotech, USA) (Figure 1B).

Antigenicity of rMSP1 conjugated to IO Nanoparticles

Freshly prepared rMSP1-IO and rMSP1-IO stored at 4^{o}C for 6 and 12 months were used. Serial dilutions of rMSP1-IO were used for coating ELISA plates. MAb 5.2 was used at a 1:200 dilution in 1% yeast extract, 0.5% BSA in BBS. Horseradish peroxidase (HRP) conjugated anti-mouse antibodies (H & L chain specific) (Kirkgaard and Perry Laboratories, Gaithersburg, MD) at a dilution of 1:2000 were used as a secondary conjugate. Color development was made using the peroxidase substrates, H_2O_2 and 2.2'-azinobis(3-ethylbenzthiazolinesulfonic acid)/ABTS (Kirkgaard and Perry Laboratories, Gaithersburg, MD). Optical density (O.D.) was determined at 405 nm. ODs for each serial dilution was plotted and the levels of reactivity were compared to the standard reactivity of mAb 5.2 against unconjugated rMSP1.

Immunizations with rMSP1-IO

Groups of SW mice (n = 6) were immunized with rMSP1-IO via intra-peritoneal (i.p), intra-muscular (i.m), and subcutaneous (s.c) routes. Injection volume for i.p and s.c routes were 100ul/dose (16 µg/dose), and i.m route was 20 ul/dose (5 µg/dose). Mice were also immunized via i.p. with rMSP1 emulsified in either CFA/IFA or Montanide ISA51. Mice were immunized three times at 21 days intervals. The first immunization consisted of a sub-optimal dose of 2µg antigen, followed by two booster injections with an optimal dose of 5µg [45]. Sera were obtained through tail bleeds on the 14th day after each immunization.

New Zealand White rabbits were also immunized with rMSP1-IO. Briefly, 0.5 ml/dose (80 µg antigen/dose) of rMSP1-IO was injected intramuscularly into the left and right thighs. A total of four immunizations were given at 4 week intervals. Sera collected 21 days after the last immunization was used in ELISAs and parasite growth inhibition assays. As a control, rabbits were similarly immunized with 50 µg of rMSP1 antigen in 250 µl PBS emulsified with an equal volume of Montanide ISA51 into the left and right thighs.

Aotus lemurinus trivirgatus monkeys were likewise immunized with rMSP1-IO, 0.5 ml/dose (80 µg antigen/dose), via the i.m. route. Immunizations were administered three times at 21 day intervals, alternating the right and left thigh. Sera were collected 21 days after the last immunization for ELISAs and parasite growth inhibition assays.

MSP1-specific Antibody Assays

Mouse, rabbit, and monkey sera were assayed for anti-MSP1 antibodies (MSP1-42 and MSP1-19 specific) by direct binding ELISA as previously described [46]. The MSP1-19 and MSP1-42 used for coating ELISA plates were expressed in yeast [47] and in baculovirus [43]; respectively. MSP1-19 and MSP1-42 was used to coat the plates at a concentration of 0.4 µg/ml. Sera were serially diluted in 1% yeast extract, 0.5% BSA in BBS. HRP-conjugated anti-mouse antibodies (H & L chain specific) (Kirkgaard and Perry Laboratories, Gaithersburg, MD) were used as a secondary conjugate at a dilution of 1:2000; HRP-conjugated anti-rabbit antibodies (Kirkgaard and Perry Laboratories, Gaithersburg, MD) were used at a dilution of 1:2000; and HRP-conjugated, anti-Aotus antibodies, graciously provided by Hawaii Biotech Inc, were used at a dilution of 1:16000. Color development was performed by using the peroxidase substrates, H_2O_2 and 2.2'-azinobis(3-ethylbenzthiazolinesulfonic acid)/ABTS (Kirkgaard and Perry Laboratories, Gaithersburg, MD). Optical density

(O.D.) was determined at 405 nm. End point titers were calculated using the serum dilutions that gave an O.D. reading of 0.2, which is greater than 4-fold of background absorbance using pre-immune mouse, rabbit, or monkey serum samples.

IFN-γ and IL-4 ELISPOT Assays.

ELISPOT assays of splenocytes from immunized mice were performed according to methods previously described. [48] Briefly, ninety-six well PVDF plates (Millipore Inc., Bedford, MA) were coated with 10 μg/ml of monoclonal antibodies (mAb) against IFN-γ (R4-642) and 5μg/ml of mAb against IL-4 (11B11) (BD Biosciences, San Diego, CA), and incubated overnight at room temperature. Plates were washed with Phosphate Buffered Saline (PBS) and blocked with 10% fetal bovine serum in DMEM for 60 minutes. Mouse spleens were harvested and single cell suspensions of splenocytes were prepared as previously described. [49] Purified splenocytes were plated at $0.5x10^6$, $0.25x10^6$, and $0.125x10^6$ cells per well and rMSP1 (4 μg/ml) was added to each well as the stimulating antigen. Positive control wells were incubated with 5 ng/ml of phorbol myristate acetate (PMA) and 1 ng/ml ionomycin. Plates were incubated at 37º C in 5% CO_2 for 48 hours. Wells were washed and incubated with biotinylated mAb against IFN-γ at 2 μg/ml (XMG1.2), or mAbs against IL-4 at 1μg/ml (BVD6-24G2) (BD, Biosciences, San Diego, CA), followed by the addition of peroxidase conjugated streptavidin (Kirkgaard and Perry Laboratories, Gaithersburg, MD) at a concentration of 1:800. Spots were developed with a solution consisting of 3,3'-diaminobenzidine tetrahydrochloride (DAB) (Sigma-Aldrich St. Louis, MO, 1mg/ml) and 30% H_2O_2 (Sigma-Aldrich St. Louis, MO) and enumerated microscopically. Data were presented as spot-forming-units (SFU) per million of isolated splenocytes.

In vitro Parasite Growth Inhibition Assay

The ability of mouse, rabbit, and monkey sera, generated by immunizations with rMSP1-IO, to inhibit parasite growth was determined using the *in vitro* assay. [50-53] For testing mouse serum samples, immunoglobulins from pooled mouse serum samples from each group were purified as previously described. [54] Briefly, antibodies were purified by ammonium sulfate precipitation followed by dialysis using an Amicon Ultra-10 (Millipore, Billerica, MA) with a molecular weight cut off of 100 kDa. Purified mouse antibody samples were reconstituted to original serum volume with RPMI 1640 medium and were used at a 20% serum concentration. For testing of rabbit and monkey samples, individual serum samples were heat inactivated, absorbed with normal RBCs, and used at a 30% final serum concentration. [47] Inhibition assays were performed using sorbitol synchronized parasite cultures (3D7 strain) as described [47]. Synchronized parasite cultures at a starting parasitemia of 0.2% and 0.8% hematocrit were incubated in antibody or serum samples for 72 hours with periodic mixing. Culture parasitemias were determined microscopically by Giemsa staining of thin blood smears, and the degree of parasite growth inhibition was determined by comparing the parasitemias of immune sera with the corresponding pre-immune sera as previously described [47, 52, 53].

Toxicity Studies on IO immunized mice and Aotus Monkeys

Mice were divided into four groups receiving escalating doses of IO nanoparticles ranging from 1.1 mgs to 4.4 mgs and one control group receiving no IO nanoparticles. Mice in each group were immunized three times every 21 days with their corresponding IO doses. All mice were bled prior to and post IO immunizations. Blood was directly placed into i-STAT EG6+ Cartridges and read by the i-STAT Blood Analyzer (Abbott Diagnostic Laboratories, Abbott Park, IL) for hematocrit, hemoglobin, blood urea nitrogen, anion gap, carbon dioxide and potassium levels.

Aotus monkeys immunized with rMSP1-IO were bled prior to and post 3rd booster immunization for blood chemistry tests. Whole blood and serum samples were sent to IDEXX Laboratories Inc. in Westbrook, Maine and blood chemistry tests were performed. Detailed results of tests performed are listed in Table 5.6.

Dendritic Cell and Macrophage Isolation and IO Uptake Assay

Immature bone marrow cells were isolated from 12-14 week old C57Bl/6 mice as described. [55] Stromal cells were purified by passage through a cell strainer to remove bone and debris. RBC lysis buffer consisting of 0.15 M NH_4Cl, 10 mM $KHCO_3$, and 0.1mM EDTA was used in order to remove red blood cells. After washings, bone marrow cells were plated in 6-well plates (Cell Star, Monroe, NC) at a density of 10^6 cells/ml together with either GM-CSF (Peprotech Inc, Rocky Hill, NJ) at a concentration of 20 ng/ml or with M-CSF (eBioscience, San Diego, CA) at a concentration of 10 ng/ml. After 24 hours, cell cultures were incubated in RPMI 1640 with GM-CSF for an additional 8 days for differentiation into dendritic cells (BMDC) or incubated for an additional 6 days in DMEM with M-CSF for differentiation into macrophages. [56] On Day 8, BMDCs in suspension were transferred to new plates and used as the cell source for all subsequent experiments. [57] Experiments were performed using macrophages from Day 6 cultures. [56]

Unconjugated IO nanoparticles were introduced at a concentration of 5 mg/ml to the 8-day old BMDCs or 6-day old macrophages and incubated for 24 hours at 37°C. To first visualize the uptake of iron oxide nanoparticles, BMDCs and macrophages were fixed with 4% paraformaldyhde (PFA) and stained with Prussian Blue (Biopal, Worcester, MA) according to manifacture's protocol (http://www.biopal.com/Molday%20ION.htm). The same cells were then stained for surface markers anti-CD11c or anti-CD11b-biotin antibodies (eBioscience, San Diego, CA) at a dilution of 1:2000 for one hour, washed, and then further labeled with

streptavidin-QDots, which has an emission wavelength of 620nm (Oceannanotech, Springdale, AR), for an additional hour for identification and purity assessment. Cells were then imaged using a fluorescent microscope (Olympus ix71) with a fluorescent cube containing the following filters: V-N41004 (ex560 and em585) and V-N41001 (ex480 and em535).

Dendritic Cell and Macrophage Activation by IOs

Unconjugated Iron Oxide nanoparticles (5 mg/ml) were introduced to 7-day old BMDCs [58] or 6-day old macrophages for 24 hours at 37°C. The cells were harvested and washed twice with FACS buffer (PBS with 2% FBS) and fixed with 0.25% PFA for 10 minutes on ice. Cells were separated by passing through a magnetic LD column (Miltenyi Biotec Inc., Auburn, CA) to obtain an enriched population of cells that have taken up the IO nanoparticles. BMDCs and macrophages were stained with cell surface markers: (APC)-labeled anti-CD80, (PE)-labeled anti-MHC II, (AlexaFluor488)-labeled anti-CD11c or (AlexaFluor488)-labeled anti-CD11b (eBiosciences, San Diego, CA), and (PE-Cy7)-labeled anti-CD86 (Invitrogen, Carlsbad, CA). Labeled cells were analyzed using the FACSAria flow cytometer with FACSDiva software (Becton Dickinson, San Jose, CA).

Cytokine Gene Expression by IO stimulated Dendritic Cells and Macrophages

BMDCs and macrophages (3×10^6 cells) were stimulated with unconjugated IO or LPS (concentration) and RNA was extracted at 0, 3, 6, and 12 hours using the RNeasy Kit (Qiagen, Valencia, CA). RNA concentrations were measured and then reversed transcribed in 50 ul reactions using the iScript cDNA synthesis kit (Bio-Rad, Hercules, CA) following manufacturer's protocol. Real-time PCR reactions using iQ SYBR Green Supermix (Bio-Rad, Hercules, CA) were run on the MyiQ Single-Color Real Time Detection System (Bio-Rad, Hercules, CA). Primers for TNF-α, TGF-β, IL-

12, IL-6, IFN-γ, IL-1β were used at 10 nM (IDT, Coralville, Iowa). Primer sequences are provided in Table 5.1. Analysis of gene expression was performed by the ΔΔCt method. [59, 60] Briefly, each sample was normalized to an endogenous control, GAPDH, and fold change for each assayed gene was determined via the ΔΔCt.

Multiplex Assay for Cytokine Detection

Supernatants from IO and LPS stimulated BMDCs were tested for the presence of cytokines/chemokine over a 12 hour period. Cytokines and chemokines were measured using the Milliplex MAP Mouse Cytokine/Chemokine 32-plex assay (Millipore Corp, Billerica, MA) as described. The following cytokines were measured: Eotaxin, G-CSF, GM-CSF, IFN-γ, IL-10, IL-12 (p40), IL-12 (p70), IL-13, IL-15, IL-17, IL-1α, IL-1β, IL-2, IL-2, IL-4, IL-5, IL-6, IL-7, IL-9, IP-10, KC-like, LIF, LIX, M-CSF, MCP-1, MIG, MIP-1α, MIP-1β, MIP-2, RANTES, TNF-α, VEGF.

Data Handling and Statistics

SigmaPlot 10 and GraphPadPrizm 4 were used to calculate the end point titers. The Mann-Whitney test was used to determine significant differences in antibody responses, and the expression of cell surface activation markers among the test groups. A p value of < 0.05 was considered statistically significant.

Results

Antigenicity of rMSP1-conjugated IO Nanoparticles

To determine if rMSP1 was successfully conjugated to IO nanoparticles, unconjugated and conjugated IOs were analyzed by agarose gel electrophoresis (Figure 5.1B). The rMSP1-IO sample (Lane 2) migrated as a single band and at a higher molecular mass than the unconjugated IO sample (Lane 1), indicating that the conjugation process had successfully produced a homogeneous species of rMSP1-IOs. To evaluate if the chemical conjugation process affected the antigenicity and stability of rMSP1, the reactivity of a conformational dependent anti-MSP1-42 monoclonal antibody, mAb 5.2, with rMSP1-IO was tested. MAb 5.2 strongly reacted with the rMSP1 conjugated to IO nanoparticles but did not recognize the unconjugated IO particles (Figure 5.2A). As a reference, an O.D. reading of 1.3 was observed with mAb 5.2 incubated with unconjugated rMSP1-42 at a plating concentration of 0.4 µg/mL. This suggests that the antigenicity of the rMSP1 antigen was preserved during the conjugation process. The conjugated nanoparticles stored at 4°C were tested over a period of 12 months for any loss of antigenicity of the rMSP1. The rMSP1-IO was equally reactive with mAb 5.2 at 6 and 12 months post-conjugation (Figure 5.2B), thus demonstrating the stability of these conjugated IO nanoparticles.

Immunogenicity of rMSP1-IO Nanoparticles in Swiss Webster Mice

The immunogenicity of rMSP1-IO was compared to that of rMSP-1 combined with conventional adjuvants. SW mice were immunized with rMSP1 conjugated to IO nanoparticles, or formulated with CFA or Montanide ISA51. Immune sera were tested for antibodies against MSP1-19 by ELISA. Vaccine responders were defined as having an ELISA O.D. >0.2 at a 1/50 serum dilution. [29, 44] which was above the O.D. values observed for pre-immune mouse sera. The rMSP1-IO induced an

antibody response in all six mice after three immunizations, resulting in a 100% response rate. The same response rate was observed with mice immunized with rMSP1-CFA. However, only five of ten mice immunized with rMSP1-ISA51 responded, resulting in a 50% response rate (Figure 5.3A).

Comparisons of antibody end-point titers of tertiary bleeds amongst the three vaccination groups showed that rMSP1-IO induced a mean antibody titer of $2.7x10^{-3}$ (Figure 5.3A), whereas the ISA51 formulation induced a lower mean antibody titer of $1.6x10^{-3}$ ($p=0.012$). The potent CFA formulation induced the highest mean antibody titer of $2.8x10^{-4}$; however, this level was not significantly higher than rMSP1-IO (Figure 5.3A). Vaccinations using CFA and ISA51 induced high and low responders within the group of immunized outbred mice, as reflected in the broad range of end-point titers. Encouragingly, rMSP1-IO induced a more uniform response (Figure 5.3A).

Mice were also immunized with rMSP1-IO via the i.m. and s.c. routes. Analysis of end-point titers revealed that the mean antibody titers induced by i.m. immunization were higher compared to that induced by i.p. or s.c. immunizations (Figure 5.3B), but the difference was not statistically significant (Figure 5.3B). Only immunizations via the i.m. and i.p. routes achieved a 100% response rate, whereas s.c. immunization resulted in a 60% response rate (Figure 5.3B).

Sera from rMSP1-IO immunized mice were also tested for their ability to inhibit parasite growth in vitro. [61, 62] Inhibition greater than 50% was considered to be biologically significant. [61, 62] As shown in Table 5.2, antibodies obtained from rMSP1-IO immunizations via the i.p. and i.m. route significantly inhibited parasite growth at 80% and 74% respectively. In comparison, antibodies from mice immunized with rMSP1 emulsified with CFA and ISA51 were both ineffective in inhibiting parasite growth (Table 5.2). In addition, IO immunization via the s.c. route was also ineffective at a 37% parasite growth inhibition (Table 5.2).

IO immunized mice showed a Predominant IL-4 Cellular Response.

ELISPOT of splenocytes from mice immunized with rMSP1-IO via the i.m., s.c., and i.p. routes showed higher production of IL-4 as compared to IFN-γ production (Figure 5.4 A and B), indicative of a TH2 type response. Immunization by i.p. rMSP1/ISA51 or rMSP1-IO via all three routes induced a significantly higher IL-4 response than that observed with rMSP1-CFA (Figure 5.4A). Of the rMSP1-IO immunizations, i.p. and s.c. delivery were especially effective, and gave a significantly higher IL-4 response than i.m. injections ($p=0.015$ and $p=0.014$ respectively) (Figure 5.4A).

Immunogenicity of rMSP1-IO Nanoparticles in New Zealand White Rabbits and in Aotus Monkeys

Rabbit sera from quaternary bleeds were tested by ELISA for antibodies specific for MSP1-19 and MSP1-42.[46] All immunized rabbits developed an antibody response (Table 5.3), with MSP1-42 specific titers ranging from 1/4,500 to 1/28,000; and MSP1-19 specific titers ranging from 1/3,500 to 1/22,000. These antibody titers were lower than those induced by rMSP1 immunized with Montanide ISA51. [44] The ability of rabbit sera generated by immunization with rMSP1-IO to inhibit in vitro parasite growth was also evaluated. [61] Only one out of three rabbits induced significant levels of growth inhibitory antibodies with a 71% inhibition (Table 5.3). In contrast, rabbits immunized with rMSP1 emulsified in ISA51 induced significant levels of inhibitory antibodies in all three animals. [44]

All four Aotus monkeys immunized with rMSP1-IO produced anti-MSP1-42 and anti-MSP1-19 antibodies (Table 5.4), with endpoint titers specific for MSP1-42 ranged from 1/2,800 to 1/29,000; and those specific for MSP1-19 ranged from 1/3,000 to 1/24,000 (Table 5.4). Sera from Aotus monkeys immunized with rMSP1-IO were also evaluated for inhibition of parasite growth as above. [61] All immunized

monkeys produced significant levels of parasite growth inhibitory antibodies, ranging from 55% to 100% inhibition (Table 5.4). This level of inhibition is comparable to studies where Aotus monkeys were vaccinated with MSP1-42-CFA. [35]

Toxicity Studies showed no Abnormalities in IO Immunized Animals

Escalating injection doses of IO nanoparticles, up to 4.4 mg per injection, did not cause any abnormalities or changes in the blood chemistries in all four groups of mice, tested after each of the three immunizations (Table 5.5). Similarly, a more comprehensive test panel of blood chemistry levels in the Aotus monkeys after three rMSP1-IO immunizations revealed no significant deviations from normal ranges (Table 5.6). In addition, no inflammation or swelling was observed at the site of injection. Thus, immunization with IO nanoparticles did not have toxic systemic affects in either animal model.

Uptake of IO Nanoparticles by Dendritc Cells and Macrophages

IO nanoparticles were introduced to 7-day old BMDC cultures and to 6-day old macrophage cultures. BMDCs and macrophages both actively internalized the IO nanoparticles as shown in Figure 5.5 (A-D). BMDCs were identified by staining for the surface marker, CD11c (Figure 5.5A) and the presence of internalized iron oxide particles was identified by Prussian Blue staining (Figure 5.5B). Approximately 89% of the BMDCs internalized IOs. Macrophages were identified by staining for the surface marker, CD11b (Figure 5.5C) and approximately 94% of these cells internalized IO nanoparticles as revealed by Prussian Blue staining (Figure 5.5D).

Dendritic Cell and Macrophage Activation by IOs

Unconjugated IO nanoparticles were introduced to immature BMDCs and macrophages and the degree of activation was determined by cell surface expression

of CD86, and CD80 using Flow Cytometry. [29] Unstimulated, IO-stimulated, and LPS-stimulated dendritic cells were first gated for the presence of CD11c, and the CD11c+ cells were analyzed for the expression of activation markers, MHC II, CD86, and CD80. IO-stimulated, CD11c positive dendritic cells (Figure 5.6A, Panel iv) were activated and showed an increase in expression of MHC II (Figure 5.6A, Panel v), CD86, and CD80 (Figure 5.6A, Panel vi). IO-stimulated dendritic cells had the highest percentage of MHC II marker (34%) and CD80 marker (28%) as compared to unstimulated dendritic cells (28% and 22% respectively). However, these increases did not reach statistical significance (Figure 5.6B). The percentages of CD86+ cells and CD80/86 double positive cells were significantly higher than those observed for unstimulated dendritic cells, with p values of 0.05 and 0.03; respectively (Figure 5.6B). LPS-stimulated DCs had significantly higher percentage of CD86+, and CD80/86+ cells than IO-stimulated DCs (p values 0.05 and 0.04 respectively) (Figure 5.6B).

Unstimulated, IO-stimulated, and LPS-stimulated macrophages (CD11b+) were similarly analyzed for the activation markers as above. IO-stimulated macrophages did not significantly up-regulate any of the markers as compared to the unstimulated macrophages (Figure 5.6C). However, LPS-stimulated macrophages expressed significantly higher levels of CD86 and CD80/CD86 than unstimulated cells (p values 0.05 and 0.03 respectively) (Figure 5.6C).

IO Uptake Induced Pro-inflammatory Cytokine and Chemokine Production by BMDCs, but not Macrophages.

Immature BMDCs were exposed to IO nanoparticles over a 12-hour period and the expression of several cytokines, IL-6, IL-12, IL-1b, TNF-α, IFN-γ, TGF-β, were monitored by RT-PCR. IO nanoparticles significantly increased the production of IL-6, TNF-α, IL1-b, IFN-γ, and IL-12 by more than two fold in BMDCs compared to

baseline, i.e. 0 hour (Figure 5.7A). In particular, IL-6 and TNF-α were highly expressed (Figure 5.7A). LPS-stimulated BMDCs induced significant expression of all cytokines assayed with the exception of TGF-β (Figure 5.7B). In general, the cytokine expression profiles of LPS- and IO-stimulated BMDCs were similar.

In order to broaden our detection targets, a 32-plex Luminex^{R} assay was performed to test for cytokine and chemokine production. BMDCs stimulated with either IO nanoparticles or LPS were found to secrete cytokines (Figure 5.8) and chemokines (Figure 5.9) over a 12 hour time course. In comparison to media alone, IO stimulated BMDCs produced higher levels of pro-inflammatory cytokines IL-1a, IL-1b, TNF-α, and IL-6 (Figure 5.8). A number of chemokines were also found to be produced as a result of IO stimulation, including CXCL1, CXCL2, CCL3, CCL4, CXCL10, and CCL2 (Figure 5.9). Among them, CCL4 reached the same levels as LPS stimulated BMDCs; and CCL3, CXCL10, and CCL2 reached levels close to those produced by LPS stimulated BMDCs at 12 hours (Figure 5.9). In general, gradual increases in both cytokine and chemokine levels were observed over time with IO stimulated BMDCs.

Cytokine expression in IO-stimulated, bone marrow derived macrophages was much more transient and modest as compared to the IO-stimulated BMDCs (Figure 5.7C). Significant levels of IL1-b, IL-6, and TNF- α were only detected in the first 3-6 hours after IO-stimulation (Figure 5.7C), and they were at lower levels as compared to IO-stimulated BMDC. The low levels of activation is not a result of an inherent defect of the cultured macrophages to respond to immune stimuli since the cytokine expression profile of LPS-stimulated macrophages was similar to LPS-stimulated BMDCs (Figure 5.7B & D).

Discussion

In a previous proof-of-concept study, we focused on the use of solid, <15 nm water-soluble, QD nanoparticles for vaccine delivery of rMSP1. [29] These nanoparticles were found to be highly effective in enhancing the immunogenicity of the recombinant MSP1 antigen. However, the Cd-based core composition of the QD particles limits their potential uses in clinical applications . Thus, the primary objective of this study is to investigate the use of the clinically accepted, Iron Oxide (IO) nanoparticles, with similar physical and surface properties as the QD nanoparticles, as an alternative vaccine delivery platform.

Our results demonstrated the effectiveness of these inorganic IO nanoparticles for the delivery of a recombinant blood stage malaria vaccine, rMSP1. Antibody levels induced by rMSP1-IO were equivalent to those induced by CFA, a highly potent but toxic adjuvant. They also surpassed the antibody responses induced by the low toxicity adjuvant, ISA51. Of equal significance was the ability of rMSP1-IO's to elicit a 100% response rate in outbred mice. The same degree of generalized responsiveness and antibody response could only be achieved with the toxic CFA adjuvant. As comparison, rMSP1-ISA51 only induced a 50% response rate (Figure 5.3A).

The route of immunization is known to affect vaccine induced immune responses. [63, 64] Our results showed that the potency of rMSP1-IO in terms of antibody titers and the induction of inhibitory antibodies were independent of the delivery route (Figure 5.3B). However, rMSP1-IO delivered via the s.c. route did not achieve a 100% response rate as observed with i.p. and i.m. injections. Among all three routes, s.c. also had the lowest parasite growth inhibition at 37%. It is possible that this percent inhibition may be increased if only the antibodies from the

responders were used, eliminating the possibility of diluting the inhibitory antibodies with non-responders' serum samples.

Antigen specific cellular responses, as analyzed by ELISOPTs revealed that IO immunizations via all three routes induced a more prominent IL-4 than IFN-γ response, which was similar in profile to immunizations with the conventional adjuvants, CFA and ISA51 (Figure 5.4). IO immunizations via i.p. and s.c. route also induced significantly higher IL-4 responses than CFA. Although the relevance of this biased IL-4 response in malaria immunity is not clear, it is possible that a more skewed TH2 response would favor antibody production, which is critical in MSP1 specific immunity. [34, 35, 37-41] No correlation between IL-4 levels and MSP1-19 specific antibody titers were observed. This is however not surprising since cytokine levels have not been shown to correlate with antibody titers, though it may change their characteristics.

Compared to our recent studies of using QD as vaccine delivery [29] rMSP1-QD induces significantly higher antibodies titers than rMSP1-IO vaccinations. Nonetheless, the rMPS1-IO formulation was capable of inducing the same responsiveness (100%) and levels of parasite inhibitory antibodies (80%) as rMSP1-QD. But unlike rMSP1-QD where no differences in immunoenhancement were observed among delivery routes, the site of immunization appeared to play a role in the effectiveness of the rMSP1-IO formulation. Injections via the i.p. and i.m. routes were more effective than subcutaneous delivery. This may be a result of the anatomical differences with respect to the fate of the IO particles once injected.

Prior studies have demonstrated that levels of parasite-inhibitory anti-MSP1 antibodies correlate with natural and vaccine induced immunity. [34, 35, 37-41] For this reason, the presence of anti-MSP1 inhibitory antibodies in rMSP1-IO vaccinated mice, rabbits, and monkeys were investigated as a measure of in vitro efficacy. We observed animal species difference in the ability of rMSP1-IO to induce inhibitory

antibodies. Accordingly, rMSP1-IO was highly effective in inducing parasite inhibitory antibodies in mice and in non-human primates, ie. Aotus monkeys; surpassing or equal to the levels achieved with CFA in the respective animal models [35], whereas it was much less effective in rabbits, and correlated with the lower antibody responses induced (Table 5.3).

Animal species difference in response to immunological adjuvants have been previously documented [65], and our present study extend this observation to the use of nanoparticles for immune enhancements. It is possible that the nanoparticles activate different cell types and/or immune pathways (see below) in different animal hosts resulting in the observed alterations in immune enhancements. The fact that the IO nanoparticles were effective in a non-human primate model, Aotus monkeys, is highly encouraging, especially in light of the apparent lack of toxicity in the vaccinated monkeys after a three doses immunization regimen (Table 5.6). This is further supported by a dose escalating toxicity study performed in SW mice that also revealed no significant systemic abnormalities (Table 5.5). This finding is extremely important, as these mice received three exceptionally large does of IO nanoparticles every 21 days without sustaining damage to kidney or liver function, indicating the safety of our platform.

Initially, it was thought that the rapid clearance of small (<15nm) nanoparticles from the body [66, 67] would impede their use as a delivery platform for polypeptide antigens due to short half-life. However, the small size and their propensity to behave as a true solution may facilitate their dispersion and allow them to easily penetrate key immunological organs and immune cells such as professional APCs. [68] Indeed, our study showed that the IO nanoparticles were efficiently taken up by antigen presenting cells (APCs), BMDC and macrophages. Furthermore, upateke of IOs by BMDC led to their activation, with increased expression of CD86, pro-inflammatory cytokines (IL-6, TNF-a, and IL-1b) and chemokines. The activation

profiles as well as the levels of some of these immune mediators (ie. CCL3 and CCL4) mimic those produced via activation with LPS It is likely that the combined effects of increased chemokine and pro-inflammatory cytokine production enhanced the migratory characteristics of these immune cells, resulting in more efficient antigen presentation and/or T cell activation. These data indicate that IO nanoparticles have the potential to activate strong immune responses, specifically through dendritic cells.

Despite efficient uptake of IO nanoparticles, macrophages were not significantly activated compared to BMDCs. Thus, it is unlikely that these cells played a major role in enhancing the immunogenicity of rMSP1. Moreover, the fact that macrophages can actively internalize these particles may result in significant loss of rMSP1-IO available for dendritic cells, thereby lowering the potency of the rMSP1-IO formulation. We are currently investigating the molecular and biological bases for the differential activation of BMDCs, but not macrophages, by the IO nanoparticles. It is possible that the observed disparity in activation pattern is the result of either the two cell types having distinct mechanisms of nanoparticle uptake and/or the possibility that once inside the cell the fate of the nanoparticles in terms of subcellular location/translocation are different, leading to differences in their ability to activate or modulate the innate immune response pathways. [69, 70] This suggests that a better understanding of the mechanism(s) by which IO nanoparticles interact with APC populations is an important next step to further improve potency and efficiency. An empirical approach at present would be to devise strategies for specific targeting of conjugated IO to dendritic cells to increase the efficiency of IO uptake by these professional APCs which may lead to a stronger immunoenhancement.

This study provides strong evidence that a water-soluble, solid inorganic nanoparticle (>15 nm) with an iron oxide core is as effective as QD nanoparticles for

enhancing the immunogenicity of a malaria vaccine antigen without requiring adjuvants. The apparent lack of toxicity of the IO nanoparticles when used in immunizations as well as its effectiveness as a vaccine platform in a non-human primate model provide the impetus to advance development of these nanoparticles for vaccine delivery. This may include optimization of parameters such as particle concentration and size, antigen conjugation methods, antigen release characteristics, and in vivo targeting methods,. Finally, the ability of the vaccine conjugated IO formulation to retain stability and antigenicity for at least 12 month in solution, as this study demonstrated, makes the IO nanoparticles an ideal vaccine platform for the deployment of vaccines under most field conditions.

Acknowledgments

We would like to thank S. Chang, W. Gosnell, K. Kramer, and S. Case for their help with the Aotus monkey immunizations. We also like to thank D. Clements of Hawaii Biotech Inc for providing the MSP1 recombinant protein. D. Clements and A. Stridiron for their technical support. This work was supported by a grant from NIH/NIAID (A1076955) and NIH/NCRR COBRE (5P20RR018727-07). K. Pusic is supported by NIH/NIDDK (DK078386).

References

1. Mbow, M. L.; De Gregorio, E.; Valiante, N. M.; Rappuoli, R., New adjuvants for human vaccines **2010,** *Curr Opin Immunol 22*, 411-6.

2. Pichichero, M. E., Improving vaccine delivery using novel adjuvant systems. *Hum Vaccin* **2008,** *4*, 262-70.

3. Lambrecht, B. N.; Kool, M.; Willart, M. A.; Hammad, H., Mechanism of action of clinically approved adjuvants. *Curr Opin Immunol* **2009,** *21*, 23-9.

4. Fischer, N. O.; Infante, E.; Ishikawa, T.; Blanchette, C. D.; Bourne, N.; Hoeprich, P. D.; Mason, P. W., Conjugation to nickel-chelating nanolipoprotein particles increases the potency and efficacy of subunit vaccines to prevent West Nile encephalitis. *Bioconjug Chem* **2010,** *21*, 1018-22.

5. Akagi, T.; Wang, X.; Uto, T.; Baba, M.; Akashi, M., Protein direct delivery to dendritic cells using nanoparticles based on amphiphilic poly(amino acid) derivatives. *Biomaterials* **2007,** *28*, 3427-36.

6. Lu, J. M.; Wang, X.; Marin-Muller, C.; Wang, H.; Lin, P. H.; Yao, Q.; Chen, C., Current advances in research and clinical applications of PLGA-based nanotechnology. *Expert.Rev.Mol.Diagn.* **2009,** *9*, 325-341.

7. Mundargi, R. C.; Babu, V. R.; Rangaswamy, V.; Patel, P.; Aminabhavi, T. M., Nano/micro technologies for delivering macromolecular therapeutics using poly(D,L-lactide-co-glycolide) and its derivatives. *J.Control Release* **2008,** *125*, 193-209.

8. Shive, M. S.; Anderson, J. M., Biodegradation and biocompatibility of PLA and PLGA microspheres. *Adv.Drug Deliv.Rev.* **1997,** *28*, 5-24.

9. Chackerian, B., Virus-like particles: flexible platforms for vaccine development. *Expert.Rev.Vaccines.* **2007,** *6*, 381-390.

10. Ludwig, C.; Wagner, R., Virus-like particles-universal molecular toolboxes. *Curr.Opin.Biotechnol.* **2007,** *18*, 537-545.

11. Sun, H. X.; Xie, Y.; Ye, Y. P., ISCOMs and ISCOMATRIX. *Vaccine* **2009,** *27*, 4388-4401.

12. Skene, C. D.; Sutton, P., Saponin-adjuvanted particulate vaccines for clinical use. *Methods* **2006,** *40*, 53-59.

13. Masotti, A.; Ortaggi, G., Chitosan micro- and nanospheres: fabrication and applications for drug and DNA delivery. *Mini.Rev.Med.Chem.* **2009,** *9*, 463-469.

14. van, d. L. I.; Verhoef, J. C.; Borchard, G.; Junginger, H. E., Chitosan for mucosal vaccination. *Adv.Drug Deliv.Rev.* **2001,** *52*, 139-144.

15. Illum, L.; Jabbal-Gill, I.; Hinchcliffe, M.; Fisher, A. N.; Davis, S. S., Chitosan as a novel nasal delivery system for vaccines. *Adv.Drug Deliv.Rev.* **2001,** *51*, 81-96.

16. Ueno, Y.; Futagawa, H.; Takagi, Y.; Ueno, A.; Mizushima, Y., Drug-incorporating calcium carbonate nanoparticles for a new delivery system. *J.Control Release* **2005,** *103*, 93-98.

17. Szmuness, W.; Stevens, C. E.; Harley, E. J.; Zang, E. A.; Oleszko, W. R.; William, D. C.; Sadovsky, R.; Morrison, J. M.; Kellner, A., Hepatitis B vaccine: demonstration of efficacy in a controlled clinical trial in a high-risk population in the United States. *N Engl J Med* **1980,** *303*, 833-41.

18. Harro, C. D.; Pang, Y. Y.; Roden, R. B.; Hildesheim, A.; Wang, Z.; Reynolds, M. J.; Mast, T. C.; Robinson, R.; Murphy, B. R.; Karron, R. A.; Dillner, J.; Schiller, J. T.; Lowy, D. R., Safety and immunogenicity trial in adult volunteers of a human papillomavirus 16 L1 virus-like particle vaccine. *J Natl Cancer Inst* **2001,** *93*, 284-92.

19. Kaba, S. A.; Brando, C.; Guo, Q.; Mittelholzer, C.; Raman, S.; Tropel, D.; Aebi, U.; Burkhard, P.; Lanar, D. E., A nonadjuvanted polypeptide nanoparticle vaccine confers long-lasting protection against rodent malaria. *Journal of Immunology* **2009,** *183*, 7268-7277.

20. Hirosue, S.; Kourtis, I. C.; van der Vlies, A. J.; Hubbell, J. A.; Swartz, M. A., Antigen delivery to dendritic cells by poly(propylene sulfide) nanoparticles with

disulfide conjugated peptides: Cross-presentation and T cell activation. *Vaccine* **2010,** *28*, 7897-906.

21. Figuerola, A.; Di Corato, R.; Manna, L.; Pellegrino, T., From iron oxide nanoparticles towards advanced iron-based inorganic materials designed for biomedical applications. *Pharmacol Res* **2010,** *62*, 126-43.

22. Raynal, I.; Prigent, P.; Peyramaure, S.; Najid, A.; Rebuzzi, C.; Corot, C., Macrophage endocytosis of superparamagnetic iron oxide nanoparticles: mechanisms and comparison of ferumoxides and ferumoxtran-10. *Invest Radiol* **2004,** *39*, 56-63.

23. Simberg, D.; Park, J. H.; Karmali, P. P.; Zhang, W. M.; Merkulov, S.; McCrae, K.; Bhatia, S. N.; Sailor, M.; Ruoslahti, E., Differential proteomics analysis of the surface heterogeneity of dextran iron oxide nanoparticles and the implications for their in vivo clearance. *Biomaterials* **2009,** *30*, 3926-33.

24. Kowalczyk, M.; Banach, M.; Rysz, J., Ferumoxytol: a new era of iron deficiency anemia treatment for patients with chronic kidney disease. *J Nephrol* **2011,** *24*, 717-22.

25. Xu, H.; Aguilar, Z. P.; Su, H. P.; Dixon, J. D.; Wei, H.; Wang, A. Y., Breast cancer cell imaging using semiconductor quantum dots. *ECS Transactions* **2009,** *25*, 69-77.

26. Xu, H.; Aguilar, Z. P.; Wang, A. Y., Quantum dot based senors for proteins. *ECS Transactions* **2010,** *25*, 1-8.

27. Xu, H.; Wei, H.; Aguilar, Z. P.; Waldron, J. L.; Wang, A. Y., Application of semiconductor quantum dots for breast cancer cell sensing. *IEEE* **2009**.

28. Alexis, F.; Pridgen, E.; Molnar, L. K.; Farokhzad, O. C., Factors affecting the clearance and biodistribution of polymeric nanoparticles. *Mol Pharm* **2008,** *5*, 505-15.

29. Pusic, K.; Xu, H.; Stridiron, A.; Aguilar, Z.; Wang, A.; Hui, G., Blood stage merozoite surface protein conjugated to nanoparticles induce potent parasite inhibitory antibodies. *Vaccine* **2011,** *29*, 8898-908.

30. Holder, A. A.; Blackman, M. J.; Burghaus, P. A.; Chappel, J. A.; Ling, I. T.; McCallum-Deighton, N.; Shai, S., A malaria merozoite surface protein (MSP1)-structure, processing and function. *Mem Inst Oswaldo Cruz* **1992,** *87 Suppl 3*, 37-42.

31. Holder, A. A.; Freeman, R. R., The three major antigens on the surface of Plasmodium falciparum merozoites are derived from a single high molecular weight precursor. *Journal of Experimental Medicine* **1984,** *160*, 624-629.

32. Kumar, S.; Collins, W.; Egan, A.; Yadava, A.; Garraud, O.; Blackman, M. J.; Guevara Patino, J. A.; Diggs, C.; Kaslow, D. C., Immunogenicity and efficacy in aotus monkeys of four recombinant Plasmodium falciparum vaccines in multiple adjuvant formulations based on the 19-kilodalton C terminus of merozoite surface protein 1. *Infection and Immunity* **2000,** *68*, 2215-2223.

33. Holder, A. A.; Guevara Patino, J. A.; Uthaipibull, C.; Syed, S. E.; Ling, I. T.; Scott-Finnigan, T.; Blackman, M. J., Merozoite surface protein 1, immune evasion, and vaccines against asexual blood stage malaria. *Parassitologia* **1999,** *41*, 409-14.

34. Singh, S.; Miura, K.; Zhou, H.; Muratova, O.; Keegan, B.; Miles, A.; Martin, L. B.; Saul, A. J.; Miller, L. H.; Long, C. A., Immunity to Recombinant Plasmodium falciparum Merozoite Surface Protein 1 (MSP1): Protection in Aotus nancymai Monkeys Strongly Correlates with Anti-MSP1 Antibody Titer and In Vitro Parasite-Inhibitory Activity. *Infection and Immunity* **2006,** *74*, 4573-4580.

35. Chang, S. P.; Case, S. E.; Gosnell, W. L.; Hashimoto, A.; Kramer, K. J.; Tam, L. Q.; Hashiro, C. Q.; Nikaido, C. M.; Gibson, H. L.; Lee-Ng, C. T.; Barr, P. J.; Yokota, B. T.; Hut, G. S., A recombinant baculovirus 42-kilodalton C-terminal

fragment of Plasmodium falciparum merozoite surface protein 1 protects Aotus monkeys against malaria. *Infection and Immunity* **1996,** *64*, 253-261.

36. Stowers, A. W.; Cioce, V.; Shimp, R. L.; Lawson, M.; Hui, G.; Muratova, O.; Kaslow, D. C.; Robinson, R.; Long, C. A.; Miller, L. H., Efficacy of two alternate vaccines based on Plasmodium falciparum merozoite surface protein 1 in an Aotus challenge trial. *Infection and Immunity* **2001,** *69*, 1536-1546.

37. Egan, A. F.; Burghaus, P.; Druilhe, P.; Holder, A. A.; Riley, E. M., Human antibodies to the 19kDa C-terminal fragment of Plasmodium falciparum merozoite surface protein 1 inhibit parasite growth in vitro. *Parasite Immunology* **1999,** *21*, 133-139.

38. Al Yaman, F.; Genton, B.; Kramer, K. J.; Chang, S. P.; Hui, G. S.; Baisor, M.; Alpers, M. P., Assessment of the role of naturally acquired antibody levels to Plasmodium falciparum merozoite surface protein-1 in protecting Papua New Guinean children from malaria morbidity. *American Journal of Tropical Medicine and Hygiene* **1996,** *54*, 443-448.

39. John, C. C.; O'Donnell, R. A.; Sumba, P. O.; Moormann, A. M.; Koning-Ward, T. F.; King, C. L.; Kazura, J. W.; Crabb, B. S., Evidence that invasion-inhibitory antibodies specific for the 19-kDa fragment of merozoite surface protein-1 (MSP-1 19) can play a protective role against blood-stage Plasmodium falciparum infection in individuals in a malaria endemic area of Africa. *The Journal of Immunology* **2004,** *173*, 666-672.

40. O'Donnell, R. A.; Koning-Ward, T. F.; Burt, R. A.; Bockarie, M.; Reeder, J. C.; Cowman, A. F.; Crabb, B. S., Antibodies against merozoite surface protein (MSP)-1(19) are a major component of the invasion-inhibitory response in individuals immune to malaria. *Journal of Experimental Medicine* **2001,** *193*, 1403-1412.

41. Perraut, R.; Marrama, L.; Diouf, B.; Sokhna, C.; Tall, A.; Nabeth, P.; Trape, J. F.; Longacre, S.; Mercereau-Puijalon, O., Antibodies to the conserved C-terminal

domain of the Plasmodium falciparum merozoite surface protein 1 and to the merozoite extract and their relationship with in vitro inhibitory antibodies and protection against clinical malaria in a Senegalese village. *Journal of Infectious Diseases* **2005,** *191*, 264-271.

42. Kirkpatrick, R. B.; Shatzman, A.; Fernandez, J.; Hoeffler, J., Drosophila S2 System for heterologous gene expression. In *Gene Expression Systems: Using Nature for the Art of Expression.*, Academic Press.: 1999; pp 289-330.

43. Chang, S. P.; Gibson, H. L.; Lee-Ng, C. T.; Barr, P. J.; Hui, G. S., A carboxyl-terminal fragment of Plasmodium falciparum gp195 expressed by a recombinant baculovirus induces antibodies that completely inhibit parasite growth. *Journal of Immunology* **1992,** *149*, 548-555.

44. Pusic, K. M.; Hashimoto, C. N.; Lehrer, A.; Aniya, C.; Clements, D. E.; Hui, G. S., T cell epitope regions of the P. falciparum MSP1-33 critically influence immune responses and in vitro efficacy of MSP1-42 vaccines. *PLoS One* **2011,** *6*, e24782.

45. Hui, G. S.; Hashimoto, A. C.; Nikaido, C. M.; Choi, J.; Chang, S. P., Induction of antibodies to the Plasmodium falciparum merozoite surface protein-1 (MSP1) by cross-priming with heterologous MSP1s. *Journal of Immunology* **1994,** *153*, 1195-201.

46. Chang, S. P.; Hui, G. S.; Kato, A.; Siddiqui, W. A., Generalized immunological recognition of the major merozoite surface antigen (gp195) of Plasmodium falciparum. *Proc Natl Acad Sci U S A* **1989,** *86*, 6343-7.

47. Hui, G. S.; Gosnell, W. L.; Case, S. E.; Hashiro, C.; Nikaido, C.; Hashimoto, A.; Kaslow, D. C., Immunogenicity of the C-terminal 19-kDa fragment of the Plasmodium falciparum merozoite surface protein 1 (MSP1), YMSP1(19) expressed in S. cerevisiae. *Journal of Immunology* **1994,** *153*, 2544-2553.

48. Hui, G.; Hashimoto, C., Interleukin-6 has differential influence on the ability of adjuvant formulations to potentiate antibody responses to a Plasmodium falciparum blood-stage vaccine. *Vaccine* **2007,** *25*, 6598-603.

49. Hui, G.; Hashimoto, C., The requirement of CD80, CD86, and ICAM-1 on the ability of adjuvant formulations to potentiate antibody responses to a Plasmodium falciparum blood-stage vaccine. *Vaccine* **2007,** *25*, 8549-56.

50. Stowers, A. W.; Cioce, V.; Shimp, R. L.; Lawson, M.; Hui, G.; Muratova, O.; Kaslow, D. C.; Robinson, R.; Long, C. A.; Miller, L. H., Efficacy of two alternate vaccines based on Plasmodium falciparum merozoite surface protein 1 in an Aotus challenge trial. *Infection and Immunity* **2001,** *69*, 1536.

51. Hui, G. S.; Gosnell, W. L.; Case, S. E.; Hashiro, C.; Nikaido, C.; Hashimoto, A.; Kaslow, D. C., Immunogenicity of the C-terminal 19-kDa fragment of the Plasmodium falciparum merozoite surface protein 1 (MSP1), YMSP1(19) expressed in S. cerevisiae. *J Immunol* **1994,** *153*, 2544-53.

52. Leung, W. H.; Meng, Z. Q.; Hui, G.; Ho, W. K., Expression of an immunologically reactive merozoite surface protein (MSP-1(42)) in E. coli. *Biochim Biophys Acta* **2004,** *1675*, 62-70.

53. Pang, A. L.; Hashimoto, C. N.; Tam, L. Q.; Meng, Z. Q.; Hui, G. S.; Ho, W. K., In vivo expression and immunological studies of the 42-kilodalton carboxyl-terminal processing fragment of Plasmodium falciparum merozoite surface protein 1 in the baculovirus-silkworm system. *Infect Immun* **2002,** *70*, 2772-9.

54. Hui, G.; Choe, D.; Hashimoto, C., Biological activities of anti-merozoite surface protein-1 antibodies induced by adjuvant-assisted immunizations in mice with different immune gene knockouts. *Clin Vaccine Immunol* **2008,** *15*, 1145-50.

55. Inaba, K.; Inaba, M.; Romani, N.; Aya, H.; Deguchi, M.; Ikehara, S.; Muramatsu, S.; Steinman, R. M., Generation of large numbers of dendritic cells from

mouse bone marrow cultures supplemented with granulocyte/macrophage colony-stimulating factor. *J Exp Med* **1992,** *176*, 1693-1702.

56. Zhang, X.; Goncalves, R.; Mosser, D. M., The isolation and characterization of murine macrophages. *Curr Protoc Immunol* **2008,** *Chapter 14*, Unit 14 1.

57. Szymczak, W. A.; Deepe, G. S., Jr., Antigen-presenting dendritic cells rescue CD4-depleted CCR2-/- mice from lethal Histoplasma capsulatum infection. *Infect Immun* **2010,** *78*, 2125-37.

58. Szymczak, W. A.; Deepe, G. S., Jr., Antigen-presenting dendritic cells rescue CD4-depleted CCR2-/- mice from lethal Histoplasma capsulatum infection. *Infect Immun* **2010,** *78*, 2125-37.

59. Livak, K. J.; Schmittgen, T. D., Analysis of relative gene expression data using real-time quantitative PCR and the 2(-Delta Delta C(T)) Method. *Methods* **2001,** *25*, 402-8.

60. Pfaffl, M. W., A new mathematical model for relative quantification in real-time RT-PCR. *Nucleic Acids Res* **2001,** *29*, e45.

61. Hui, G.; Choe, D.; Hashimoto, C., Biological activities of anti-merozoite surface protein-1 antibodies induced by adjuvant-assisted immunizations in mice with different immune gene knockouts. *Clin Vaccine Immunol* **2008,** *15*, 1145-1150.

62. Hui, G.; Hashimoto, C., Plasmodium falciparum anti-MSP1-19 antibodies induced by MSP1-42 and MSP1-19 based vaccines differed in specificity and parasite growth inhibition in terms of recognition of conserved versus variant epitopes. *Vaccine* **2007,** *25*, 948-56.

63. Peek, L. J.; Middaugh, C. R.; Berkland, C., Nanotechnology in vaccine delivery. *Adv.Drug Deliv.Rev.* **2008,** *60*, 915-928.

64. Shahiwala, A.; Vyas, T. K.; Amiji, M. M., Nanocarriers for systemic and mucosal vaccine delivery. *Recent Pat Drug Deliv.Formul.* **2007,** *1*, 1-9.

65. Hui, G. S., Liposomes, muramyl dipeptide derivatives, and nontoxic lipid A derivatives as adjuvants for human malaria vaccines. *Am J Trop Med Hyg* **1994,** *50*, 41-51.

66. Ferrari, M., Cancer nanotechnology: opportunities and challenges. *Nat.Rev.Cancer* **2005,** *5*, 161-171.

67. Peer, D.; Karp, J. M.; Hong, S.; Farokhzad, O. C.; Margalit, R.; Langer, R., Nanocarriers as an emerging platform for cancer therapy. *Nat.Nanotechnol.* **2007,** *2*, 751-760.

68. Gao, X.; Cui, Y.; Levenson, R. M.; Chung, L. W.; Nie, S., In vivo cancer targeting and imaging with semiconductor quantum dots. *Nat Biotechnol* **2004,** *22*, 969-76.

69. Barton, G. M.; Kagan, J. C., A cell biological view of Toll-like receptor function: regulation through compartmentalization. *Nat Rev Immunol* **2009,** *9*, 535-42.

70. Pasare, C.; Medzhitov, R., Toll-like receptors: linking innate and adaptive immunity. *Adv Exp Med Biol* **2005,** *560*, 11-8.

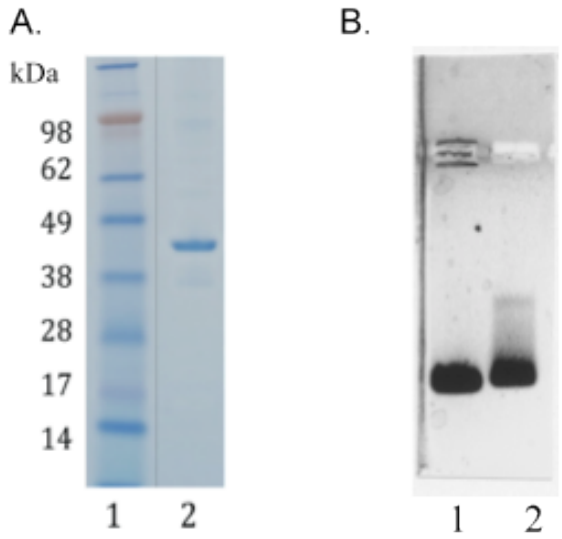

Figure 5.1 Purification and conjugation of rMSP1 recombinant protein to IO nanoparticles. Panel A, SDS-PAGE gel of purified rMSP1 protein. Lane 1: Molecular Marker, Lane 2: Purified rMSP1 recombinant protein. Panel B, agarose gel electrophoresis of unconjugated IO nanoparticles (Lane 1) and rMSP1 conjugated IO nanoparticles (Lane 2).

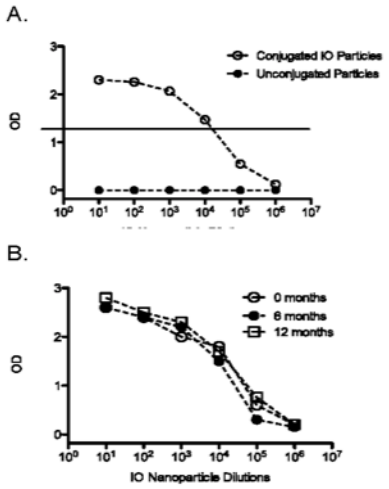

Figure 5.2 Antigenicity analysis of rMSP1 protein to IO nanoparticles. Panel A, antigenicity of rMSP1 conjugated IO nanoparticles. ELSIA titration curves of rMSP1 conjugated nanoparticles (open circles) and unconjugated nanoparticles (filled circles) against MSP1-42 specific monoclonal antibody, mAb 5.2. Straight line represents OD reading of mAb 5.2 reactivity to native MSP1-42 at a coating concentration of 0.4 ug/ml. Panel B, antigenicity stability of rMSP1 conjugated IO nanoparticles over a 12 month period. ELISA titration curves of rMSP1 conjugated nanoparticles at 0 months (open circles), 6 months (filled circles), and 12 months (open squares) post-conjugation against MSP1-42 specific monoclonal antibody, mAb 5.2.

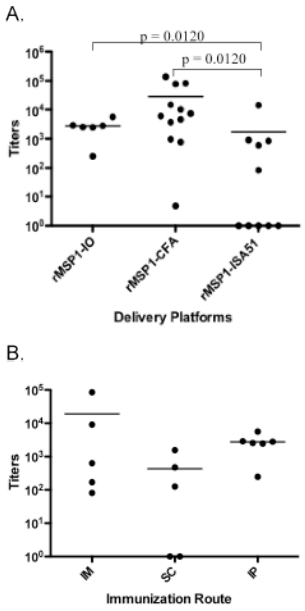

Figure 5.3 ELISA antibody response against MSP1-19 in SW mice immunized with rMSP1. Panel A, antibody titers of SW mice immunized with different adjuvant/delivery platforms (rMSP1-IO, rMSP1-CFA, rMSP1-ISA51). Results of the tertiary bleed are shown. Panel B, antibody response in mice vaccinated with rMSP1-IO via different immunization routes (IP, IM, SC). Results of tertiary bleed are shown. Significant differences in antibody titers among the vaccination groups are shown with p-values (Mann-Whitney test).

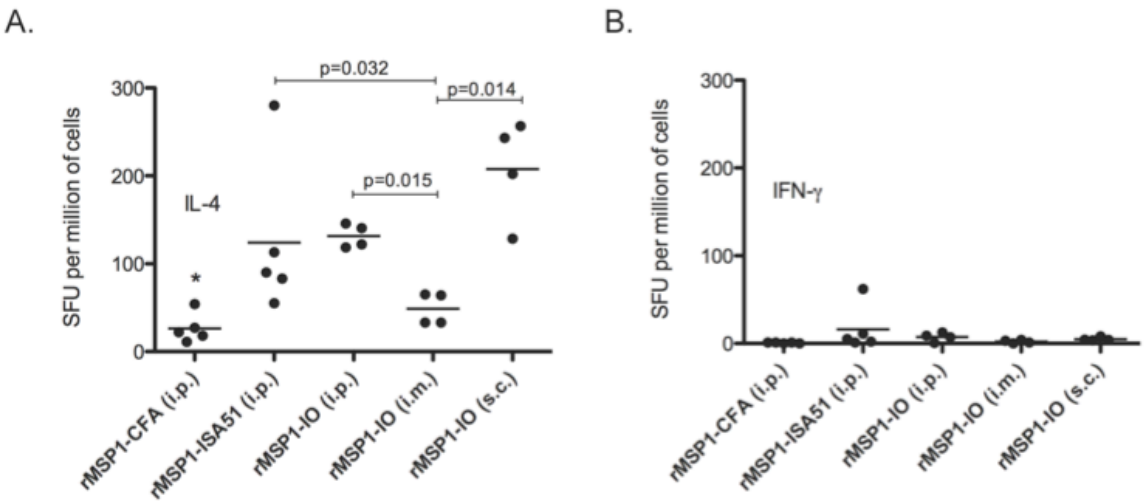

Figure 5.4 MSP1-specific IL-4 and IFN-γ responses to rMSP1 with different delivery platform/adjuvants. IL-4 (Panel A) and IFN-γ (Panel B) responses as determined by ELISPOT in SW immunized mice. Horizontal lines indicate mean SFU.

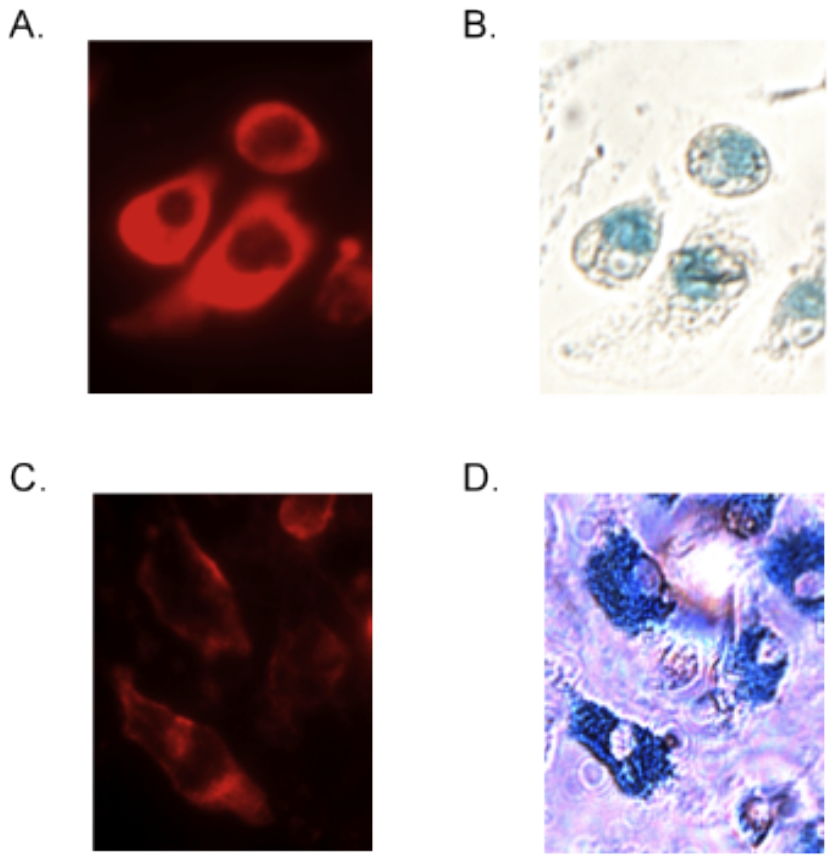

Figure 5.5 Uptake of IO nanoparticles by bone marrow derived dendritic cells (BMDCs) and macrophages. Panel A, surface staining of BMDCs with QDot labeled anti-CD11c (red). Panel B, localization of IO nanoparticles (blue) in the same BMDC cultured cells. Panel C, surface staining of macrophages with QDot labeled anti-CD11b (red). Panel D, localization of IO nanoparticles (blue) in the same macrophage culture.

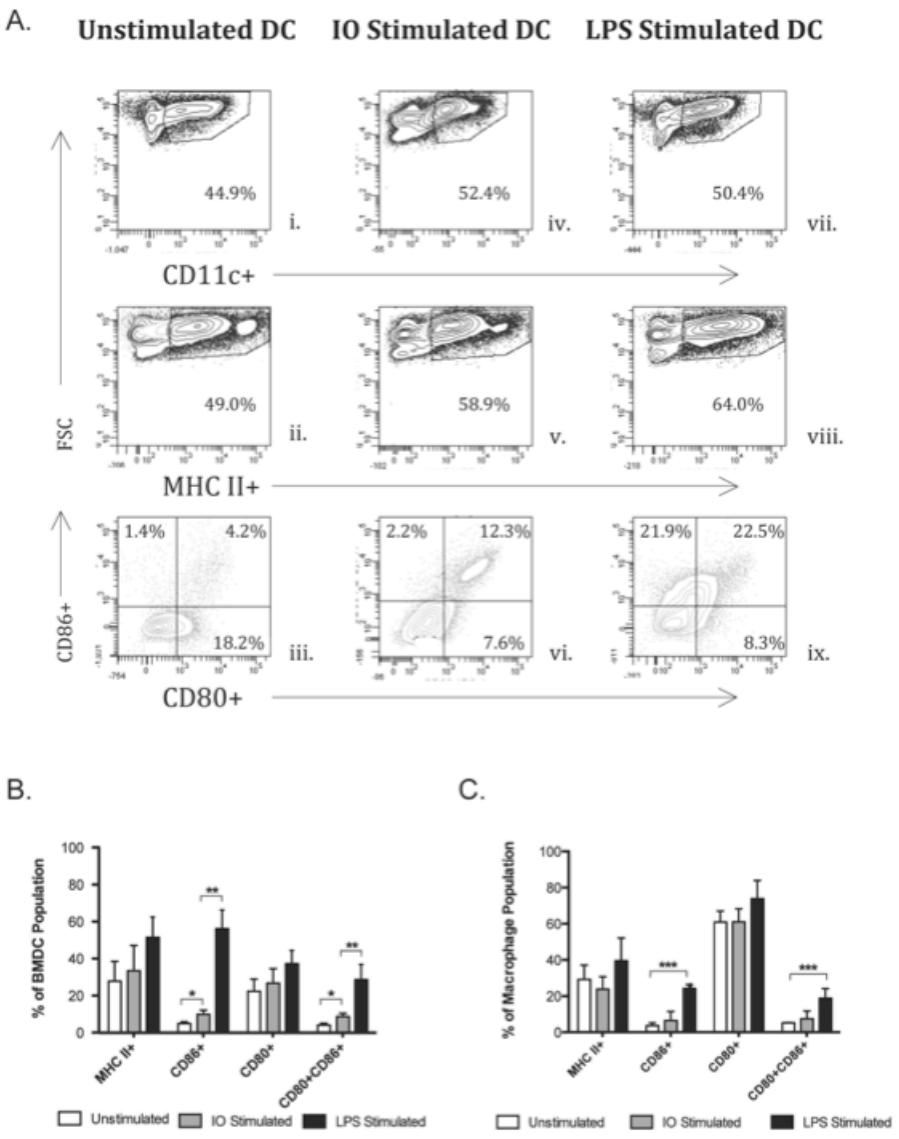

Figure 5.6 Activation of BMDCs and macrophages by IO nanoparticles. Panel A, a representative of one experiment. BMDCs ($1x10^6$ cells) were incubated with media alone, IO nanoparticles, or LPS at 37°C for 24 hours. Cells were stained for surface markers: CD11c-FITC, MHC II-PE, CD80-APC, and CD86-PE-Cy7 and analyzed by flow cytometry. Panel i. gated for CD11c+ cells, Panel ii & iii. are live gates of Panel i. and stained for MHC II, CD80, and CD86. Panel v. and vi. are live gates of Panel iv.; and Panel viii and ix are live gates of Panel vii. Panel B, summary of three BMDC activation experiments. Panel C, summary of three macrophage activation experiments. Significant differences were observed between unstimulated and IO-stimulated BMDCs (*) for CD86+ (p=0.05) and CD80+/CD86+ (p=0.03) and also between IO-stimulated DCs and LPS-stimulated DCs (**) for the expression of CD86+ (p=0.05) and CD80+/CD86+ (p=0.04). Significant differences were observed between unstimulated and IO-stimulated macrophages (***) for the expression of CD86+ (p=0.05) and CD80+/CD86+ (p=0.03).

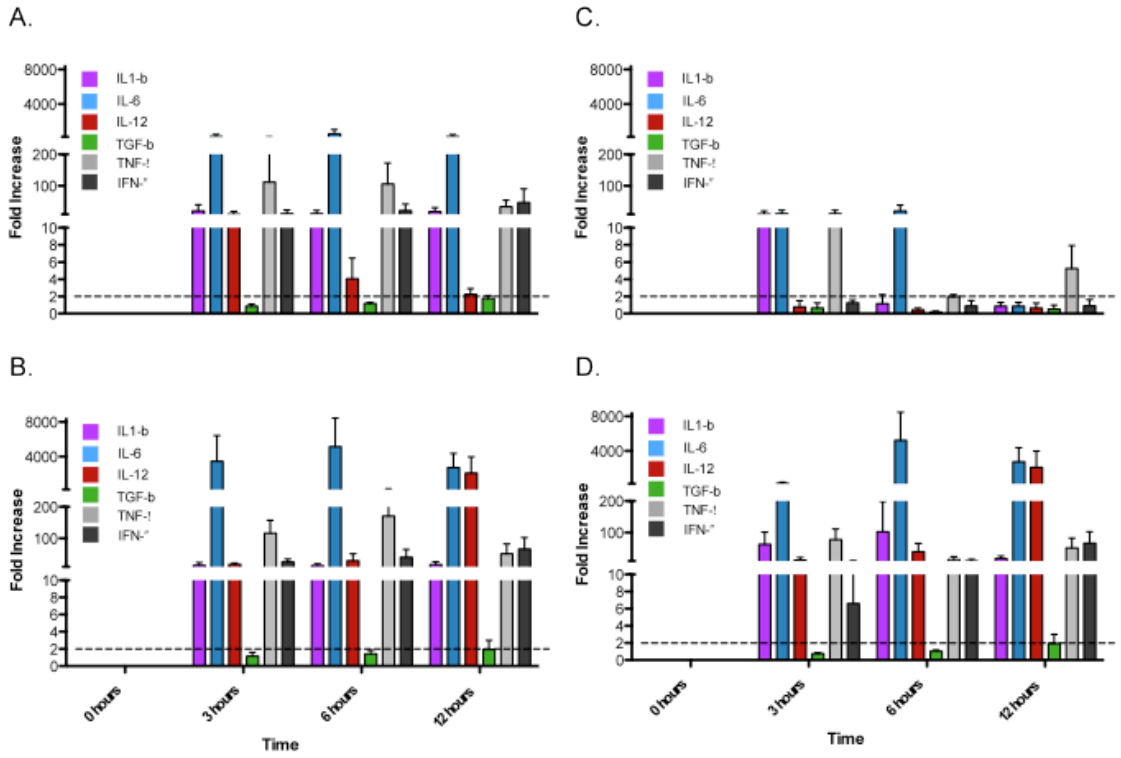

Figure 5.7 Cytokine expression of stimulated BMDCs and macrophages. RT-PCR quantification of six different cytokine gene expressions in IO-stimulated BDMCs (Panel A), LPS-stimulated BMDCs (Panel B), IO-stimulated macrophages (Panel C), and LPS-stimulated macrophages (Panel D). Expression was monitored over a 12 hour period. Data were normalized to GAPDH and fold changes were calculated based on "0 hour" samples.

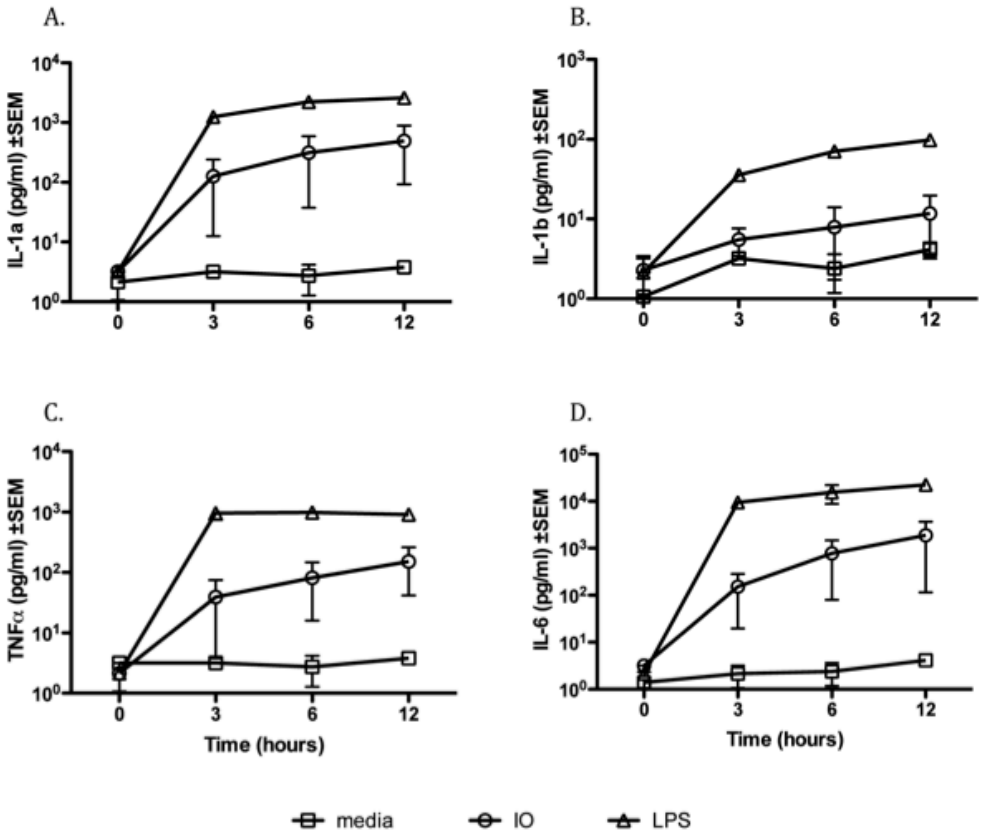

Figure 5.8 Cytokines production by stimulated BMDCs. BMDCs ($1x10^6$) were incubated with media alone (open squares), IO nanoparticels (open circles), or LPS (100 ng/ml)(open triangles). Culture supernatants were measured for the presence of cytokines IL-6 (A), IL-1b (B), TNFα (C), and IL-6 (D) at 0, 3, 6, and 12 hours by Luminex using the Milliplex MAP Mouse Cytokine/Chemokine 32 plex assay. Cell supernatants were measured in triplicates and only the cytokines with the highest expression are depicted.

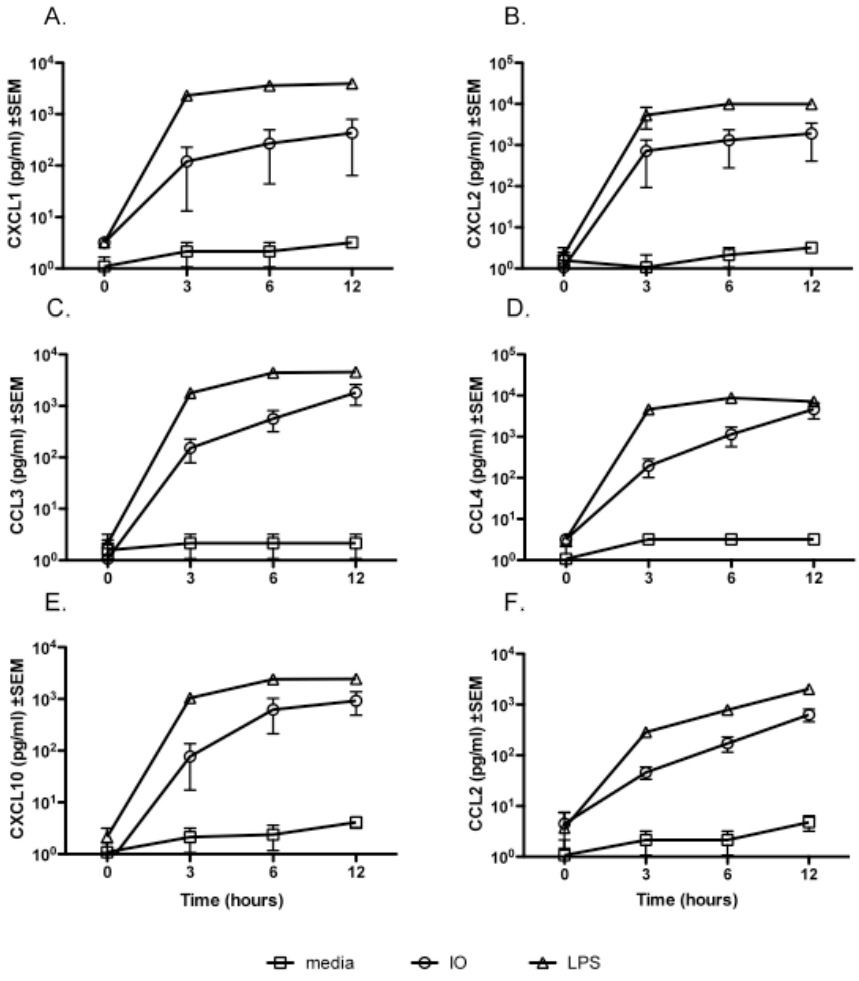

Figure 5.9 Chemokine production by stimulated BMDCs. BMDCs ($1x10^6$) were incubated with media alone (open squares), IO nanoparticels (open circles), or LPS (100 ng/ml) (open triangles). Culture supernatants were measured for the presence of chemokines CXCL1 (A), CXCL2 (B), CCL3 (C), CCL4 (D), CXCL10 (E), and CCL2 (F) at 0, 3, 6, and 12 hours by Luminex using the Milliplex MAP Mouse Cytokine/Chemokine 32 plex assay. Cell supernatants were measured in triplicates and only the chemokines with the highest expression are depicted.

Table 5.1 Sequences of RT-PCR primers

Gene	GenBank Accession #	Primer*	Sequence (5' ➔ 3')
IL-1β	NM_008361	F	TGGAGAGTGTGGATCCCAAGCAAT
		R	ATGGTTTCTTGTGACCCTGAGCGA
IL-6	NM_031168	F	ATCCAGTTGCCTTCTTGGGACTGA
		R	TGGTACTCCAGAAGACCAGAGGAA
IL-12p40	NM_008352	F	ACCTGTGACACGCCTGAAGAAGAT
		R	AGAGACGCCATTCCACATGTCACT
TGF-β	M13177	F	TAAAGAGGTCACCCGCGTGCTAAT
		R	TTTGCTGTCACAAGAGCAGTGAGC
TNF-α	NM_008352	F	AGCTCAAACCCTGGTATGAACCCA
		R	AGTCCTTGATGGTGGTGCATGAGA
IFN-γ	XM_125899	F	TGCATCTTGGCTTTGCAGCTCTTC
		R	TGGGTTGTTGACCTCAAACTTGGC
GAPDH	M32599	F	TGTGATGGGTGTGAACCACGAGAA
		R	GAGCCCTTCCACAATGCCAAAGTT

* F, forward primer; R, reverse primer

Table 5.2 In vitro Parasite Growth Inhibition of Purified Mouse Anti-MSP1 Antibodies

Pooled Mouse Purified Antibody (Tertiary Bleeds)	% Parasite growth inhibition*
rMSP1-IO (i.p.)	80%
rMSP1-IO (i.m.)	74%
rMSP1-IO (s.c.)	37%
rMSP1-CFA (i.p.)	17%
rMSP1-ISA51 (i.p.)	0%

* Mean of two growth inhibition assays

Table 5.3 In vitro Parasite Growth Inhibition of Rabbit Anti-MSP1 Antibodies

Rabbit Serum (Quaternary Bleed)	Anti-MSP1-42 antibody titers	Anti-MSP1-19 antibody titers	% Parasite growth inhibition
Rbt#1	4,500	3,500	48%
Rbt#2	6,000	5,600	0%
Rbt#3	28,000	22,000	71%

Table 5.4 In vitro Parasite Growth Inhibition of Monkey Anti-MSP1 Antibodies

Monkey Serum (Tertiary Bld)	Anti-MSP1-42 Antibody Titers	Anti-MSP1-19 Antibody Titers	% Parasite growth inhibition
Monkey #1	2,800	3,000	82%
Monkey #2	29,000	24,000	100%
Monkey #3	4,500	10,000	55%
Monkey #4	10,000	20,000	66%

Table 5.5 Clinical Chemistry on Immunized Aotus Monkeys

	Monkey #1		Monkey #2		Monkey #3		Monkey #4	
	Prior to Vaccination	End of Vaccination	Prior to Vaccination	End of Vaccination	Prior to Vaccination	End of Vaccination	Prior to Vaccination	End of Vaccination
Alk phosphatase, U/L	65	62	132	92	70	79	65	87
ALT (SGPT), U/L	53	30	76	141	37	40	78	41
AST (SGOT), U/L	128	75	258	538	125	121	195	161
CK, U/L	3.4	3.2	1322	1304	569	66	551	145
GGT, U/L	466	89	8	7	9	8	12	7
Albumin, g/dL	11	12	3.1	2	4.1	3.8	3.8	4.2
Total protein, g/dL	6.9	6.5	7	5.6	7.6	7	7.2	7.6
Globulin, g/dL	3.5	3.3	3.9	3.6	3.5	3.2	3.4	3.4
Total bilirubin, mg/dL	0.8	0.1	0.4	0.3	0.3	0.4	0.2	0.2
Direct bilirubin, mg/dL	0.4	0.1	0.2	0.3	0.3	0.3	0.2	0.2
BUN, mg/dL	11	10	13	7	8	11	8	6
Creatinine, mg/dL	0.5	0.5	0.5	0.5	0.5	0.6	0.4	0.5
Cholesterol, mg/dL	144	144	125	129	116	117	118	108
Glucose, mg/dL	130	232	153	164	143	173	167	181
Calcium, mg/dL	9.1	8.6	8.7	8.4	9.7	9.6	9.2	9.1
Phosphorus, mg/dL	5	3	6.6	5.2	3.3	4.1	5.5	5.6
Chloride, mEg/L	107	109	108	103	102	106	105	108
Potassium, mEg/L	4.5	3.7	4.6	4.8	4.3	5.3	5.9	5.1
Sodium, mEg/L	152	146	149	146	148	148	149	152
A/G Ratio	1	1	0.8	0.6	1.2	1.2	1.1	1.2
B/C Ratio	22	20	26	14	16	18.3	20	12
Indirect Bilirubin, mg/dL	0.4	0	0.2	0	0	0.1	0	0
Na/K Ratio	34	39	32	30	34	28	25	30
Hemolysis Index	N	N	+	N	N	N	+	N
Lipemia Index	N	N	N	N	N	N	N	N
WBC, THOUS/ul	-	-	34.1	21.1	-	-	-	-
RBC, MILLION/uL	18	11.5	5.03	4.5	7.4	7.5	14.4	6
HGB, g/dL	4.8	6.1	13.2	11.4	5.8	6.2	6.2	6.6
HCT, %	13.3	14.9	39.7	35.4	14.1	13.9	16.5	15.2
MCV, fL	40.6	45.9	79	78	43.3	43.8	48.9	46.3
MCH, pg	83	75	26.2	25	74	71	79	69
MCHC, g/dL	27.3	24.4	33.2	32.2	24.1	22.4	26.5	22.8
NRBC, /100 WBC	32.8	32.5	-	18	32.6	31.7	33.7	32.8
NEUTROPHIL SEG, %	48	58	24	43	28	34	34	31
LYMPHOCYTES, %	39	27	55	43	67	51	58	60
MONOCYTES, %	9	10	5	9	4	10	3	3
EOSINOPHIL, %	4	5	6	5	1	5	5	6
AUTO PLATELET, THOUS/uL	572	511	586	611	298	386	364	182

Table 5.6 Blood Chemistry on IO Immunized Swiss Webster Mice

IO dose groups *:	Control		250ul IO		450ul IO		650ul IO		850ul IO	
	Pre-injection	Post-injection	Pre-injection	Post-injection	Pre-injection	Post-injection	Pre-injection	Post-injection	Pre-injection	Post-injection
Hematocrit, %PCV	52.5	52	56.7	54.7	56.3	49	54.8	52.5	56.5	53
Hemoglobin, g/dL	17.8	17.7	19.3	18.6	19.1	16.7	18.6	17.9	19.2	18
Blood Urea Nitrogen, mg/dL	27	25.5	23.75	23.25	24.3	26	21	25	29.5	26.3
Anion Gap, mmol/L	16	15.5	14.5	14.5	12	12.3	14.8	14.3	15	11
Carbon Dioxide, mmol/L	25.5	25	27.75	27	28.3	27	26	26.8	24.3	26
Potassium, mmol/L	8.3	8.2	7.85	8.3	7.8	8	8.1	7.9	7.7	8.7

* Values consist of the average readings of six mice/group

CONCLUSION

As one of the leading malaria vaccine candidates, MSP1-42 has been the focus of many vaccine and immunological studies [1,2,3,4]. Animal studies with MSP1-42-based vaccines have demonstrated varying degrees of protection against malaria blood infection [5,6,7,8,9]. However, despite encouraging animal data, clinical studies with MSP1-42 have been disappointing and have failed to induce protection [10,11]. Therefore, focused our studies have been on designing modified MSP1-42 subunit proteins to overcome the immunological shortcomings that have confound the current vaccines.

The development of vaccines based on MSP1-19 and MSP1-42 is based on the concept of eliciting specific antibody responses against the MSP1-19 region that have parasite inhibition activity. This is the biological relevance of these vaccine candidates. MSP1-19 based vaccines have been unsuccessful, primarily due to the fact that this antigen lacks T cell epitopes to allow for consistent and robust antibody responses. Current efforts to develop MSP1-42 vaccines are based on the assumption that T cell epitopes that reside in the MSP1-33 region can provide help in eliciting specific anti-MSP1-19 antibody responses. In has also been assumed that all functional T cell epitopes from MSP1-33 contribute to immunogenicity by providing help to induce anti-MSP1-19 antibodies [12,13,14,15,16,17]. Here, we have proven that functional T helper epitopes can contribute either positively or negatively to the development of an enhanced anti-MSP1-19 response by influencing immune responsiveness and antibody specificity [3]. Additionally, we show that an epitope's influence is magnified or dampened by virtue of its relative dominance [3]. This novel concept has provided us with the scientific rationale for engineering a significantly more potent vaccine candidate than the MSP1-42 by selectively including and/or excluding T epitopes [3]. The use of this approach has led to the

identification of two truncated constructs consisting of T helper epitopes regions of MSP1-33 expressed in tandem with MSP1-19, ie. Constructs D and I [3]. These truncated MSP1-42 vaccines elicit a more robust immune response than naïve MSP1-42. Additional analyses of these two constructs has further validated their potential as malaria vaccine candidates. Both constructs are able to maintain or enhance their immunogenicity in animals that have already been exposed to MSP1-42 [3]. These results indirectly suggest that deployment of the two candidate vaccines in malaria endemic areas may be effective.

This approach of utilizing T cell epitoptes to enhance immunogenicity of an antigen is not a new idea, since numerous studies have used the addition of a universal T cell epitope to try to enhance the immunogenicity of vaccines. An example of this is the use of tetanus toxoid conjugated to a malaria sporozoite vaccine [18]. This vaccine was found in induce antibody response which recognized native sporozoite peptide and generated measurable levels of immunity, however it was not very efficacious [18]. Our concept of utilizing T cell epitopes is much different. Here we select T helper epitopes in a way that can positively lead to the development of an enhanced anti-MSP1-19 response by it's ability to help influence immune responsiveness and antibody specificity [3]. Additionally, we understand that the epitope's influence is magnified or dampened by virtue of its relative dominance and so in this fashion the correct T cell epitopes are selected for vaccine development.

Immunological studies of these two candidates indicate that Construct I, consisting of only conserved sequences of MSP1-33, is particularly promising. The immunogenicity of this construct was not parasite strain specific, as it cross-reacted with both allelic forms of MSP1-42. Furthermore, fusion of the conserved sequence regions of MSP1-33 that make up Construct I led to the formation of new T cell

epitopes, of which four were identified to have helper function in inducing anti-MSP1-19 antibodies. These data provide the scientific basis to further refinements of Construct I to produce an even more effective MSP1-42-based malaria vaccine. In addition, the series of studies on MSP1-42 described here also provide new insights into the development of anti-MSP1-42 antibody responses that can be modulated during natural malaria exposures, whereby a full complement of MSP1-42 specific T epitopes, with differing effects on antibody production and specificity are presented. Our studies on the characterization of T epitopes of Construct I provide evidence that not all immunogenic T epitopes can efficiently provide helper function to induce antibody responses. Further our studies indicate the need for caution when designing vaccines based on *in-vitro* antigen-stimulated T cell studies.

As substantial baseline studies on the natural and vaccine-induced immune responses in humans are already available for MSP1-42 our current work is highly translational and may have considerable impact on malaria vaccine development. The identification of these two constructs mentioned above, and particularly Construct I, have excellent potential as the next generation MSP1-42 vaccine.

Additional studies will be required to examine the function of the newly identified T cell epitopes on Construct I, the phenotypes of T cells they produce; and the potential crossreactive sequences on MSP1-42. The information may be used to further refine vaccine design. In parallel, it will be necessary to evaluate whether the candidate constructs can be recognized and be immunogenic in malaria exposed individuals. More specifically, it will need to be determined if malaria primed human PBMCs can recognize the constructs and start proliferating and inducing cytokines. Additional modifications of the candidate constructs based on studies with human reagents will facilitate the fine tuning and eventual evaluation and the deployment of the most suitable vaccines for clinical studies.

Successful development of recombinant protein and peptide based vaccines not only require careful design of the immunogen but must also depend on effective antigen delivery and judicial enhancement of protective immune effectors, as measured by the induction of parasite inhibitory antibodies. We have not yet established this assay as *in vitro* correlate of *in vivo* protection, however this may be one measurement of protection. Other measurements of protection may involve other immune effector mechanisms such as Antibody Dependant Cell Cytotoxicity (ADCC), which involves Fc-dependent killing of parasites through neutrophils and macrophages [19,20]. Thus in conjunction with studies to improve the MSP1-42 vaccine, the efficacy of adjuvant-free, solid nanoparticles as a delivery platform for the candidate immunogens was explored. This is of importance as there are currently a very limited number of adjuvants that are registered for use in human vaccines [21].

In the studies described here, the use of novel inorganic nanoparticles as effective antigen delivery vehicles was investigated. Of note is that solid, inorganic nanoparticles (<15 nm) were used for these studies. As the use of nanoparticles for vaccine delivery is not entirely novel, the specific use of small iron oxide nanoparticles for vaccine delivery is novel. In theory, the small sizes of these nanoparticles will enable them to act as true solutions, thus allowing the antigen-conjugated nanoparticles to be readily dispersed and efficiently penetrate tissues to reach key immunological sites/cells [22,23,24].

The data presented here, indicates that the efficacy of these nanoparticles is likely due to their capacity to be readily taken up by, and induce the activation of, antigen presenting cells (APC), specifically dendritic cells, resulting in the induction of strong immune responses. The initial studies with the QD nanoparticles provide for the first time the proof of concept that solid inorganic nanoparticles can be used as a

vaccine delivery platform [25]. Additionally, we tested a clinically approved form of solid inorganic nanoparticles, iron oxide (IO), and verified its use as a vaccine delivery platform. IO nanoparticles were able to enhance the immunogenicity of the malaria antigen without requiring an adjuvant, and had no evidence of toxicity in mice or Aotus monkeys. Furthermore, vaccine conjugated to IO, as demonstrated by conjugation of MSP1-42, are stable at 4°C over a span of one year. This makes our malaria vaccine and delivery platform extremely suited for transport and deployment in field conditions. Unlike the current RTS,S vaccines, which have to be formulated at the bedside, the MSP1-42/IO formulation is ready for administration without further manipulations, thus eliminating the need for an experienced personnel at the point of administration. These promising attributes make IO a strong candidate for clinical development, not only for malaria vaccines, but for numerous other parenterally administered vaccines.

As promising as they appeared, our studies with IO nanoparticles are nevertheless preliminary and based on relatively un-optimized parameters. Further optimization of key parameters such as particle concentration, size, antigen conjugation methods, and/or antigen release characteristics will most likely improve the potency of the platform. In parallel, there is a need to better understand the immunological mechanism(s) by which these nanoparticles interact with the APC populations in order to improve potency and efficiency. The involvement of TLRs, inflammasome pathways and NOD-Like Receptors are among the key candidates we will explore.

The future of an efficacious MSP1-42 malaria vaccine lies in the careful selection and pairing of the antigen and the delivery platform/adjuvant system. Identifying the ideal pair of immunogen and delivery platform/adjuvant that overcomes the obstacles in current vaccine design is indeed a tall order to fill.

However, we believe that our current studies give cautious optimism that an effective blood stage malaria vaccine is an attainable goal.

References

1. Holder AA, Guevara Patino JA, Uthaipibull C, Syed SE, Ling IT, et al. (1999) Merozoite surface protein 1, immune evasion, and vaccines against asexual blood stage malaria. Parassitologia 41: 409-414.
2. Hui G, Hashimoto C (2007) Plasmodium falciparum anti-MSP1-19 antibodies induced by MSP1-42 and MSP1-19 based vaccines differed in specificity and parasite growth inhibition in terms of recognition of conserved versus variant epitopes. Vaccine 25: 948-956.
3. Pusic KM, Hashimoto CN, Lehrer A, Aniya C, Clements DE, et al. (2011) T cell epitope regions of the P. falciparum MSP1-33 critically influence immune responses and in vitro efficacy of MSP1-42 vaccines. PLoS One 6: e24782.
4. Nagata M, Wong T, Clements D, Hui G (2007) Plasmodium falciparum: immunization with MSP1-42 induced non-inhibitory antibodies that have no blocking activities but enhanced the potency of inhibitory anti-MSP1-42 antibodies. Exp Parasitol 115: 403-408.
5. Singh S, Miura K, Zhou H, Muratova O, Keegan B, et al. (2006) Immunity to recombinant plasmodium falciparum merozoite surface protein 1 (MSP1): protection in Aotus nancymai monkeys strongly correlates with anti-MSP1 antibody titer and in vitro parasite-inhibitory activity. Infect Immun 74: 4573-4580.
6. Kumar S, Collins W, Egan A, Yadava A, Garraud O, et al. (2000) Immunogenicity and efficacy in aotus monkeys of four recombinant Plasmodium falciparum vaccines in multiple adjuvant formulations based on the 19-kilodalton C terminus of merozoite surface protein 1. Infect Immun 68: 2215-2223.
7. Chang SP, Case SE, Gosnell WL, Hashimoto A, Kramer KJ, et al. (1996) A recombinant baculovirus 42-kilodalton C-terminal fragment of Plasmodium

falciparum merozoite surface protein 1 protects Aotus monkeys against malaria. Infect Immun 64: 253-261.

8. Stowers AW, Cioce V, Shimp RL, Lawson M, Hui G, et al. (2001) Efficacy of two alternate vaccines based on Plasmodium falciparum merozoite surface protein 1 in an Aotus challenge trial. Infect Immun 69: 1536-1546.
9. Hirunpetcharat C, Tian JH, Kaslow DC, van Rooijen N, Kumar S, et al. (1997) Complete protective immunity induced in mice by immunization with the 19-kilodalton carboxyl-terminal fragment of the merozoite surface protein-1 (MSP1[19]) of Plasmodium yoelii expressed in Saccharomyces cerevisiae: correlation of protection with antigen-specific antibody titer, but not with effector CD4+ T cells. J Immunol 159: 3400-3411.
10. Ogutu BR, Apollo OJ, McKinney D, Okoth W, Siangla J, et al. (2009) Blood stage malaria vaccine eliciting high antigen-specific antibody concentrations confers no protection to young children in Western Kenya. PLoS One 4: e4708.
11. Malkin E, Long CA, Stowers AW, Zou L, Singh S, et al. (2007) Phase 1 study of two merozoite surface protein 1 (MSP1(42)) vaccines for Plasmodium falciparum malaria. PLoS Clin Trials 2: e12.
12. Udhayakumar V, Anyona D, Kariuki S, Shi YP, Bloland PB, et al. (1995) Identification of T and B cell epitopes recognized by humans in the C-terminal 42-kDa domain of the Plasmodium falciparum merozoite surface protein (MSP)-1. J Immunol 154: 6022-6030.
13. Malhotra I, Wamachi AN, Mungai PL, Mzungu E, Koech D, et al. (2008) Fine specificity of neonatal lymphocytes to an abundant malaria blood-stage antigen: epitope mapping of Plasmodium falciparum MSP1(33). J Immunol 180: 3383-3390.

14. Tian JH, Miller LH, Kaslow DC, Ahlers J, Good MF, et al. (1996) Genetic regulation of protective immune response in congenic strains of mice vaccinated with a subunit malaria vaccine. J Immunol 157: 1176-1183.

15. Hui GS, Gosnell WL, Case SE, Hashiro C, Nikaido C, et al. (1994) Immunogenicity of the C-terminal 19-kDa fragment of the Plasmodium falciparum merozoite surface protein 1 (MSP1), YMSP1(19) expressed in S. cerevisiae. J Immunol 153: 2544-2553.

16. Stanisic DI, Martin LB, Good MF (2003) The role of the 19-kDa region of merozoite surface protein 1 and whole-parasite-specific maternal antibodies in directing neonatal pups' responses to rodent malaria infection. J Immunol 171: 5461-5469.

17. Tian JH, Good MF, Hirunpetcharat C, Kumar S, Ling IT, et al. (1998) Definition of T cell epitopes within the 19 kDa carboxylterminal fragment of Plasmodium yoelii merozoite surface protein 1 (MSP1(19)) and their role in immunity to malaria. Parasite Immunol 20: 263-278.

18. Herrington DA, Clyde DF, Davis JR, Baqar S, Murphy JR, et al. (1990) Human studies with synthetic peptide sporozoite vaccine (NANP)3-TT and immunization with irradiated sporozoites. Bull World Health Organ 68 Suppl: 33-37.

19. Bouharoun-Tayoun H, Oeuvray C, Lunel F, Druilhe P (1995) Mechanisms underlying the monocyte-mediated antibody-dependent killing of Plasmodium falciparum asexual blood stages. J Exp Med 182: 409-418.

20. McIntosh RS, Shi J, Jennings RM, Chappel JC, de Koning-Ward TF, et al. (2007) The importance of human FcgammaRI in mediating protection to malaria. PLoS Pathog 3: e72.

21. Mbow ML, De Gregorio E, Valiante NM, Rappuoli R New adjuvants for human vaccines. Curr Opin Immunol 22: 411-416.

22. Gao J, Gu H, Xu B (2009) Multifunctional magnetic nanoparticles: design, synthesis, and biomedical applications. Acc Chem Res 42: 1097-1107.

23. Ferrari M (2005) Cancer nanotechnology: opportunities and challenges. NatRevCancer 5: 161-171.

24. Peer D, Karp JM, Hong S, Farokhzad OC, Margalit R, et al. (2007) Nanocarriers as an emerging platform for cancer therapy. NatNanotechnol 2: 751-760.

25. Pusic K, Xu H, Stridiron A, Aguilar Z, Wang A, et al. (2011) Blood stage merozoite surface protein conjugated to nanoparticles induce potent parasite inhibitory antibodies. Vaccine 29: 8898-8908.